AD-A164 916 JOINT SERVICES ELECTRONICS PROGRAM(U) OHIO STATE UNIV 1/2
COLUMBUS ELECTROSCIENCE LAB DEC 85 ESL-710816-10
N00014-78-C-0049

UNCLASSIFIED F/G 9/5 NL

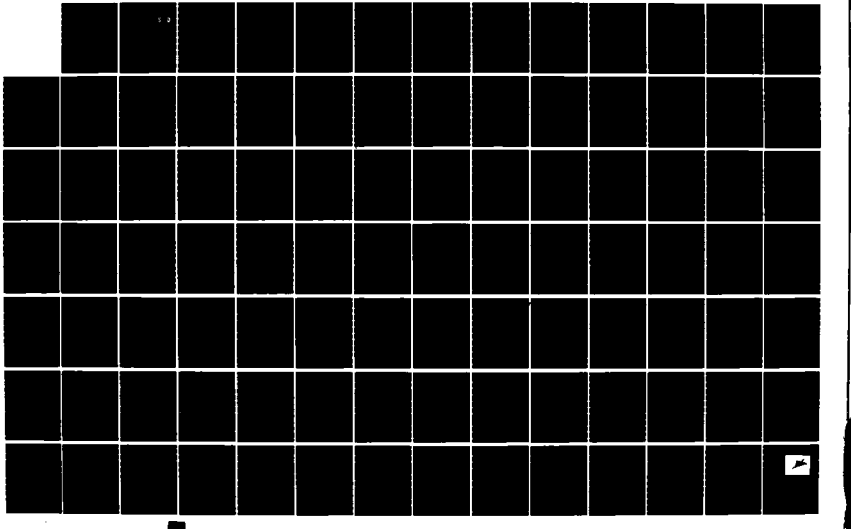

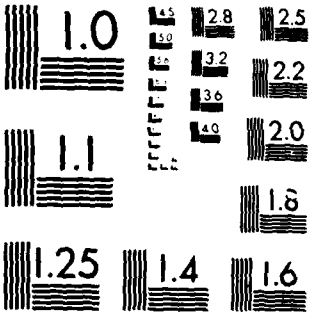

OSU

The Ohio State University

JOINT SERVICES ELECTRONICS PROGRAM

The Ohio State University

ElectroScience Laboratory

Department of Electrical Engineering
Columbus, Ohio 43212

Eighth Annual Report 710816-18
Contract N00014-78-C-0049
December 1985

Department of the Navy
Office of Naval Research
800 Quincy Street
Arlington, Virginia

NOTICES

When Government drawings, specifications, or other data are used for any purpose other than in connection with a definitely related Government procurement operation, the United States Government thereby incurs no responsibility nor any obligation whatsoever, and the fact that the Government may have formulated, furnished, or in any way supplied the said drawings, specifications, or other data, is not to be regarded by implication or otherwise as in any manner licensing the holder or any other person or corporation, or conveying any rights or permission to manufacture, use, or sell any patented invention that may in any way be related thereto.

ADA 164916

50272-101

REPORT DOCUMENTATION PAGE	1. REPORT NO.	2.	3. Recipient's Accession No.
4. Title and Subtitle: JOINT SERVICES ELECTRONICS PROGRAM EIGHTH ANNUAL REPORT			5. Report Date: December 1985 6.
7. Author(s)			8. Performing Organization Rept. No. 710816-18
9. Performing Organization Name and Address: The Ohio State University ElectroScience Laboratory 1320 Kinnear Road Columbus, Ohio 43212			10. Project/Task/Work Unit No. 11. Contract(C) or Grant(G) No. (C) N00014-78-0049 (G)
12. Sponsoring Organization Name and Address: Department of the Navy Office of Naval Research 800 Quincy Street Arlington, Virginia			13. Type of Report & Period Covered: Annual Report Oct. 1984 - Sept. 1985 14.

15. Supplementary Notes

16. Abstract (Limit: 200 words)

17. Document Analysis a. Descriptors

b. Identifiers/Open-Ended Terms

c. COSATI Field/Group

18. Availability Statement	19. Security Class (This Report)	21. No. of Pages
APPROVED FOR PUBLIC RELEASE: DISTRIBUTION IS UNLIMITED.	Unclassified	177
	20. Security Class (This Page) Unclassified	22. Price

(See ANSI-Z39.18) See Instructions on Reverse OPTIONAL FORM 272 (4-77)
(Formerly NTIS-35)
Department of Commerce

TABLE OF CONTENTS

LIST OF TABLES

LIST OF FIGURES

I. DIRECTOR'S OVERVIEW

This report represents the eighth annual summary at the Ohio State University sponsored by the Joint Services Program (JSEP).

There has been a total of 14 Ph.D. and 13 M.Sc. degrees in Electrical Engineering degrees obtained under JSEP sponsorship. There are currently 8 Ph.D. and 3 M.Sc. students being partially supported under JSEP.

As may be seen in the Annual Report Index, 18 reprints have been included in the period March 1984 to September 1985. In addition, 12 papers have already been accepted for publication in the coming year, an additional 5 papers have been submitted, and an additional 10 papers are already in preparation.

II. DESCRIPTION OF SPECIAL ACCOMPLISHEMENTS AND TECHNOLOGY TRANSITION

In the Sixth Annual Report we made the following statements:

> "Our major research area continues to be the analysis of electromagnetic radiation and scattering. Associated with this primary goal is a substantial program for improving our experimental capabilities. This was supported in part by the JSEP program and has expanded recently with other sponsorship so that our anechoic chamber compact scattering range is probably the best of its kind at the present time. This is emphasized by the fact that we have provided information to Scientific Atlanta (the reflector manufacturer) for improving these facilities. We have also been contacted by several other manufacturers requesting assistance in building the next generation of compact ranges. It is noted that the stepped frequency concept originated under JSEP was then developed using the comapct range under separate funding by ONR. Additional improvements were made under funding from NASA. This has indeed been a most rewarding area of research."

In the Seventh Annual Report we observed that:

> "These statements turn out to be an understatement. We can now report that Scientific Atlanta is incorporating our designs in their compact reflector. In fact, they have donated the first modified compact reflector to the ESL (500K value). We have discussed compact range technology with many organizations including Sandia, Hughes, Rockwell, NASA, Martin Marietta, MacDonald Douglas, SPC, Westinghouse, Motorola, etc., Thus, this work started under JSEP is being rapidly converted to practice by many major industries. Also, there have been further developments funded by various agencies based on this technology initiated originally under JSEP. One of these is rather interesting, i.e,. using the compact reflector to simulate ranges from 50 feet to infinity by displacing the feed four feet from the focal point (50 foot range)."

More recently we are currently involved with Boeing in establishing the design for a very large compact range facility for studying the EM properties of full scale vehicles. They have borrowed the reflector donated by Scientific Atlanta and are to return it to us with an updated blended edge of our design.

We have also provided the Avionics Laboratory at Wright Patterson Air Force Base with a blended edge design which should be installed before this is being read. After it is installed they should have the best compact range facility in existance. Prof. Burnside and Dr. Young of our laboratory have recieved a written commendation for timely and professional support in providing these designs at the Navy's Indoor RCS Measurement Conference from Admiral J.B. Mooney, Chief of Naval Research, ONR.

Not only has the compact range work extended the state-of-the-art of RCS measurements, but we have also collected a substantial amount of

phasor RCS data as a funciton of aspect, polarization and frequency for a variety of targets. This data is of substantial value to target identification groups both at the ElectroScience Laboratory and elsewhere.

It is emphasized that this complete Compact Range Technology was initiated under our Time Domain Studies JSEP and transferred to other agencies including ONR and NASA as such support became available. There is no doubt that this modernized compact range technology will be used for most free space EM measurements in the long range future.

The diffraction studies continue to provide the basis for the extension of our radar scattering analyses of complex objects under other sponsorship. These studies were originally being directed toward generating computer codes for EM scattering from bodies of complex shape. However, security regulations at that time required a secure computer to make such calculations. Thus, our sponsors were undertaking this role while we continued to provide guidance to this effort.

However, this approach has not produced the desired results. As a consequence, we discussed this with the appropriate DOD office and we have just been granted an exception to these regulations. This is essential if these codes are to be developed since the basic EM concepts and the technical staff required to further expand the appropriate theoretical concepts are here at the ElectroScience Laboratory. Again this resevoir of talent and knowledge is available because of JSEP support and as this program develops, JSEP support will be essential in further expanding basic scattering mechanisms such as corner diffraction, edge waves, diffraction from coated bodies, etc.

A major conclusion of the EM Planning Workshop, November 14 and 15, 1985, at the U.S. Naval Postgraduate School were that the above topics are essentially those required to extend the state-of-the-art of electromagnetics for the coupling problem. Observe that we had applied the hybrid techniques to coupling (see the previous Annual Report, p. 63). Again our JSEP support is being used to generate timely complex theoretical concepts.

As we reported for the past several years computer codes based on the high frequency asymptotic techniques for antennas mounted on various types of vehicles are now used throughout the aerospace industry. During the past year, 97 copies of the computer tape containing these codes, were sent to various organizations who could provide a DOD contract number, at their request. This is up from the 35 copies distributed the year before. These codes have been declared to be sensitive and now fall under the export control laws. Computer codes obtained from the integral equation and surface patch modeling studies are also being widely distributed and this year 29 copies of this code were distributed.

The basic work conducted under JSEP sponsorship is being used under other sponsorship for the development of these codes. The transfer of technology is being greatly assisted by the distribution of computer codes.

There is a continued concentrated effort to develop asymptotic techniques for treatment of penetrable bodies in addition to our continued research on asymptotic solutions for conducting bodies.

Another substantial DOD payoff has been in the area of the hybrid solutions which has been supported by JSEP. There have been several rewarding efforts that have subsequently been funded by other agencies. The scattering from jet intakes has been funded by AFOSR, NWC and NASA. We have found one remarkable result. The hybrid solution uses waveguide modes in the scattering in internal structure and UTD solutions for the external scattering. The internal structure can be treated using only a very small number of modes for very large intake-like structures. Recall that a waveguide mode in a rectangular waveguide can be represented by a pair of homogeneous plane waves propagating at an angle with respect to the waveguide axis. Then, these modes are selected so that rays representing these plane waves are directed near the shadow boundary associated with the incident radar wave. Thus, for the first time very large intake-like structures can be analyzed accurately.

Yet another structure of importance to DOD is the crack. Such cracks take on a significant role for low observabable vehicles in that after other scattering mechanisms are reduced, the cracks (due to access panels, landing wheel doors, etc.) are the remaining scatterers. The crack study initiated in the hybrid studies under JSEP program has since been picked up by other DOD agencies and Aerospace Companies. Again our contribution to these programs has been substantial due to the available JSEP support.

The work on hybrid solutions is continuing. The study of scattering from cracks is not the only result obtained via the hybrid solution. Problems being attacked by this approach include: 1) diffraction involving special edges, 2) diffraction between edges coated with dielectric, 3) coupling by apertures, 4) analysis of microstrip antennas, 5) reflector antenna synthesis and 6) the properties of a dipole over a lossy media. This last is an alternative approach to the very difficult and complex Sommerfeld problem and is an important advance because of its simplicity.

The focus on the integral equation or moment method solutions is to generate concepts that will extend the usefulness of these solutions. This is of great importance since this approach represents the only "exact" solution for complex geometries. It is not quite exact since it becomes approximate when the integral equations are digitized in some form. The major role being pursued here is primarily in the creation of novel basis functions that substantially extend the potential of the integral equation approach.

The research involving integral equation solutions for penetrable media has resulted in several technical advances. First, Dr. Newman incorporated polarization currents to represent a dielectric slab in the presence of a conducting edge. By using the Green's function for the half plane he has been able to eliminate computational problems associated with the edge singularity.

Professor Richmond, under the study of Scattering by Penetrable Geometries, has shown that he can represent a rather large thin flat

dielectric sheet by only three unknowns. This work, properly extended, will make the new so called "physical basis" technique a standard analysis, available for many applications and avoid the problem of treating huge matrices. Both of these studies will not only provide check cases and guidance for the asymptotic cases already discussed but will become a design tool for any case where a thin penetrable layer ($< 0, 2\lambda$ thick) is used.

The original time domain studies are now being funded elsewhere. The target identification work is being pursued under contract with ONR and NWC. Some spectacular results have been obtained but cannot be disclosed here because of classification. Further, impulse response forms the basis for all of our high resolution measurements. We are now directing our JSEP effort to concentrate on the K-pulse concept.

It is observed that there is a group of four senior engineers involved in these studies that are supported by the basic JSEP studies.

A JSEP paper by Professors Kennaugh and Moffatt was used as the lead paper in the Proc. of NATO Advanced Research Workshop on Inverse Methods in Electromagnetic Imaging. The entire workshop was dedicated to the memory of Professor Kennaugh, who (along with Professor Moffatt) was a major contributor to our JSEP activities in this improtant area of research. The book resulting from this meeting has been dedicated to Professor Kennaugh with a full page photograph as the frontispiece. Over the past several years there has been substantial progress in the general area of time domain measurements and target identification. It may be worth noting that the ERA in Leatherhead, England, after a

complete review of target identification techniques for mine detection came to the conclusion that the OSU approach was optimum for detecting and identifying mines in the Falklands. Remarkable improvement has been achieved in obtaining the impulse response of a cone-cylinder simply by replacing the sphere with a circular disk as a calibration target. The problem, that was eliminated, was caused by the isotropic scattering nature of the sphere. The resulting time domain pattern is in excellent agreement with predictions. This is the only known result when such agreement has indeed been obtained. A method of combining low frequency calculated or measured scattering data with high frequency asymptotic computations has been demonstrated for the case of a cavity-type target. Frequencies in the vicinity of low or first cutoff are spanned using rational function approximants. We repeat that the source of the time domain processing in our compact range is our JSEP transient studies.

It is observed that the prediction - correlation target recognition procedure developed under JSEP sponsorship is now being extensively tested on a large noncooperative target recognition program. Procedures for complex natural resonance extraction from measured scattering data also developed under JSEP sponsorship are being utilized on other programs. The impulse response concepts, while not initially developed on JSEP, have been continuously refined on this program. It is now generally recognized in the electromagnetics area that broadband scattering or radiation data are most easily interpreted in the time domain. Thus, target recognition, radar cross section control and scattering mechanisms analysis all are utilizing time domain waveforms.

Data from broadband compact reflectivity measurement ranges are used to produce complete time-dependent polarization scattering matrices.

The time domain portion of our research was initially based primarily on the problem of radar target identification under the direction of Professor Moffatt with a small effort on the K-pulse concept conducted by Professor Kennaugh, now deceased. All of the target identification research is now supported on other research programs and JSEP supported effort now is concentrated on the K-pulse problem development, radar cross section control and in target identification.

It is emphasized that while the K-pulse has been carried as a topic on JSEP for a number of years, the level of effort has been very small. As might be expected in any novel basic concept, results have been slow in appearing. However recently we have been successful. This is a result of directing all of our JSEP support in this direction and moving other time domain topics including the compact range technology to other supporting agencies. Among other things, these papers involving K-pulse studies are now being published in referred journals. Unfortunately, the low level of JSEP funding in this area for the forthcoming year will prohibit sustaining this level of effort.

III. RESEARCH SUMMARY

Researchers: R.G. Kouyoumjian, Professor
(Phone: 614/422-7302)

P.H. Pathak, Assistant Professor
(Phone: 614/422-6097)

N. Wang, Senior Research Associate
(Phone: 614/422-0220)

R. Tiberio, Visiting Professor and Consultant

O.M. Buyukdura, Senior Research Associate
(Phone: 614/-422-1760)

R.G. Rojas, Senior Research Associate
(Phone: 614/422-2530)

A. DIFFRACTION STUDIES

1. Diffraction by Non-Conducting Surfaces

(a) Diffraction by a Discontinuity in Surface Impedance

The need for analyzing EM scattering by discontinuities in surface impedance arise not only in the control of the RCS of perfectly conducting structures by impedance loading, but they also arise, for example, in the design of flush mounted aircraft/missile antennas with a thin coating (or a radome), of finite extent, and in the studies for improving the isolation among a pair of flush mounted antennas by placing an absorber (which can be modeled by a lossy impedance surface) in between those two antennas.

During the present period, work has continued on the analysis of electromagnetic scattering by discontinuities in surface impedance.

Tiberio, et al. published two papers in 1982-1983, which dealt with the solutions for diffraction by a strip with two face impedances, and by a three part planar impedance surface. In the above mentioned papers, Tiberio, et al., employed a spectral expansion for the field diffracted by the first edge to then calculate the field diffracted from the second edge in the case when the direction of incidence lines up along the direction of grazing incidence on the strip thereby giving rise to an overlap of shadow boundary transition regions associated with each edge. In such a situation, the diffraction of the field incident on the second edge after diffraction from the first edge cannot be calculated via a direct application of the uniform geometrical theory of diffraction (UTD); however, a spectral expansion for the field diffracted from the first edge can be used in conjunction with the UTD to handle the doubly diffracted field in this special case. The UTD result employed in these papers was based on an extension of Maliuzhinet's solution for the diffraction by an impedance wedge. Specifically the extension involved making Maliuzhinet's [1] results for the fields diffracted by a half plane with two face impedances and by a planar two part impedance surface, respectively uniformly valid across the geometrical optic incident and reflection shadow boundaries. It is noted that the original Maliuzhinet's asymptotic analysis in [1] is non-uniform and so it does not remain valid within the geometrical optics shadow boundaries.

A further extension of Maliuzhinet's work [1] has been performed; namely, his non-uniform asymptotic analysis of the diffraction integrals has been made uniform so that this uniform result now remains valid within the geometrical optics incident and reflection shadow boundaries associated with an impedance wedge of any interior angle (rather than for just the previously mentioned half plane or a planar two part configuration, both of which are special cases of the general wedge configuration). In addition, this uniform version of Maliuzhinet's solution has been cast into the UTD form for the diffraction by a perfectly-conducting wedge together with appropriate multiplying factors which account for the non-zero surface impedance. Such a UTD form of Maliuzhinet's solution may provide the clues to simplifying it further using some approximations without really sacrificing it's accuracy. All of this work has been reported recently as an oral as well as a written paper; these oral and written presentations are indicated below:

"A Uniform GTD Formulation for the Diffraction at a Wedge with Two Face Impedances", R. Tiberio, G. Pelosi and G. Manara, paper presented at the 1984 International IEEE APS/Radio Science meeting, Westin Hotel, Boston, Massachusetts, June 25-29, 1985.

"A Uniform GTD Formulation for the Diffraction by a Wedge with Impedance Faaces", R. Tiberio, G. Pelosi and G. Manara, IEEE Trans. AP-33, No. 8, pp. 867-873, August 1985.

Also, it was reported in the previous JSEP annual report (June 1986) that EM plane and surface waves by a planar, two part surface in which one part is a perfect electric or magnetic conductor and the other

part is characterized by a non-zero surface impedance. This two-dimensional analysis is based on the Wiener-Hopf procedure together with Weinstein's method of factorization, and it leads to solutions which are simpler than those obtained by specializing the UTD form of Maliuzhinet's solution for the wedge to the case of a two part planar impedance discontinuity. These Wiener-Hopf based solutions, which have been obtained by Rojas and Pathak for both the TE and TM polarizaitons, provide uniform GTD or (UTD) diffraction coefficients for the discontinuity in surface impedance; furthermore, they constitute solutions to canonical problems which are crucial to the development of a uniform GTD analysis for the problems of the diffraction by the edge of a thin dielectric or ferrite half plane, and by the edge of a thin dielectric or ferrite half plane on a perfectly conducting surface. For this reason, these Wiener-Hopf solutions are described in an invited paper entitled:

> "A Uniform GTD Analysis of EM Diffraction by an Impedance Discontinuity in A Planar Surface", by P.H. Pathak and R. Rojas, paper accepted for publication in the Journal of Wave-Material Interaction.

The solution of the diffraction by a thin dielectric or ferrite half plane is discussed later in Part (b), along with a mention of the paper which has been recently submitted on this topic.

An analysis of the high frequency EM radiation by a magnetic line (or line dipole) source on a uniform impedance surface which partially covers a smooth perfectly-conducting convex surface has been performed

in the past. A manuscript describing this work has been recently submitted for publication; namely,

> "An Asymptotic High Frequency Analysis of the Radiation by a Source on a Perfectly-Conducting Convex Cylinder with an Impedance Surface Patch", L. Ersoy and P.H. Pathak, paper submitted to the IEEE Trans. AP.

The preceding work is of interest, for example, in the study of fuselage mounted airborne slot antennas with a finite dielectric cover for the purpose of controlling the field radiated near the horizon (or shadow boundary) over that in the absence of the cover. The impedance surface approximation can be employed here to model the dielectric patch or covering if the dielectric is sufficiently thin.

It is often of interest in practical applications to analyze the isolation between two flush mounted antennas on either side of an absorber panel which is placed on a planar perfectly-conducting surface containing the flush mounted antennas. Such a study is expected to provide information on the size and value of the impedance patch (corresponding to the absorber coated surface) which is generally required to achieve a prescribed level of antenna isolation. Work has been initiated to analyze this geometry and some preliminary results were reported recently in an oral paper:

> "GTD Analysis of the Coupling Between Two Slots Separated by an Impedance Patch on a Ground Plane," R. Tiberio, G. Pelosi, G. Manara, P.H. Pathak, R.G. Rojas, IEEE/APS Symposium and National Radio Science Meeting at the University of British Columbia, Canada, June 1985.

The work on the type of diffraction analysis described above, dealing with structures possessing a discontinuity in surface impedance, will be continued in the future phases of this study in order to extend these solutions to treat more general situations (e.g., to treat 3-D problems as described in the last JSEP proposal (1985).

(b) Diffraction at Dielectric/Ferrite Loaded Edges

In situations where an equivalent uniform surface impedance boundary condition, which was discussed in the previous section, cannot effectively model uniform coatings on perfectly-conducting structures, it then becomes necessary to deal with such coatings in a less approximate fashion. Such a situation typically arises when the coating is not sufficiently thin. Nevertheless, the solutions based on the surface impedance approximation are useful not only for treating very thin coatings, but also for offering clues as to the generalizations of such solutions so that they remain valid for coatings which cannot be modeled sufficiently accurately by the impedance boundary condition. Geometries involving the scattering by the edge of dielectric/ferrite structures are commonly encountered in of metallic aerospace vehicles coated by absorber patches, or in estimating the diffraction by edges in composite materials which may occur as wings or stabilizers in such vehicles. In view of such interest, we analyzed the diffraction by a dielectric/ferrite half plane on a planar perfect electric or magnetic conductor of infinite extent. More importantly, these solutions for the diffraction by dielectric/ferrite half planes on perfect electric and

magnetic conductors, respectively, were employed to synthesize the solution for of the diffraction by a dielectric/ferrite half plane of twice the thickness in the absence of the conductors using the image bisection principle. In relation to the latter geometry, the former are referred to as the even or odd bisection configurations, (depending on the field polarization in each case). The latter geometry along with the former even and odd bisection type geometries constitute important canonical configurations involving edges in penetrable (dielectric/ferrite) structures. The procedure employed to solve the even and odd bisection type geometries was briefly described in the last annual report (1984). It was indicated therein that the solutions to the canonical even and odd bisection geometries of the diffraction by dielectric/ferrite half planes on electric and magnetic walls were obtained indirectly from the solutions to appropriate planar two part diffraction problems which exhibited in a more simple fashion all the essential characteristics of the odd and even bisection problems. In those planar two part geometries, one part was a perfect electric or magnetic conductor while the other part was an impedance surface. In the case of plane wave illumination, those two part solutions were obtained by the Wiener-Hopf procedure. A key step was to express the solutions to the two-part geometries in the format of the well-known UTD solution for the diffraction by a perfectly-conducting edge [2]; once this was done, the two-part solutions offered direct clues as to how these could be generalized approximately, but accurately, to handle the even and odd bisection configurations pertaining to of plane wave

diffraction by dielectric/ferrite half planes on electric and magnetic walls. It was then a straight forward matter to generalize the plane wave incidence case to include cylindrical wave illumination using the UTD concepts of [2,3]. The solutions to the 2-D even and odd bisection case are useful in their own right as canonical UTD solutions; they can be used directly to study the diffraction by the edges of absorber panels of moderate thickness (in terms of the wavelength) when those finite size panels are placed on larger planar conducting surfaces. A superposition of the solutions using the even and odd bisection configurations led to the solution of the other useful canonical problem in the UTD; namely, to the solution for the 2-D problem of plane and cylindrical wave diffraction by a dielectric/ ferrite half plane as mentioned above. That work was reported in a previous JSEP annual report. Furthermore, the solution to the 2-D diffraction by a two part impedance surface was very recently generalized in a rigorous fashion to treat the corresponding 3-D configuration of waves obliquely incident to the edge of the two part impedance discontinuity. As a result, following procedures similar to those employed in the generalization of the two part impedance solutions from 2-D to 3-D, the corresponding 2-D solutions to the problems of odd and even bisection configurations pertaining to a dielectric/ferrite half plane on electric or magnetic walls were likewise extended to the 3-D case. The 3-D solutions to the even and odd bisection cases when appropriately superposed also then led directly to the solution for the 3-D diffraction of EM plane, conical, spherical and surface waves obliquely incident on the edge of a

dielectric/ferrite half plane. In all of this work, the dielectric/ ferrite half plane is assumed to be thick enough so that only the dominant TE and TM surface wave modes can be excited. The UTD solution for the 3-D diffraction by a dielectric/ferrite half plane constitutes an important addition to the class of solutions using ray methods. It is noted that there is a coupling between the TE and TM scattered fields in the 3-D diffraction by a dielectric/ferrite half plane which further added to the complexity of the analysis; such a coupling is absent for the 2-D case or the case of normal incidence on the edge.

Presently, the 2-D UTD solution obtained for the scattering by a dielectric/ferrite half-plane and related configuration has been described in the following:

> "EM Scattering by a Thin Dielectric/Ferrite Half Plane and Related Configurations-Two Dimensional Case", P.H. Pathak and R.G. Rojas, paper submitted for publication to the IEEE Trans. AP-S.

A second paper describing the corresponding 3-D UTD solution for the scattering by a dielectric/ferrite half-plane and related configuration was presented orally, and it is also being written for publication as indicated below:

> "A UTD Analysis of the Diffraction by a Thin Dielectric/Ferrite Half-Plane (Oblique Incidence Case)", R.G. Rojas, P.H. Pathak, IEEE/APS Symposium and National Radio Science Meeting at the University of British Columbia, Vancouver, Canada, June 1985.

> "EM Scattering by a Thin Dielectric/Ferrite Half-Plane and Related Configurations-Three Dimensional Case", R.G. Rojas and P.H. Pathak, paper in preparation.

2. Vertex Diffraction

The analysis of vertex diffraction is important because flat plates are frequently used to model aircraft wings and vertical or horizontal stabilizers. The radiation from an antenna mounted on the aircraft or the backscatter from the aircraft is strongly affected by both edge and vertex diffraction. As we shall see, these effects may be strongly coupled.

A typical vertex in a planar, perfectly-conducting surface is shown in Figure 1. A more general vertex in a planar surface is formed by the intersection of two otherwise smooth, curved edges. The angle α is the internal angle formed by the tangents to each of the curved edges at the vertex.

The asymptotic high-frequency analysis of electromagnetic vertex diffraction is rather complicated. Vertices not only shadow the incident field, but they also shadow the edge diffracted fields. The shadow boundary of an edge diffracted field is a conical surface whose tip coincides with the vertex and whose axis is an extension of the shadowed edge. The vertex introduces a diffracted ray which penetrates the shadow regions; furthermore, the vertex diffracted field must also compensate the discontinuities in the incident and edge diffracted fields at their shadow boundaries. At these boundaries the vertex diffracted field assumes its largest magnitude and, hence, its greatest importance. If the vertex diffracted field is omitted in the GTD solution, then substantial discontinuities connected with the shadowing

of the incident and edge diffracted fields may occur in the calculated radiation pattern.

A simple, approximate vertex diffraction coefficient which appears to work reasonably well in certain cases has been obtained at the ElectroScience Laboratory [3,4]. However, this result has been found heuristically using a combination of theory and experiment; therefore, it needs to be improved in order to be useful in the general situations encountered in practice. Nevertheless, this diffraction coefficient offers some clues for constructing the more refined and useful vertex diffraction coefficient, which we expect to obtain from asymptotic analysis.

One objective of this research is to obtain a uniform asymptotic solution for the electromagnetic field scattered by the vertex, which can be interpreted ray optically in terms of contributions from the reflected ray, the rays diffracted from edges 1 and 2 and the vertex diffracted ray; these rays originate at the critical points Q_R, Q_1, Q_2 and Q_V, respectively. It is assumed here that the source 0 is not close to either edge. The approach is to approximate the current away from the edges by the geometrical optics current. Near the edges, but away from the vertex, the local half-plane current is used and near the vertex the first few terms of the eigenfunction solution [5] are employed. The integral representation of the field radiated by these currents could be evaluated numerically, but it is important to avoid this clumsy, inefficient procedure. For this reason, as well as to obtain the aforementioned ray optical contributions, the integral representation should be evaluated asymptotically.

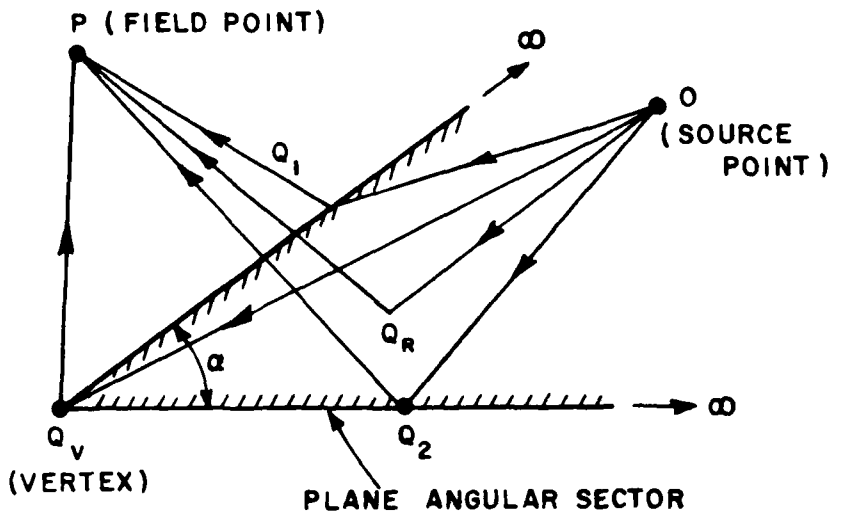

Figure A.1. Various rays associated with the reflection and diffraction by a plane angular sector.

A method for asymptotically approximating the field of the current near an edge or vertex is being investigated. Recently this method has been successful in the case of currents near an edge; it will be applied next to the eigenfunction representation of the current near the vertex to obtain the vertex diffraction coefficient.

The confluence of the critical points has been examined using the geometrical optics current everywhere on the vertex. When all the critical points are close to each other, the expression obtained for the transition function is so complicated it does not appear to be useful. An effort is being made to simplify this expression.

Vertex diffraction is of special importance when plate geometries are illuminated at or near grazing incidence. The vertex is strongly excited by waves guided along the edge of the plate. The existence of these traveling edge waves has been shown analytically [6], and the scattering by objects illuminated by them has been studied [7]. It is found that reflected and transmitted edge waves are excited as well as a space wave. The vertex is clearly an edge scatterer so the same phenomena are to be expected in this case, as is illustrated in Figure A.2. The incident edge wave is excited by a source or scatterer at 0 very near the edge, or by a second vertex illuminated by a space or edge wave. A solution to this geometry is under study. The total field has been obtained in the form of a (vector) eigenfunction expansion. A transformation of this representation is being sought which will permit its asymptotic approximation.

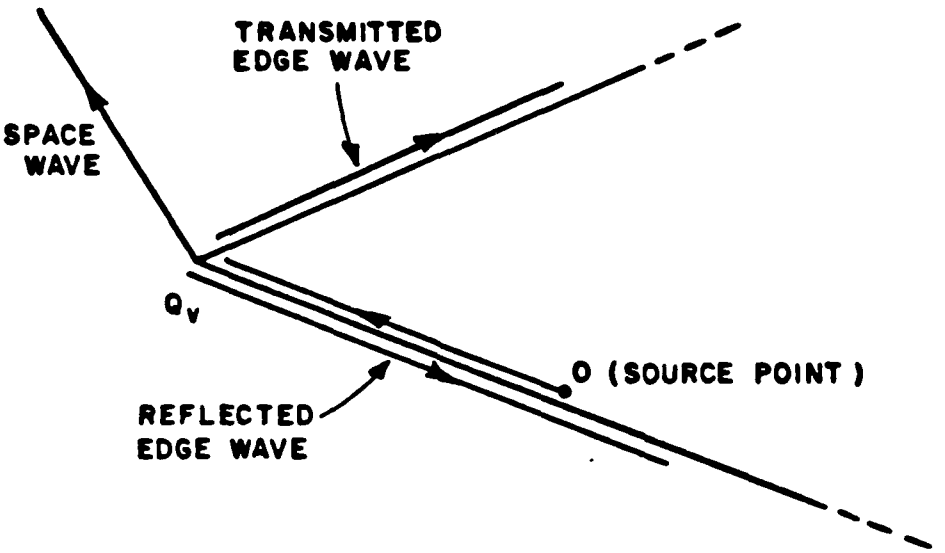

Figure A.2. Various rays associated with the diffraction of an edge wave by the vertex.

3. Diffraction by Wedges

(a) Diffraction by a Pair of Interacting Edges

Configurations consisting of a pair of interacting edges are often involved in modelling geometries of actual interest. Geometries of this type are shown in Figures A.3a,b,c. In addition to the field of the rays singly diffracted from the two edges, the contributions from the higher order diffracted fields are usually important. The most significant of these is the doubly-diffracted field, i.e., the field of the ray which is first diffracted from Q_1 and then diffracted a second time from Q_2. In calculating this field an ordinary application of the Uniform Geometrical Theory of Diffraction (UTD) [2] augmented by slope diffraction, provides useful results when the singly diffracted field which impinges on the second edge exhibits a ray optical behavior. However, at those aspects where the second edge lies in the transition region of the first, this solution may fail, particularly at aspects which are in the overlapping transition regions of the two edges. In earlier work suppored by this program, it was shown that accurate high-frequency expressions for the doubly-diffracted field can be obtained at grazing illumination, where the source is at 0, by means of a spectral extension of the UTD [8,9,10]. Although this result is valuable because it yields an accurate solution where the ordinary UTD fails, it is awkward to have it apply only at grazing incidence.

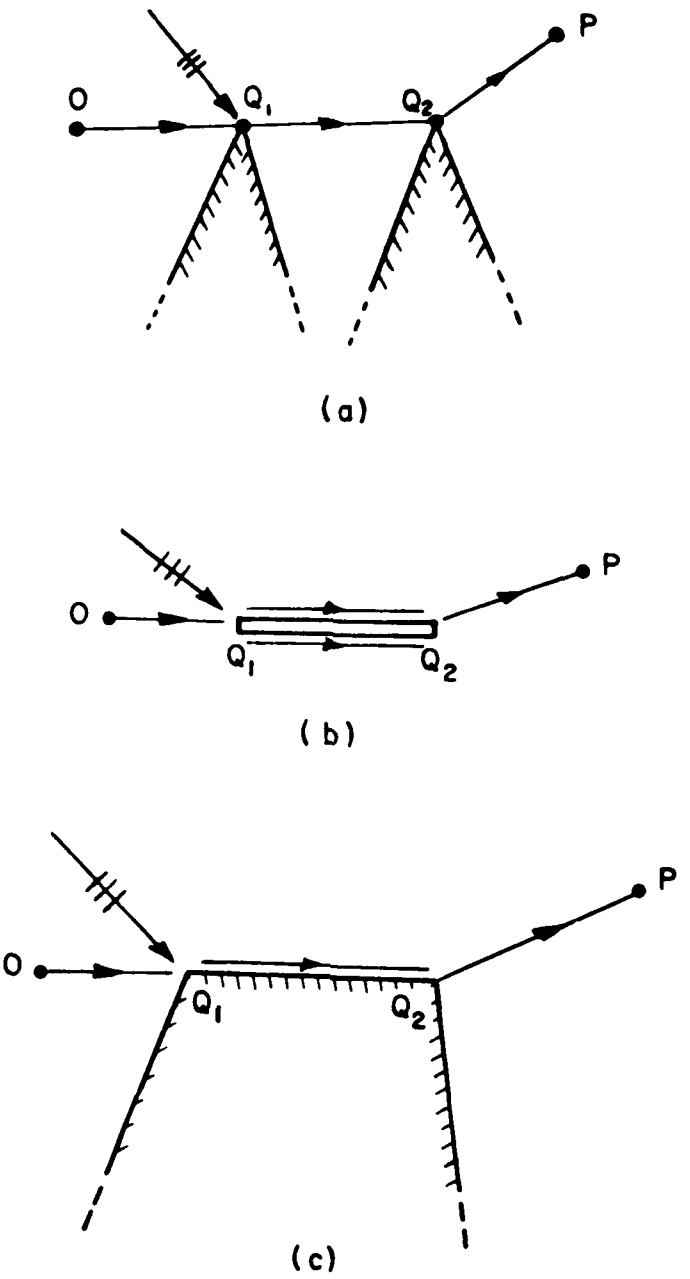

Figure A.3. Examples of interacting double edge structures.

In the present period it was found that the restriction to grazing incidence could be removed in the case of plane wave incidence. Except for some minor modifications, the method of analysis closely parallels that described in [10]. Solutions have been obtained for both the TE (incident electric field perpendicular to the edge) and TM (incident magnetic field perpendicular to the edge) polarizations. The extension to oblique incidence wiht arbitrary polarization of the incident plane wave is readily accomplished as described in [2,10].

Outside the overlapping transition regions the expression for the doubly diffracted field reduces to the UTD solution augmented by slope diffraction, as it should. At grazing incidence and observation this expression becomes infinite, but so does that for the singly-diffracted ray. It was found that the doubly-diffracted field compensates both the discontinuities and singularities which may occur in the singly diffracted field. Therefore the new solution when combined with the contributions from other diffracted fields provides a result which is uniformly valid at any incidence and observation aspects.

At present this solution is being tested by applying it to several polygonal scatterers. The calculated scattered fields will be compared with those obtained from a moment method solution.

A paper describing this work was presented at the 1985 International IEEE/AP-S Symposium held in Vancouver, Canada. It is planned to write a paper describing this work when the aforementioned calculations are completed.

(b) An Improved UTD Solution for Wedge Diffraction

The most important high frequency scattering mechanism (excluding those phenomena accounted for by geometrical optics, i.e., reflection and shadowing) is edge diffraction. Although the uniform geometrical theory of Diffraction (UTD) solution for edge diffraction properly compensates all jump discontinuities in the geometrical optics field, some components of the geometrical optics field have discontinuous derivatives across shadow and reflection boundaries which are not compensated by the UTD even when slope diffraction is included. To eliminate these unwanted "kinks" and obtain greater accuracy generally speaking, a new UTD solution for the wedge has been obtained.

Let an electromagnetic spherical wave with its center at 0 illuminate a perfectly conducting wedge. The distances of 0 and the field point from the point of diffraction Q_ξ are s' and s respectively, as shown in igure 1. The total high-frequency field is the sum of the geometrical optics field and a diffracted field, which is based on an asymptotic approximation. The accuracy of the approximation depends upon a large parameters, which in this case is

$$\kappa = \frac{k_0 ss'}{s+s'} \sin^2\beta_0 \quad , \tag{1}$$

where k_0 is the wave number of the medium surrounding the wedge and β_0 is the angle of incidence to the edge. The error in the expression for the diffracted field increases as κ decreases; however, during the period covered by this report we have been able to reduce κ without sacrificing accuracy. This has been accomplished by retaining the

higher order terms in the asymptotic approximation. The method of solution is described in the next paragraph.

An electric dipole parallel to the edge is introduced at O. Its magnetic vector potential, which is also parallel to the edge, is represented in terms of a scalar Green's function which satisfies the Dirichlet boundary condition on the surface of the wedge. This Green's function is expressed as the Fourier transform of a 2-D Green's function. A uniform asymptotic approximation for the 2-D Green's function which employs D_s is used. The Fourier transform is then evaluated asymptotically for field points outside the transition regions. Next the electric dipole is replaced by an edge-directed magnetic dipole and the above procedure is repeated using an electric vector potential. Since the expressions for the diffracted electric field obtained from these vector potentials are valid only outside the transition regions, they must be modified to obtain a uniform solution. This is done by imposing the following conditions:

1) the total field should be continuous and have continuous first derivatives across the shadow and reflection boundaries,

2) the solution should reduce to that obtained outside the transition regions,

3) as $s' \to \infty$ the solution should reduce to that obtained for plane wave incidence,

4) the reciprocity principle should be satisfied.

The resulting expression for the diffracted field is

$$\begin{bmatrix} E^d_{\beta_o} \\ E^d_{\phi} \\ E^d_{s} \end{bmatrix} = \left\{ \begin{bmatrix} -D_s + D_1 & D_2 \\ D_3 & -D_h + D_4 \\ D_5 & D_6 \end{bmatrix} \begin{bmatrix} E^i_{\beta'_o}(Q_E) \\ E^i_{\phi'}(Q_E) \end{bmatrix} + \begin{bmatrix} -d_s & d_2 \\ d_3 & -d_h \\ 0 & 0 \end{bmatrix} \begin{bmatrix} \frac{\partial E^i_{\beta'_o}}{\partial n'}(Q_E) \\ \frac{\partial E^i_{\phi'}}{\partial n'}(Q_E) \end{bmatrix} \right\} \sqrt{\frac{s'}{s(s+s')}}\, e^{-jk_o s} \tag{2}$$

where again D_s and D_h are given in [2],

$$D_1 = \frac{\cot^2\beta_o}{jk_o}\left(\frac{s+s'}{s'}\right)\left[\left(\frac{s+s'}{s'}\right)\frac{\partial}{\partial s} - \frac{1}{2s}\right] D_s, \tag{3}$$

$$D_2 = -\frac{\cos\beta_o}{jk_o \sin^2\beta_o}\left(\frac{s+s'}{ss'}\right)\frac{\partial D_h}{\partial \phi}, \tag{4}$$

$$D_3 = \frac{\cos\beta_o}{jk_o \sin^2\beta_o}\left(\frac{s+s'}{ss'}\right)\frac{\partial D_s}{\partial \phi}, \tag{5}$$

$$D_4 = \frac{1}{jk_o \sin^2\beta_o}\left(\frac{s+s'}{s'}\right)\left[\left(\frac{s+s'}{s'}\right)\frac{\partial}{\partial s} - \frac{1}{2s}\right] D_h, \tag{6}$$

$$D_5 = \frac{\cot\beta_o}{jk_o}\left[\left(\frac{s+s'}{s'}\right)\frac{\partial}{\partial s} - \frac{1}{2s}\right] D_s, \tag{7}$$

$$D_6 = -\frac{1}{jk_o s \sin\beta_o}\frac{\partial D_h}{\partial \phi}, \tag{8}$$

$$d_s = \frac{1}{jk_o \sin\beta_o}\frac{\partial D_s}{\partial \phi'}, \tag{9}$$

$$d_h = \frac{1}{jk_o \sin\beta_o}\frac{\partial D_h}{\partial \phi'}, \tag{10}$$

$$d_2 = \frac{s\cot\beta_o}{jk_o}\left[\left(\frac{s+s'}{s'}\right)\frac{\partial}{\partial s} - \frac{1}{2s}\right] D_s, \tag{11}$$

$$d_3 = -\frac{s\cot\beta_o}{jk_o}\left[\left(\frac{s+s'}{s'}\right)\frac{\partial}{\partial s} - \frac{1}{2s}\right] D_h \tag{12}$$

and the various geometrical quantities are defined in Figure A.4, except for the partial derivative with respect to distance n which is taken at Q_E in the direction of $\hat{\phi}'$.

While the scalar diffraction coefficients D_s and D_h are of order $k_o^{-1/2}$ outside the transition regions, the new coefficients D_1 to D_6, d_2 and d_3 are of order $k_o^{-3/2}$, as are the slope diffraction coefficients d_s and d_h given earlier [3]. As the frequency decreases the importance of these higher order terms increases, and the importance of these terms is further enhanced for small values of the large parameter κ.

During the period covered by this report an extensive study of the accuracy of the improved UTD solution has been carried out. Numerical results obtained from this solution were compared with those obtained from the rigorous eigenfunction solution [6]. The accuracy of the new solution is found to be very dependent on the wedge angle. In the case of the half plane the improvement is dramatic; κ can be reduced by a factor of 10^3, so that the new solution is valid deep in the paraxial region. For example, β_o may be as small as 1° with s'=2λ; also the soure is clearly very close to the edge in this case. The largest errors occur in diffraction from a 90° wedge, and even for this wedge angle κ can be reduced by at least a factor of 2 to a value of less than one.

A paper describing this work was presented at the 1985 International IEEE/AP-S Symposium in Vancouver, Canada. A written version of this papaer is in preparation.

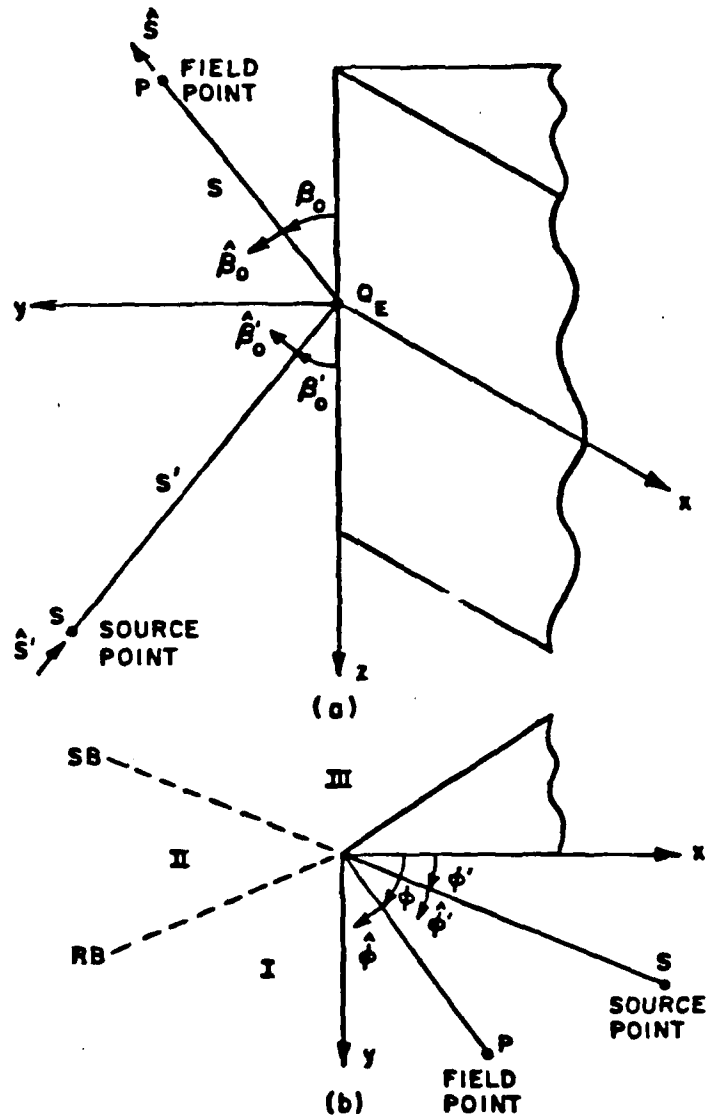

Figure A.4. Geometry associated with the wedge diffraction problem.

(c) The Radiation from Scatterers at the Edge of a Wedge

Work has continued on the radiation from scatterers positioned at the edge of a perfectly-conducting wedge. The type of scattering is interesting because the guiding effect of the edge causes strong interaction between the scatterers, thereby greatly enhancing the scattered field as compared with that of the scatterers in free space. This configuration also can be used to model the scattering from a rough edge.

As a first step, the dyadic Green's function for a conducting sphere at the edge was obtained. For a small sphere, it was observed that the field close to the edge can be approximated by the sum of two terms: the field in the absence of the sphere, and an edge guided wave due to an equivalent point source placed close to the edge at the position of the sphere.

Next, scattering by an irregularly shaped object at the edge was considered. A generalized T-Matrix formulation is used for this case. The incident field is defined as the field in the absence of the scatterer but with the wedge present; it is expanded in terms of a set of spherical vector wave functions which satisfy the boundary condition on the surface of the wedge together with the edge condition. The dyadic Green's function used in this formulation is the one previously obtained for the perfectly conducting wedge (R.G. Kouyoumjian and O.M. Buyukdura, Proceedings of the 1983 International URSI Symposium, Universidad de Santiago de Compostela, Spain, pp. 151-154). It too is expanded in terms of these vector wave functions. Again, for a small scatterer, the field close to the edge is given by the sum of

the field in the absence of the scatterer and an edge wave. The T-Matrix formulation is also used along with a self-consistent method to solve the problem of multiple scatterers located along the edge of the wedge. Numerical results show the enhanced scattering from small objects positioned at the edge of a wedge. Also there is excellent agreement between backscatter cross sections calculated by the self-consistent method with those calculated by the complete modal (T-Matrix) method for the problem in Figure A.5 as is evident in Figure A.6.

A paper describing this work was presented at the 1985 North American Radio Science Meeting held in Vancouver, Canada. A written version of this paper is in preparation.

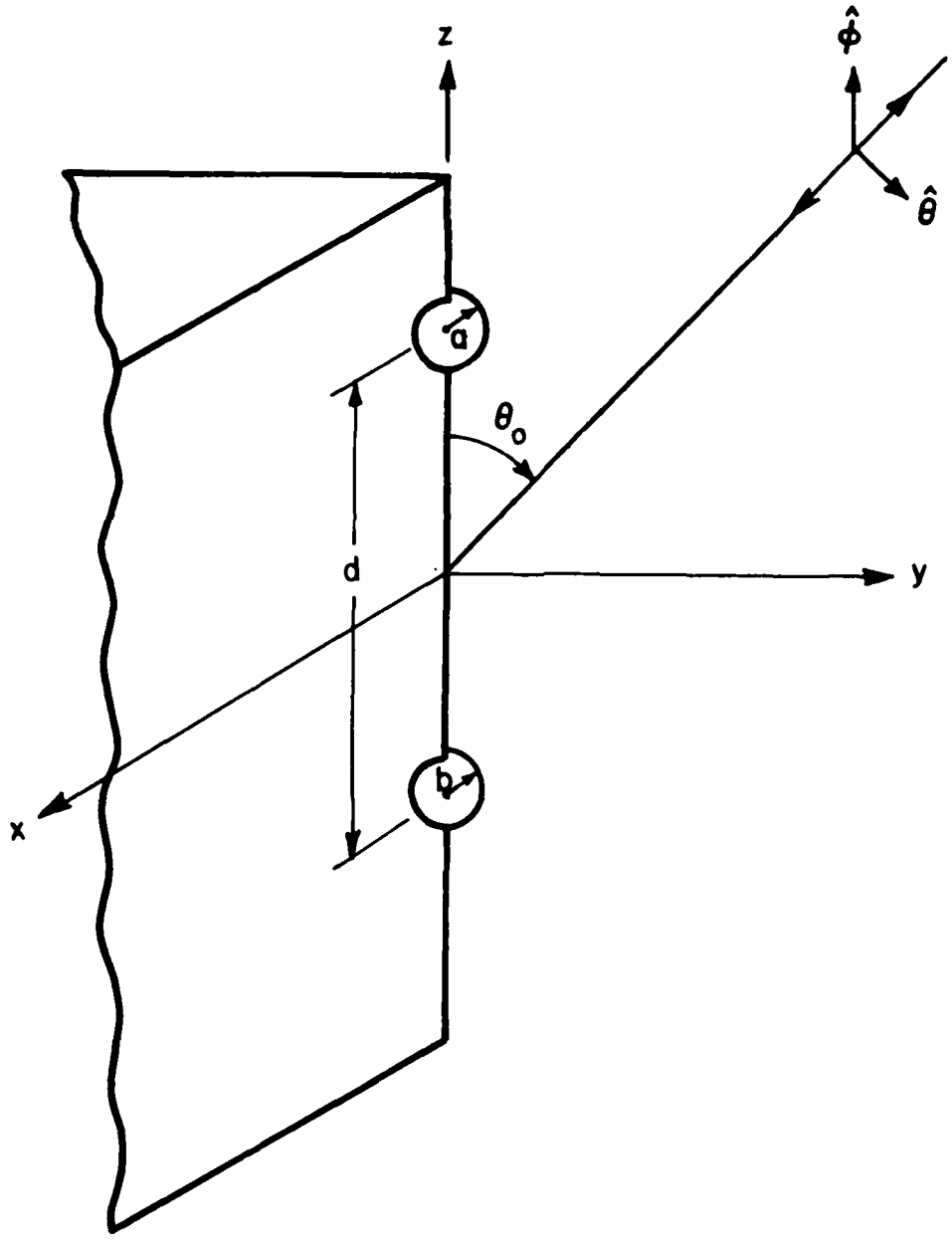

Figure A.5. Scattering by two spheres on a wedge.

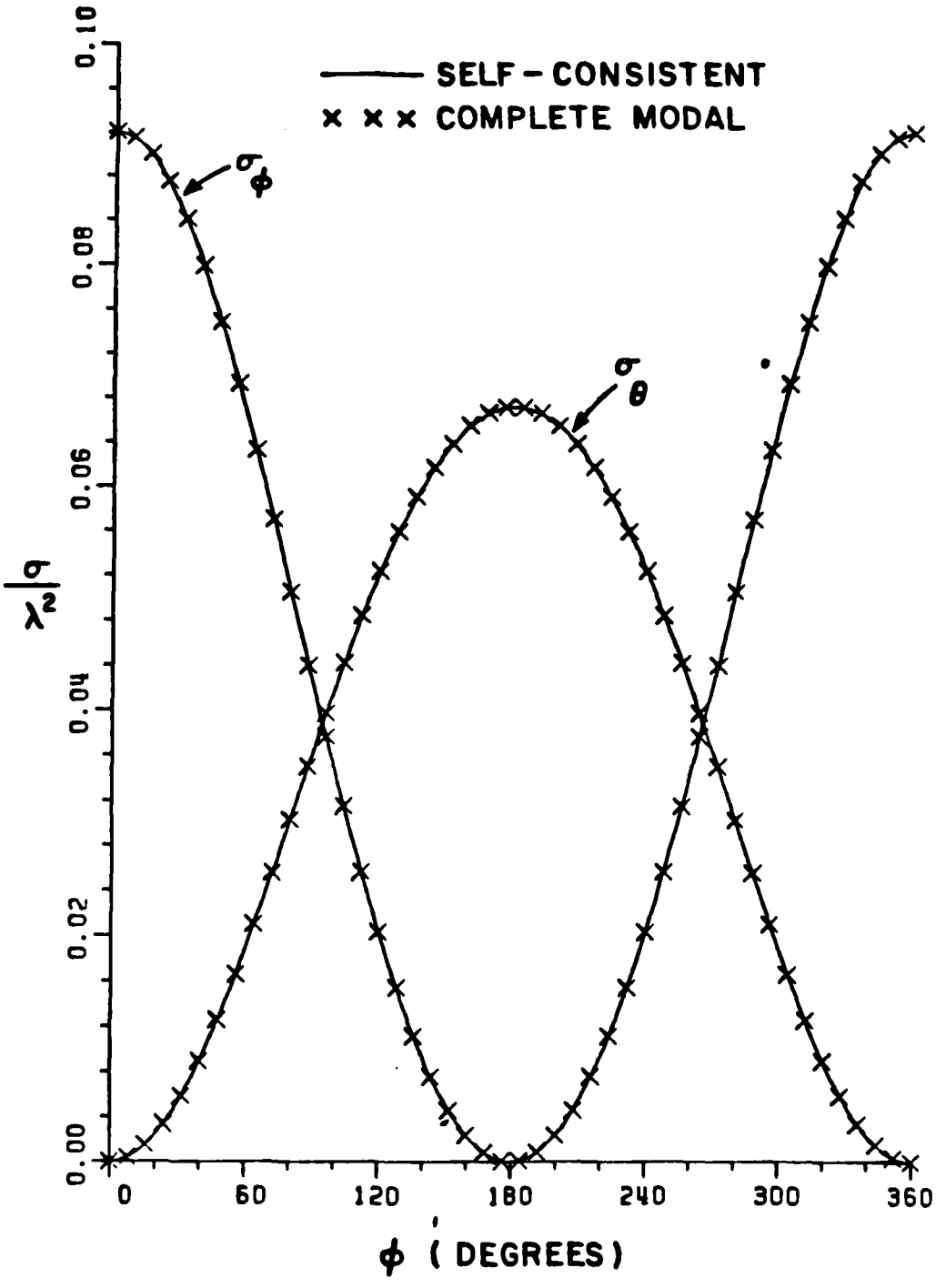

Figure A.6. Backscattering cross-sections σ_θ and σ_ϕ which are associated with two small spheres at the edge of a wedge. $a = n = 0.04\lambda$, $d = 3\lambda$, $\theta_0 = 30°$.

4. Diffraction in the Paraxial Regions of Smooth Quasi-Cylindrical Convex Surfaces

Several papers were written (under the JSEP program) and published [11,12,13] which describe Uniform GTD (UTD) solutions for the diffraction by perfectly-conducting convex surfaces. In particular, efficient UTD solutions for the problems of the radiation from sources both off and on a convex surface and the mutual coupling between sources on a convex surface were presented in [11,12,13]. These UTD solutions, for the problems of scattering, radiation, and mutual coupling, which are associated with the radiation by antennas in the presence of an arbitrary, smooth perfectly-conducting convex surface, represent an important and useful contribution to the area of ray methods for analyzing the EM radiation and scattering from complex structures. It is noted that the effects of surface ray torsion on the diffracted fields are explicitly identified in these solutions. Here, the diffracted fields are associated with surface rays as well as with rays shed from the surface rays. It is noted that these surface rays on a convex surface traverse geodesic paths which in general are torsional; i.e., the surface ray paths are twisted (or they do not lie in a plane).

While the above mentioned UTD solutions for sources on or off a smooth perfectly-conducting convex surface are valid under very general conditions, they must be modified within the paraxial regions. For example, these solutions must be modified for an observation point (either on or off the surface) which lies in the paraxial region of an

elongated or cigar shaped (quasi-cylindrical) convex surface whenever the rays from the source to that observation point traverse paths which lie within the paraxial zone. At the present time, the solution for the surface fields of a source on the convex surface in [13] has been extended so as to include higher order terms which improve the accuracy within the paraxial region of quasi-cylindrical, or elongated convex surfaces. This surface field (or mutual coupling related) solution provides the electric current density which is induced by a source on the same surface. Such a surface current density can be incorporated into the usual radiation integral to find the field radiated by this current; that step has also been performed presently. Thus, the field radiated by the source on the surface has been obtained via an asymptotic high frequency evaluation of the radiation integral containing this surface current density which remains valid in the paraxial zone. The asymptotic evaluation of this radiation integral associated with a general convex surface has been done carefully in order to obtain a simple and useful uniform solution for the radiated field which is not only expected to be valid in the paraxial region but, which also contains all the leading terms of the previous radiation solution of [12]. Work on this paraxial region radiation which has been reported earlier by others, was based on a far less accurate asymptotic evaluation of such radiation integrals associated with a general convex surface, because of a simplifying assumption which is inherent in their work. Our present analysis reveals that such as asymptotic analysis must be done by a different approach which circumvents the inherent approximation present in the previously reported approaches to recover

the leading terms in [12] which are valid outside the paraxial zone. The theoretical solution to the problem of EM radiation in the paraxial zone by sources on a convex surface is presently nearly complete and is now being tested for accuracy by comparison with other independent approaches. When the work on the radiation problem is completed, it will be extended subsequently to deal with the EM scattering within the paraxial regions in almost the same manner as the radiation solution was obtained via an extension of the surface field (mutual coupling related) solution through the use of the appropriate surface currents in the radiation integral.

5. Caustic Field Analysis

The GTD or its uniform version, the UTD, is a very convenient and accurate procedure for analyzing high frequency radiation, scattering, and diffraction phenomena. However, the GTD/UTD suffers from a limitation inherent in ray methods; namely, it cannot be employed directly to evaluate fields at and near focal points or caustics of ray systems. The fields at a caustic must, therefore, be found from separate considerations [14,15].

In certain problems such as in the diffraction by smooth, closed convex surfaces or by surfaces with a ring-type edge discontinuity, it is possible to employ the GTD indirectly to evaluate the fields in the caustic regions via the equivalent ring current method [16,17]. However, even the equivalent ring current method fails if the incident or reflection shadow boundaries are near or on a caustic.

The recently developed uniform G.[illegible] (or UTD) solution for the scattering and diffraction of waves by a convex surface [11] offers clues as to how it may be employed indirectly to obtain the far zone fields in caustic regions where the surface is illuminated by a distant source. In the latter case, the shadow boundary and caustic transition regions tend to overlap. The far zone fields in the near axial direction of a closed surface of revolution illuminated by an axially directed plane wave can be expressed in terms of an equivalent ring current contribution plus a dominant term which may be interpreted as an "effective aperture integral". The latter integral can be evaluated in closed form for surfaces of revolution with on-axis illumination. This work will be described in a paper which will be prepared in the near future. The generalization of that solution to treat non-axial incidence and also closed convex surfaces which are not necessarily surfaces of revolution would form the subject of future investigation.

Another related and interesting problem which is presently under study involves the analysis of high frequency electromagnetic diffraction by perfectly conducting planar surfaces (or plates) with an edge contour which has a smooth convex boundary. The planar face of the plate gives rise to caustic effects. For certain aspects, the caustic and specular reflection directions can coincide so that a direct use of UTD becomes invalid. The present study is aimed at determining a proper modification of the UTD so that a new and efficient equivalent current method can be used in these situations. Away from the caustic and confluence of caustic and specular directions, the modified UTD solution

must reduce to the conventional GTD solution. At the present time, a study of this difficult problem has revealed that the equivalent currents obtained from a purely asymptotic analysis exhibit spurious singularities at certain aspects. Consequently, a better description for the equivalent currents is essential; approaches are being investigated to achieve such a description.

Recently work has been initiated to analyze the RCS of rotationally symmetric bodies which are characterized by a pair of inflexion points on the generator of that surface (e.g., as for a body shaped like a peanut shell). Consequently, the shadow boundary of reflected geometrical optics field coincides with the caustic of the reflected rays. A uniform asymptotic solution is being obtained for this problem for angles of incidence away from grazing at the points of inflexion; preliminary results are very encouraging.

Diffraction by Non-Conducting Surfaces

(a) Smooth Dielectric Covered and Impedance Convex Surface

A study of the electromagnetic scattering and radiation from a conducting surface with dielectric loading is of great interest in that it provides an understanding of the effects, due to the loading, on the electromagnetic scattered fields. There is also an emphasis in the design of second generation air-borne vehicles to achieve maximum radar cross section (RCS) reduction by fabricating the structure from radar absorbing material. Therefore, there is a strong need for an analytical tool to predict the electromagnetic scattered field from a dielectric-loaded conducting surface. Although an efficient, approximate uniform GTD solution has been obtained for the electromagnetic scattering from a smooth, perfectly-conducting convex surface [18,19], no such solution exists for a conducting surface covered with dielectric material.

As a first step leading to the problem of scattering from a dielectric coated circular cylinder, we study the electromagnetic scattering from a circular cylinder with a constant surface impedance bounbdary condition. It is known that for a thin dielectric coating on a conducting surface, the surface impedance model is a useful and convenient approximation.

We have developed an approximate UTD solution for the electromagnetic scattering from a circular cylinder with a constant surface impedance (an impedance cylinder). The solution is convenient for engineering application due to its simple ray format. The ray paths associated with the solution for the perfectly-conducting cylinder [18] remain unchanged for the impedance cylinder. The UTD solution is uniform in the sense that it is valid in the transition regions adjacent to the shadow boundaries where the pure ray-optical solution fails, and it reduces to the GTD solution in terms of the incident, reflected, and surface diffracted rays exterior to the transition regions. Numerical values for an essential transition function

$$e^{-j\frac{\pi}{4}} p^*(x,q) \triangleq \frac{e^{-j\pi/4}}{\sqrt{\pi}} \int_{-\infty}^{\infty} \frac{V'(t) - qV(t)}{W_1'(t) - qW_1(t)} e^{-jxt} dt + \frac{e^{-j\frac{\pi}{4}}}{2x\sqrt{\pi}} \tag{1}$$

is deduced, via a heuristic approach, from alternative representations of the Green's functions for an impedance cylinder. The functions V_1, W_1, are the usual Airy functions (e.g., Ref. [18]). Figure A.7 presents some typical examples of the transition functions for various values of q.

The transition integral is then employed to calculate the electromagnetic field scattered from a circular impedance cylinder. Figure A.8 illustrates the geometry of the problem. The two-dimensional line source is located at $Q'(\rho_1', \phi' = 0°)$, and the reciever is located at $P(\rho_1, \phi)$. For the electrical line source excitation, the pattern is

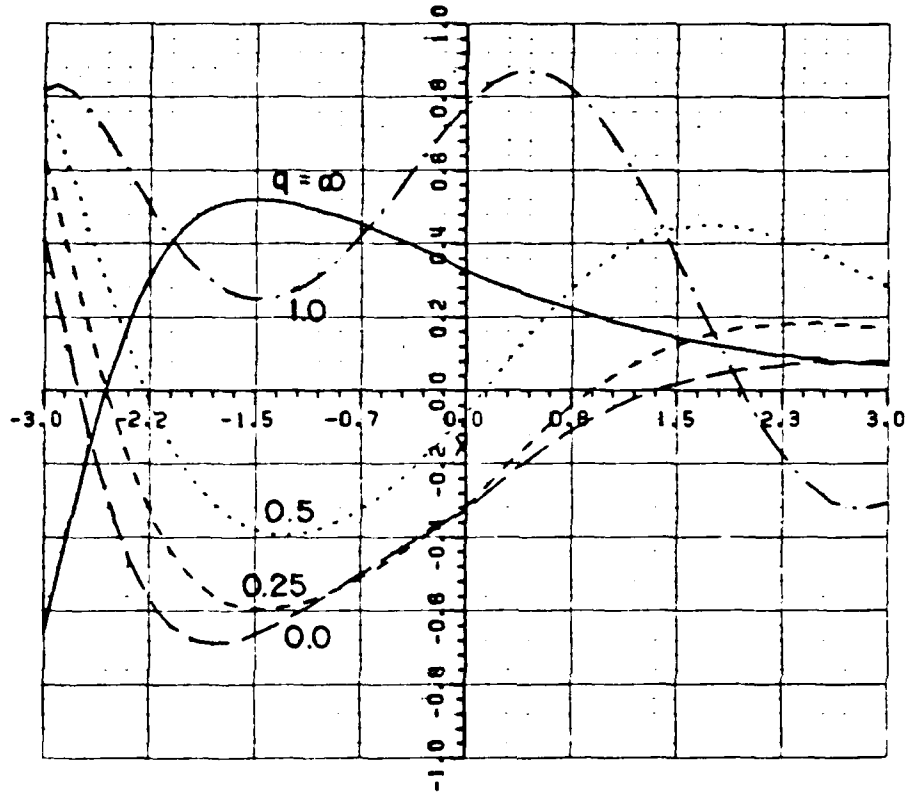

(a) The real part of $e^{-j\pi/4}p^*(x,q)$

Figure A.7. The transition integral $e^{-j\pi/4}p^*(x,q)$.

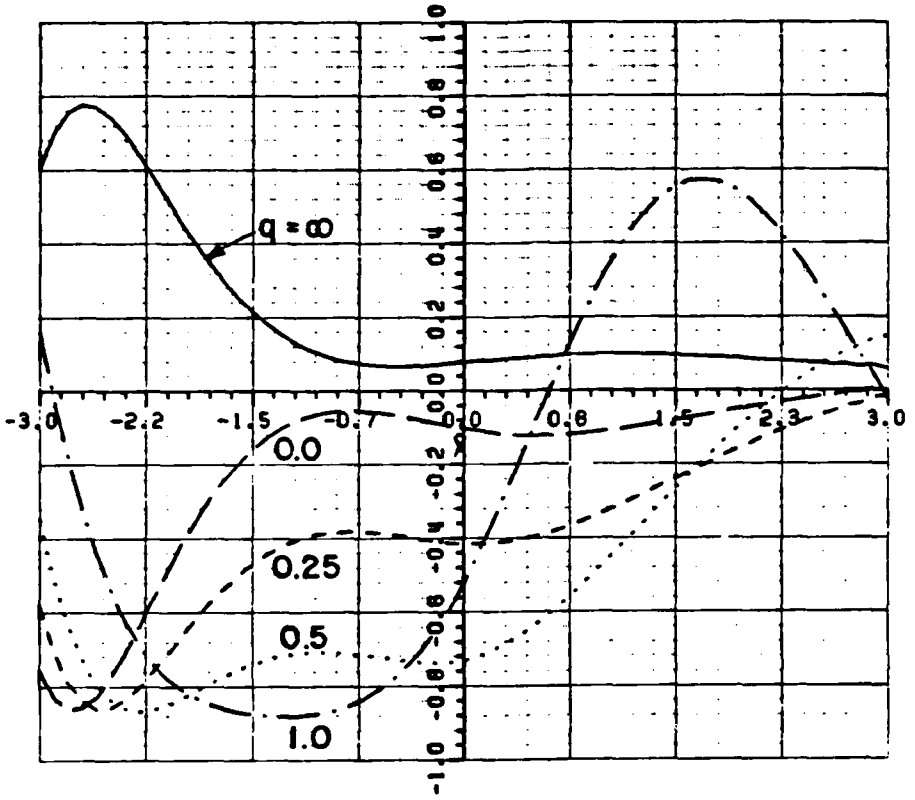

(b) The imaginary part of $-e^{-j\pi/4}p^*(x,q)$

Figure A.7. (continued)

plotted for the total electric field intensity E_z, and for the magnetic line source excitation, the pattern is shown for the total magnetic field intensity H_z. For numerical calculations, the strength of the line source is normalized such that the direct incident field is given as $e^{-jkR}/\sqrt{kR}$, where R is the distance between the source and the receiver.

As shown in Figure A.8, the asymptotic UTD solutions employ two ray paths, one is $Q'Q_1Q_2P$ and the other one is $Q'Q'_1Q'_2P$. For the situation shown in Figure A.8b, the ray path $Q'Q_1Q_2P$ is replaced by the path $Q'Q_RP$, where Q_R is the specular reflection point defined by $\theta_i=\theta_r$. Figures A.11 to A.12 illustrate some examples for the total field surrounding the circular cylinder with a constant surface impedance. Here q is equal to $-j(\frac{ka}{2})^{1/3}\bar{c}$, and $\bar{c}$ is the normalized surface impedance. The eigenfunction results are shown as the solid curves and the results obtained from the UTD solution are shown as the dashed curves. It is seen that the agreement is excellent. It should be mentioned that all the UTD results are obtained using the transition integral shown in Figure A.7.

As a continuation of the study on the impedance cylinder, we propose to investigate the electromagentic bistatic scattering from a circular cylinder with dielectric coating with a plane wave at normal incidence.

A high frequency GTD solution has been developed (under JSEP support) for the backscattering from a dielectric-coated circular cylinder [20]. However, for the bistatic scattering case, the

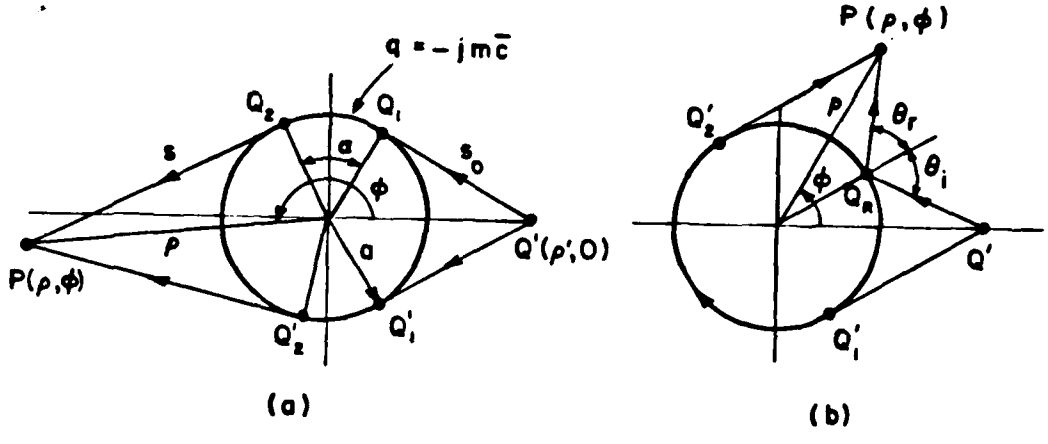

Figure A.8. Ray paths employed for the UTD solution, $x=(ka/2)^{1/3}\alpha$.

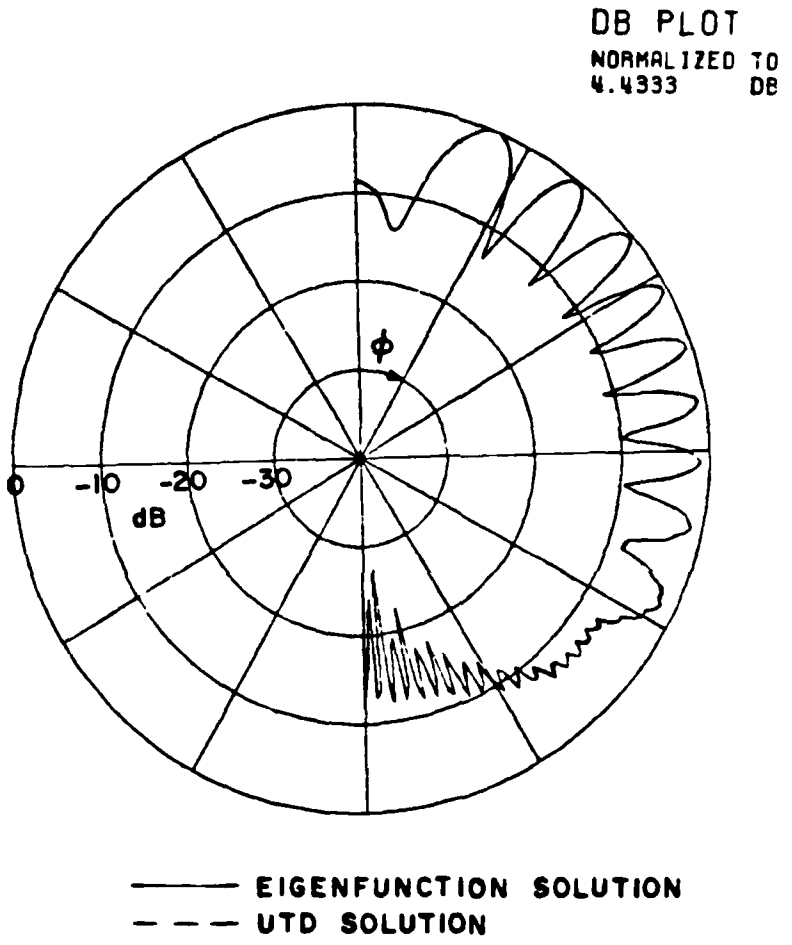

Figure A.9. Total field surrounding the circular cylinder excited by a line source. ka=50, kρ'=80, kp→∞, q=0.5.

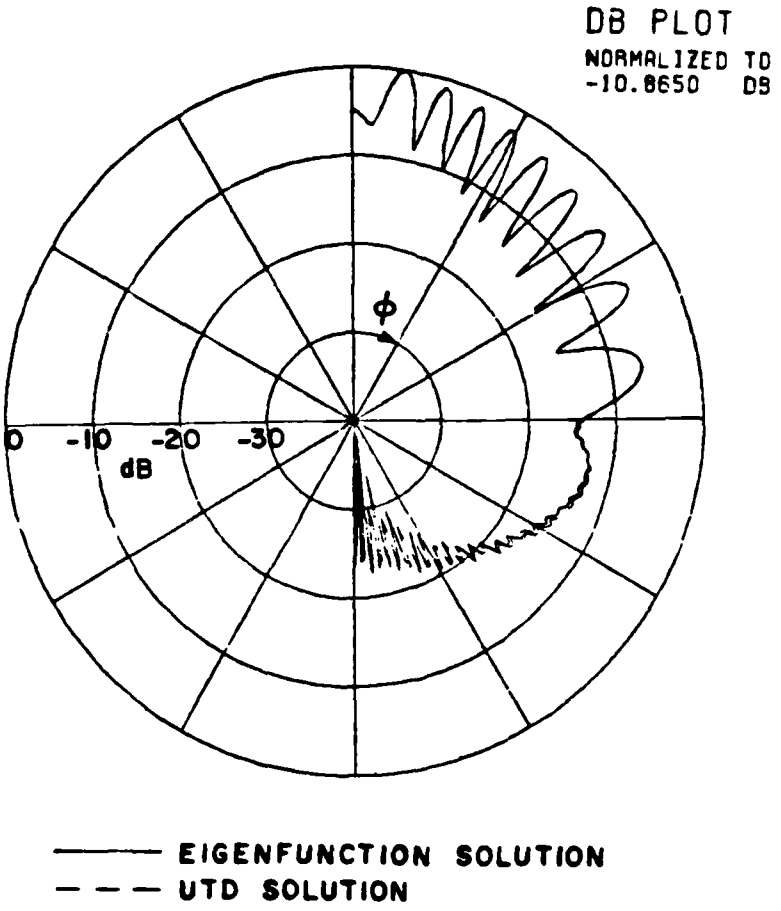

Figure A.10. Total field surrounding the circular cylinder excited by a line source. ka=50, kρ'=80, kρ=100, q=0.5.

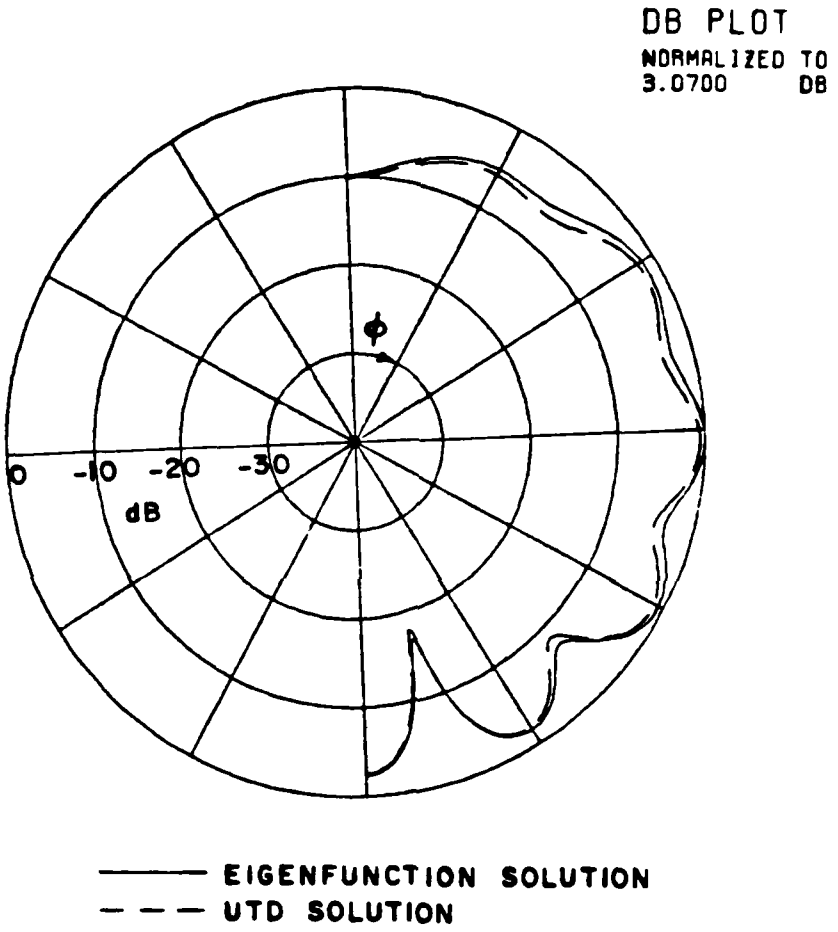

Figure A.11 Total field surrounding the circular cylinder excited by a line source. ka=5, kρ'=6, kρ=→∞, q=0.5.

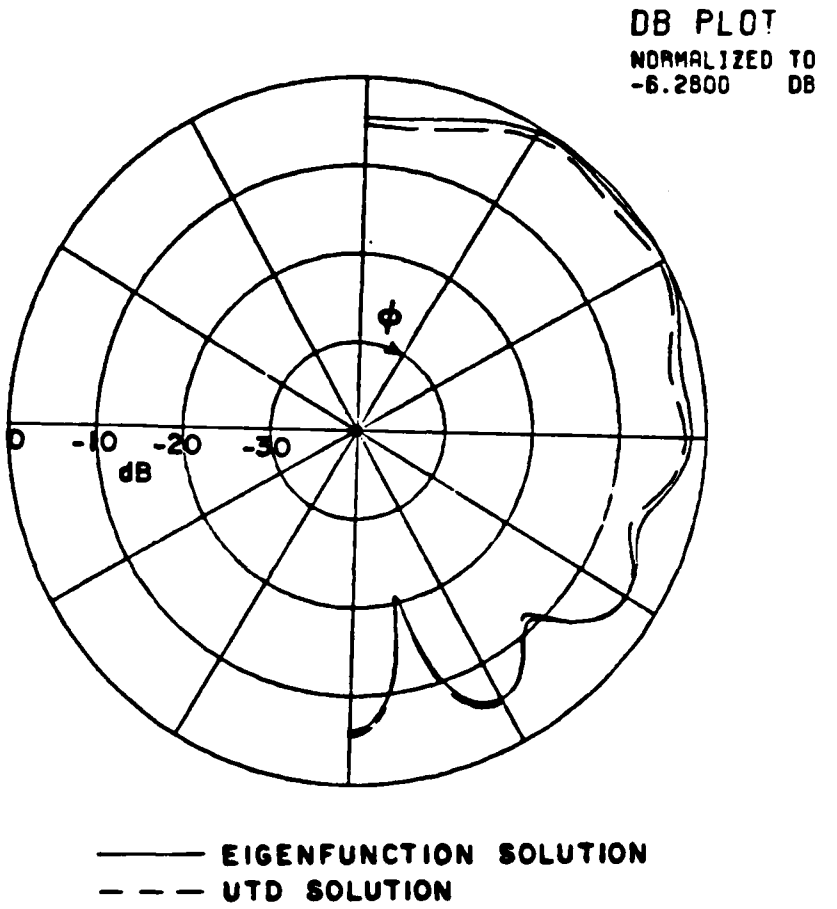

Figure A.12. Total field surrounding the circular cylinder excited by a line source. ka=5, kρ'=6, kρ=10, q=0.5.

challenging task of deriving the transition function remains to be pursued. It is anticipated that a UTD solution similar to the one for the impedance cylinder could be obtained. And it is hoped that the ray paths shown in Figure A.8 will be valid for the coated cylinder. It is recalled that, for the impedance cylinder case, the transition integral $p^*(x,q)$ is a function of two parameters. The parameter q characterizes the impedance cylinder via the normalized surface impedance. On the other hand, the characteristics of the coated cylinder depends upon the thickness of the coating, and the relative permittivity and permeability of the dielectric coating. Therefore, one needs to investigate whether it is possible to characterize the coated circular cylinder with one universal parameter such as the "q" employed for the impedance cylinder. Preliminary study seems to suggest that it is indeed possible, at least for the thin coating case, to define a q parameter to characterize the coated circular cylinder. This task together with developing the UTD solution for the coated cylinder will be pursued in the future.

The electromagnetic characteristic associated with the creeping waves supported by a dielectric coated cylinder are investigated. The propagation constants and wave impedances of the creeping waves are obtained numerically. Higher order modes which are significant for a thick coating are also investigated. The propagation constants and creeping wave modal impedance are compared with those obtained for a planar dielectric slab backed by a ground plane. It is found that, contrary to the planar configuration, no cutoff frequencies exist for

the creeping waves associated with the coated cylinder. In fact, the coated cylinder supports an infinite number of modes. However, depending upon the thickness of the coating, only a few Elliott-type creeping wave modes with low attenuation can exist. Furthermore, for each of the Elliott-type creeping waves, there is a corresponding, critical radius for the coated cylinder, below which the Elliott-type creeping wave cannot exist. Some typical results for the propagation constants and modal impedances of the creeping waves for the coated circular cylinder are illustrated in Figures A.13 to Figure A.16. Detailed analysis and more numerical results can be found in Pakny's dissertation [21].

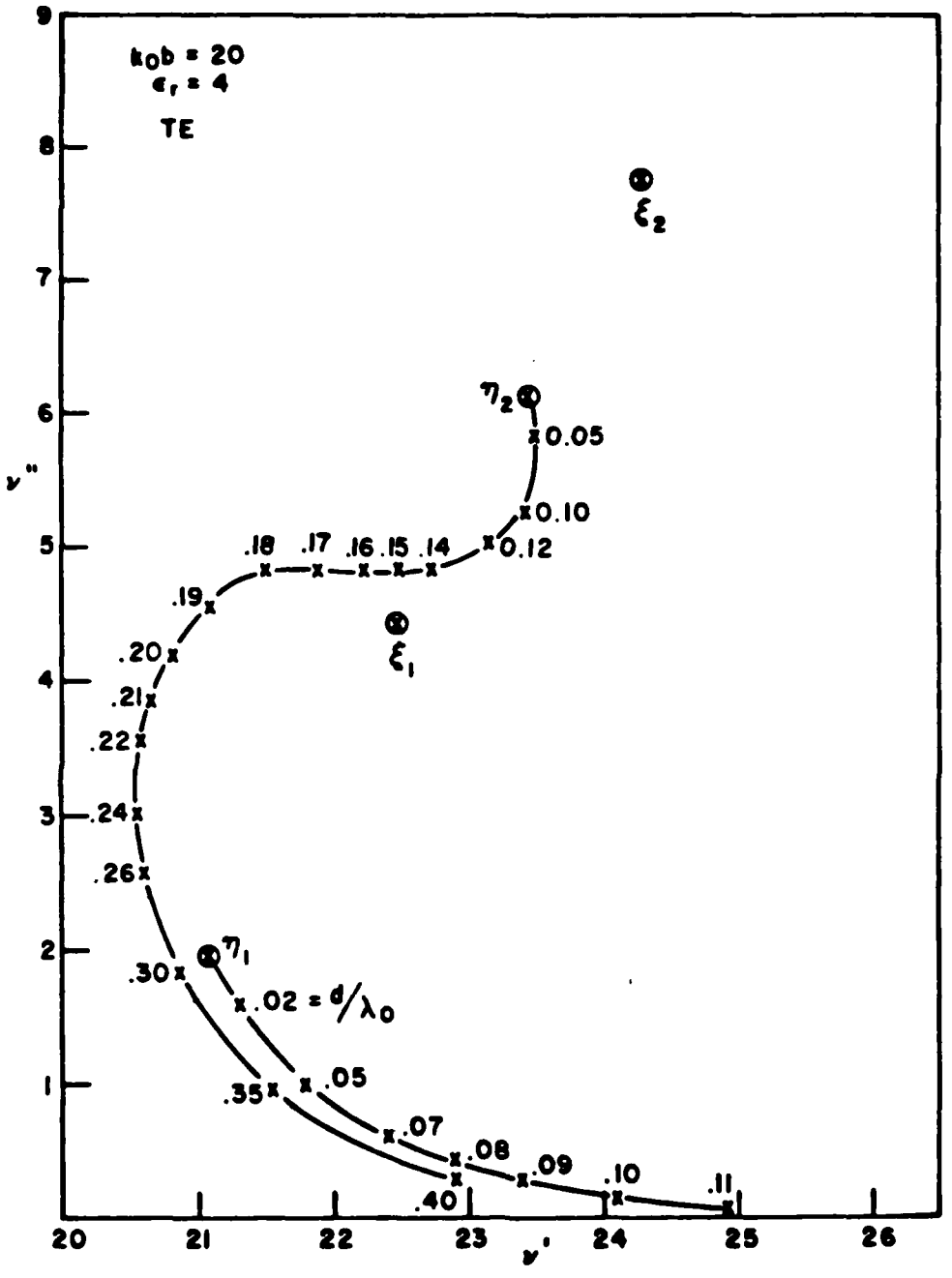

Figure A.13 TE azimuthal propagatoin constants for the coated cylinder.

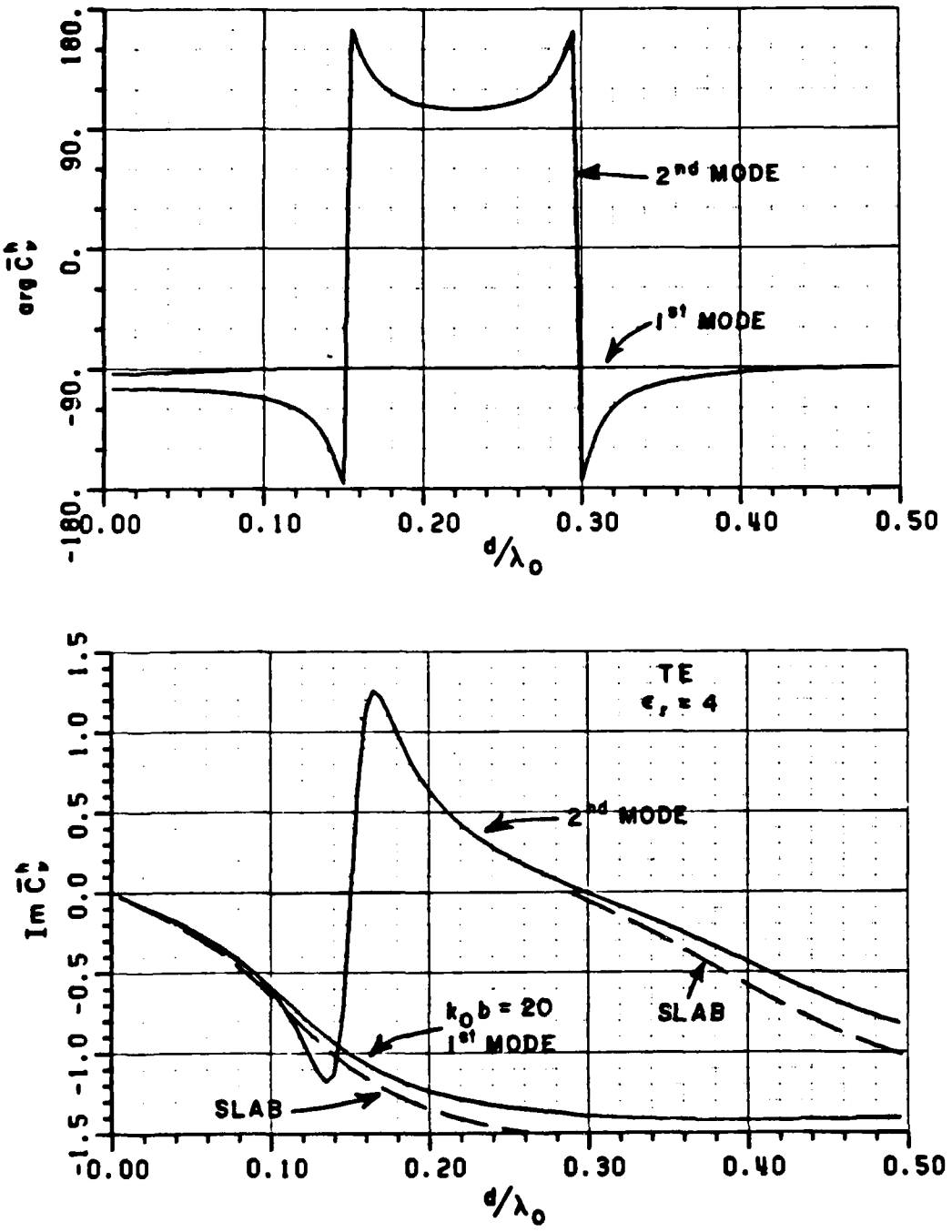

Figure A.14. Impedance function associated with the first two TE modes.

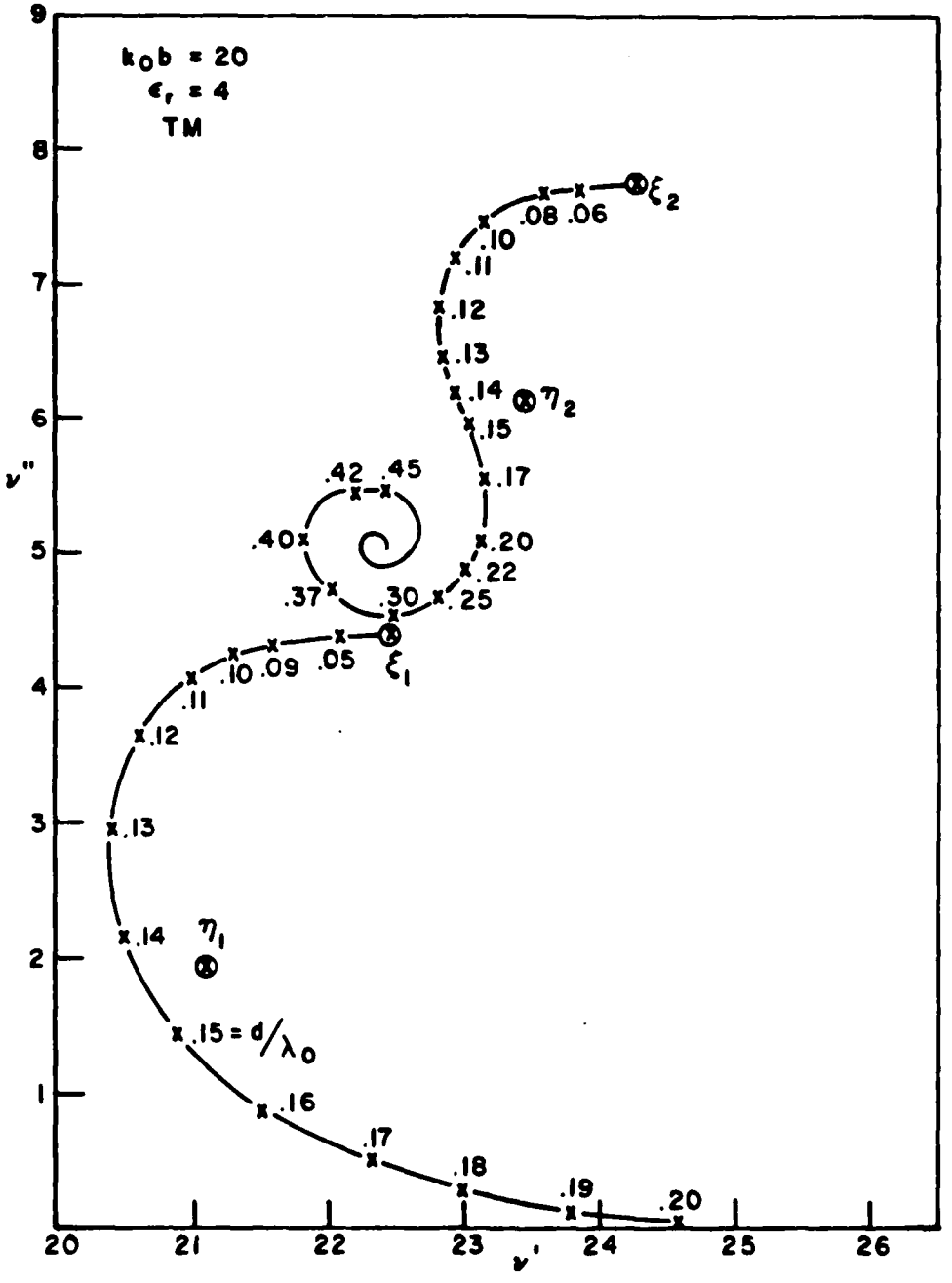

Figure A.15. TM azimuthal propagation constants for the coated cylinder.

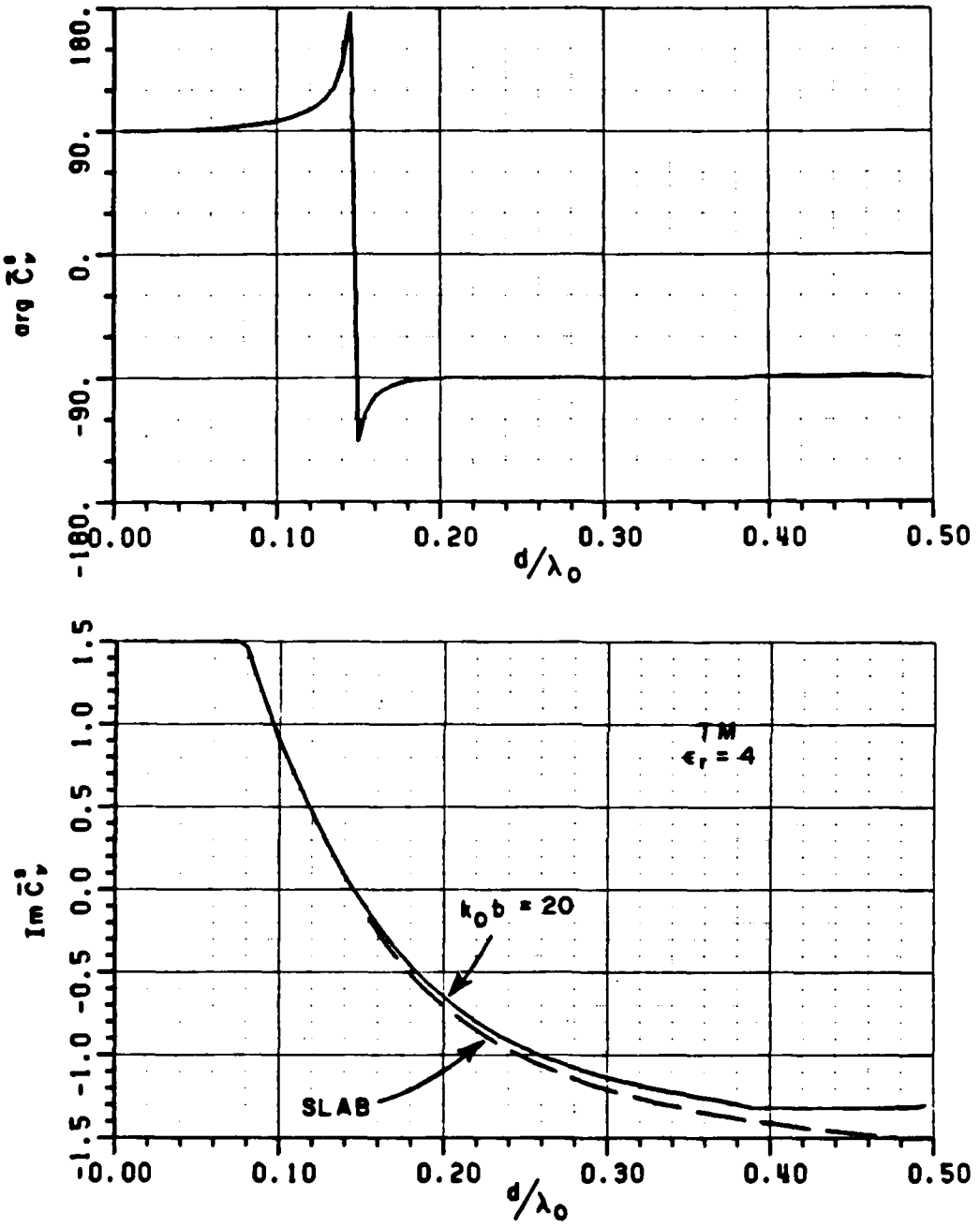

Figure A.16. Admittance function associated with the first TM mode.

REFERENCES

[1] Maliuzhinets, G.D., "Excitation, Reflection and Emission of Surface Waves from a Wedge with Given Face Impedances", Sov. Phys. Dokl., 3(4), pp. 752-755, 1959.

[2] Kouyoumjian, R.G. and P.H. Pathak, "A Uniform Geometrical Theory of Diffraction for an Edge in a Perfectly-Conducting Surface", Proc. IEEE, Vol. 62, pp. 1448-1461, 1974.

[3] Kouyoumjian, R.G., P.H. Pathak, and W.D. Burnside, "A Uniform GTD for the Diffraction by Edges, Vertices, and Convex Surfaces", 65 pages in Theoretical Methods for Determining the Interaction of Electromagnetic Waves with Structures, ed., J.K. Skwirzynski, Sijthoff and Noordhoff, Netherlands, 1981.

[4] Burnside, W.D. and P.H. Pathak, "A Corner Diffraction Coefficient', to be published.

[5] Satterwhite, R. and R.G. Kouyoumjian, "Electromagnetic Diffraction by a Perfectly-Conduting Plane Angular Sector", Report 2183-2, 1970, The Ohio State University ElectroScience Laboratory, Department of Electrical Engineering; prepared under Contract AF 19(628)-5929 for Air Force Cambridge Research Laboratories.

[6] Kouyoumjian, R.G. and O.M. Buyukdura, "Paraxial Edge Diffraction", 1983 International URSI Symposium held 23-26 August at Santiago de Compostela, Spain.

[7] Buyukdura, O.M., "Radiation from Sources and Scatterers Near the Edge of a Perfectly-Conducting Wedge", Ph.D. Dissertation, The Ohio State University, 1984.

[8] Tiberio, R. and R.G. Kouyoumjian, "A Uniform GTD Solution for the Diffraction by Strips Illuminated at Grazing Incidence", Radio Science, Volume 14, pp. 933-941, 1979.

[9] Tiberio, R. and R.G. Kouyoumjian, "Calculation of the High-Frequency Diffraction by Two Naerby Edges Illuminated at Grazing Incidence", IEEE Trans. Antennas and Propagation, Vol. 32, Nov. 1984.

[10] Tiberio, R. and R.G. Kouyoumjian, "An Analysis of Diffraction at Edges Illuminated by Transition Region Fields", Radio Science, Vol. 17, pp. 323-336, 1982.

[11] Pathak, P.H., W.D. Burnside and R.J. Marhefka, "A Uniform GTD Analysis of the Scattering of Electromagnetic Waves by a Smooth Convex Surface", IEEE Transactions on Antennas and Propagation, Vol. AP-28, No. 5, September 1980, pp. 631-642.

[12] Pathak, P.H., N.N. Wang, W.D. Burnside and R.G. Kouyoumjian, "A Uniform GTD Solution for the Radiation from Sources on a Perfectly-Conducting Convex Surface", IEEE Transacations on Antennas and Propagation, Vol. AP-29, No. 4, July 1981, pp. 609-621.

[13] Pathak, P.H. and N.N. Wang, "Ray Analysis of Mutual Coupling Between Antennas on a Convex Surface", IEEE Transactions on Antennas and Propagation, Vol. AP-29, No. 6, November 1981, pp. 911-922.

[14] Kay, I. and J.B. Keller, "Asymptotic Evaluation of the Field at a Caustic", J. Appl. Physics, Vol. 25, No. 7, pp. 876-886, July 1954.

[15] Ludwig, D., "Uniform Asymptotic Expansions at a Caustic", Commun. Pure Appl. Math, 19, pp. 215-250, 1966.

[16] Burnside, W.D. and L. Peters, Jr., "Radar Cross Section of Finite Cones by the Equivalent Current Concept with Higher Order Diffraction", J. Radio Science, Vol. 7, No. 10, pp. 943-948, October 1972.

[17] Knott, E.F. and T.B.A. Senior, "A Comparison of Three High-Frequency Diffraction Techniques", Proc. IEEE, Vol. 62, No. 11, pp. 1468-1474, November 1974.

[18] P.H. Pathak, "An asymptotic analysis of the scattering of plane waves by smooth convex cylinder", Radio Science, V-14, No. 3, May-June 1979.

[19] P.H. Pathak, W.D. Burnside and R.J. Marhefka, "A uniform GTD analysis of the diffraction of electromagnetic waves by a smooth convex surface", IEEE Trans. on Antennas and Propagation, AP-28, No. 5, September 1980.

[20] N. Wang, "Electromagnetic scattering from a dielectric coated circular cylinder", IEEE Trans. on Antennas and Propagation, Vol. AP-33, No. 9, September, 1985.

[21] R. Paknys, "High frequency surface fields excited by a line source on a dielectric coated cylinder", Ph.D. Dissertation, The Ohio State University, ElectroScience Laboratory, Dept. of Electrical Engineering, Cols., Ohio, Winter 1985.

B. HYBRID TECHNIQUES

Researchers: P.H. Pathak, Assistant Professor
(Phone: 614/422-6097)

C.D. Chuang, Senior Research Associate
(Phone: 614/422-5851)

S. Barkeshli, Graduate Research Associate
(Phone: 614/422-2530)

I. Choi, Graduate Reserach Associate
(Phone: 614/422-5754)

J. Lyons, Graduate Research Associate
(Phone: 614/422-5040)

Introduction

Hybrid techniques constitute a very powerful procedure for extending the capabilities of more specialized analytic tools by combining the best features of each individual tool. Indeed, hybrid techniques are being employed to analyze the electromagnetic scattering by important geometries such as cavities and cracks. Here, cavities could be shallow and wide as in the case of antenna cavities, or they could be shallow and thin as in the case of a notch; furthermore, they could be deep as in the case of jet inlets. The analysis of such configurations are rather complex as they involve a coupling of the exterior incident field into the interior and the re-radiation of that interior field back into the exterior after it has undergone multiple wave reflections between the open front end of the cavity and the termination at the back end of the cavity. If the latter termination is

removed, then the cavity which is now open at the front and the back ends reduces to a crack through which part of the incident energy can be transmitted. The treatment of cracks and notches was initiated under JSEP and then picked up mostly by other funding sources which are also supporting the analysis of antenna and inlet cavities. In fact, research on cavity scattering is a natural extension of the research on crack scattering. Electromagnetic scattering by cracks and notches is mentioned here because of their great importance to DOD. The cracks are created by doors and other openings in aerospace vehicles; they become dominant scatterers when all the other scattering mechanisms have been reduced. Likewise, the antenna and jet inlet cavities can also be significant scatterers whose effects must be included when analyzing the radar cross section of modern aerospace vehicles. In the analysis of cracks and notches which was initiated under JSEP, an integral equation was formulated for the unknown equivalent magnetic currents only in the aperture at the open front end, and this integral equation was solved numerically via the method of moments. The generalized scattering matrix was then employed to couple these aperture fields to the interior waveguide region in a simple and efficient way which automatically accounted for either a short circuit termination at the back end corresponding to a notch, or an open circuit termination corresponding to a crack. Furthermore, utilizing the concept of equivalent currents it was possible to directly extend these solutions for the two-dimensional crack/notch problems to the corresponding three-dimensional solutions for cracks/notches of finite length.

Obviously, the hybrid technique can combine a variety of methodologies. For example, in the analysis of the scattering by inlet cavities, the geometrical theory of diffraction (GTD) can be used to analyze the part of the field which is scattered by just the open front end; whereas, the GTD, the equivalent current method (ECM), or a modification of the physical theory of diffraction (PTD) can be employed to efficiently calculate the various generalized scattering matrices associated with the reflections and radiation of the modes coupled into the interior cavity region. It is important to note that the high frequency techniques (such as GTD, ECM, or PTD) provide information in a rather simple way on the waveguide modes coupled into the cavity from the external incident field, and also on the modes reflected back and forth between the front and back ends of the cavity, as well as on the re-radiation of the interior modes from the front end after they have undergone these multiple reflections. In contrast, conventional solutions based on a classical mode matching procedure would have proven to be very inefficient and cumbersome in dealing with the inlet problem. Scattering by cracks and cavities are but only two examples which are being treated by the hybrid procedure. It should be noted that the hybrid techniques discussed above are distinct from the integral equation solutions being developed by Newman and Richmond (see later sections) who use a special Green's function and physical basis functions, respectively. The following paragraphs discuss the various hybrid techniques that have been introduced under these studies.

The method of moments (MM) provides a means of generating electromagnetic boundary value solutions in terms of a set of simultaneous linear equations. In general, the electromagnetic boundary value solution is formulated as an integral equation for the unknown surface fields on the antenna or scatterer and the integral equation is then reduced to a system of equations by expanding the unknown in terms of a basis set and by enforcing the resulting equation to hold true in some average sense through the use of testing functions. However, the MM procedure can become inefficient and cumbersome if the number of unknowns (coefficients of the expansion of basis functions) becomes large as is the case for antennas or scatterers which are not small in terms of wavelength. On the other hand, the geometrical theory of diffraction (GTD) exploits the local nature of high frequency wave propagation, diffraction and radiation, thereby reducing the antenna radiation or scattering problem to calculating the fields associated with just a few rays emanating from edges, tips, and shadow boundaries (of smooth convex surfaces), and also from other discontinuities in the geometrical and electrical properties of the antenna or scatterer. Although the GTD is a high frequency technique, it works rather well, even for structures which are only moderately large in terms of the wavelength. However, the use of the GTD is limited by the number of available diffraction coefficients for characterizing a particular type of electrical and/or geometrical discontinuity. It is obvious that a procedure is desirable which would overcome the limitations of the individual MM and GTD approaches enumerated above. Such a procedure,

referred to as the "hybrid" GTD-MM procedure, can indeed overcome the limitations of the individual MM and GTD approaches by actually combining the best features of both methods. The hybrid GTD-MM (or MM-GTD) procedure may be classified into at least three basic types as indicated below:

(i) In the first type of hybrid GTD-MM approach, the GTD provides the form of the local field over any part of the antenna or scattering structure, which is at least moderately large in terms of the wavelength; hence, the form of the GTD field could be viewed as a set of basis functions for the expansion of the unknowns in the MM formulation. The unknown coefficients associated with this type of GTD basis or expansion functions are then the diffraction coefficients for the surface field calculations if the unknown in the integral equation happens to be the surface field. Thus, by using the local GTD field form outside the region where the structure is small in terms of the wavelength, the number of unknowns is thereby vastly reduced in the MM procedure. The expansion for the unknown within regions (of the structure) which are small in terms of wavelength can of course be done according to the conventional MM approach (perhaps using a subsectional basis set such as rectangular pulses, etc). This type of approach was originally introduced at The Ohio State University by Burnside et al. [1].

Examples where this first type of hybrid GTD-MM approach was used previously on the JSEP contract happened to deal with an analysis of the diffraction by a discontinuity in curvature, and by a perfectly-

conducting half-cylinder. This type of approach is useful in obtaining a numerical diffraction coefficient for situations where an analytical diffraction coefficient is not available; also, it can provide a useful check on future diffraction coefficients as and when they become available.

(ii) In the second type of hybrid GTD-MM approach, the GTD provides a fully known asymptotic high frequency approximation to a "special" Green's function which constitutes the kernel of the integral equation for the unknown actual or equivalent currents. The unknown currents in this approach exist only over those regions of the source and/or scatterer which are not accounted for by the "special" Green's function. The unknown currents can then be solved via the conventional MM procedure as done at The Ohio State University by Thiele and Newhouse [2] who introduced this type of GTD-MM approach. In [2], Thiele and Newhouse essentially employed the GTD Green's function for a circular disc (using the edge diffraction coefficient) to find the current distribution on an excited monopole antenna which was positioned over that conducting circular disc. Later, Thiele and Eckelman [3], and Thiele and Henderson [4] solved for the currents on an excited wire antenna which radiated in the presence of conducting circular and elliptic cylinders, respectively. Again, if the disc, and the cylinders in [3] and [4] are large in terms of the wavelength, then the use of the GTD Green's functions for these electrically large structures allows a significant reduction of the unknowns in the MM procedure as the unknown currents are now confined only to the wire antennas and not to the rest

of the electrically large structure. Such a type of hybrid GTD-MM procedure is currently being employed to obtain an efficient numerical solution to the microstrip antenna (or antenna array) configuration; in this case, an asymptotic microstrip Green's function is being sought so that the only unknowns in this case reside on the electrically small conducting microstrip patch. The "special' microstrip Green's function accounts for the complete effect of the rest of the grounded substrate on which the microstrip patch resides.

It is noted that in this second type of hybrid GTD-MM approach, one may also employ an exact form of the "special" Green's function (rather than an asymptotic/GTD approximation) if it is available, and if it is not too cumbersome for numerical computations as compared to its asymptotic/GTD approximation which is generally far simpler to use.

(iii) A third type of hybrid GTD-MM approach can involve a combination of the first two types. For example, one might be able to employ a special Green's function in the integral equation formulation to reduce the extent of the region over which the unknown current has to be evaluated. This special Green's function may be used either in its exact form if it is available or in it's approximate (asymptotic) form if the exact form is numerically cumbersome to use. Up to this point, such a procedure is of type (ii); however, if the region over which the unknown is to be evaluated is electrically large even after a special Green's function is employed (to account for the remaining electrically large structure), then one may be able to employ local GTD type basis functions over most of this region of the currents to reduce the number

of unknowns according to the type (i) approach. Thus, the idea present in both types of approaches are employed in this type (iii) approach. Previously, the problem of EM scattering by cracks and notches in perfectly conducting surfaces was studied under the JSEP contract (with some additional funding from Rockwell and PMTC); in time however, most of the support for this type of work was picked up primarily by AFOSR, so that it is now being continued only with a minimal support from JSEP. Indeed, the scattering by dielectric loaded antenna cavities in conducting surfaces is the main topic of this AFOSR sponsored research; this is a natural extension of the work initiated on the scattering by cracks and notches under JSEP. The EM scattering by shallow open ended cavities in perfectly-conducting surfaces in which the cavities may be large or small (e.g., as in the case of a notch or a crack) is being analyzed via this type (iii) approach. The unknown equivalent current exists only in the aperture of the open face of the cavity after using special Green's function (as in the type (ii) hybrid GTD-MM approach). For small cavities with a width (as in the notch case), it has been found that basis functions which satisfy the edge conditions (rather than GTD type basis functions) must be used. For cavities with a large width, other GTD type basis functions do well (as is the case in the type (i) hybrid GTD-MM approach).

While the hybrid GTD-MM procedure will in general be employed to essentially obtain diffraction coefficients numerically, other hybrid techniques which combine high frequency methods and numerical methods different from the MM procedure will also be studied as is being done

for instance in the analysis of scattering by jet inlet cavities. Thus, in a broader sense, the area of hybrid techniques will emphasize useful combinations of high frequency techniques with numerical methods to generate a variety of interesting and useful electromagnetic radiation and scattering solutions. For example, the numerically efficient fast Fourier transform (FFT) method and the asymptotic high frequency approximation are being combined to efficiently analyze the focal region fields received by a parabolic reflector antenna with an arbitrary rim contour, when it is illuminated by a distant EM plane wave. This current research is expected to provide a simple, physically appealing and efficient procedure for designing parabolic reflector antennas and feeds for multiple and contour beam applications.

During the present period, progress has been made in the following areas of research which come under the hybrid methods.

1. Diffraction by Perfectly-Conducting Surfaces

During the recent past, the radiation or scattering by surfaces with discontinuity in curvature and by a half-cylinder were analyzed via the hybrid GTD-MM procedure. In addition, some analytical solutions were also developed for the problems of radiation and scattering by a surface with a discontinuity in curvature. The work performed in analyzing the diffraction by a half cylinder was described in the previous annual report (June 1984); it was indicated therein that a M.Sc. thesis on this topic was also published in 1984. In addition, a

paper on this subject has been recently accepted for publication as indicated below:

> "Hybrid UTD-MM Analysis of the Scattering by a Perfectly-Conducting Semi-Circular Cylinder", S. Srikanth, P.H. Pathak and C.W. Chuang, paper accepted for publication in the IEEE Trans. AP.

Progress made in the high frequency analysis of the diffraction by a discontinuity in surface curvature is described next in part (a); it is followed by a brief description of the work, which has been recently initiated to analyze the EM diffraction by a cone tip in part (b).

(a) Diffraction by a Perfectly-Conducting Surface with a Discontinuity in Surface Curvature

The radiation by a magnetic line source mounted on a flat plate which is smoothly joined to a convex cylinder was previously solved using a hybrid technique and published in two papers [5,6]. That hybrid technique combines the moment method with the geometrical theory of diffraction. Although the hybrid approach is conceptually simple, it still requires a fair amount of computation. Recently, an analytical solution to the same radiation problem has been obtained. This analytical solution can also be applied to solving the diffraction of a plane wave propagating along the flat plate towards the join where the curvature discontinuity occurs. The new solution is expressed in terms of well tabulated functions of one variable. Its calculation is very simple and efficient. Calculated results agree very well with those obtained by the hybrid approach. A paper [7] describing the new

solution has been accepted for publication in IEEE Transactions on Antennas and Propagation.

As an extension of the work described in the last paragraph, an analytical solution is obtained to describe the current distribution induced by a high frequency plane wave incident upon a conducting surface composed of a flat plate smoothly-joined to a parabolic cylinder with the join in the penumbra region. The modified Fock function which describes this current distribution is given by

$$-\frac{1}{\pi j}\int_{-\infty}^{\infty}\frac{\int_{q}^{\infty e^{-j2\pi/3}} w_1(v)\cos[m\alpha(v-q)]\,dv}{w_1'(q)}\,e^{jq\xi}dq\,,$$

where α = angle of incidence measured from the flat plate.

$m = (ka/2)^{1/3}$

a = radius of curvature of the parabola at the join.

$w_1(q)$ = an Airy function.

An efficient analytical formula is developed for calculating this function. Figure B.1 shows the several magnitudes and phases of the modified Fock function as compared to those of the corresponding Fock function.

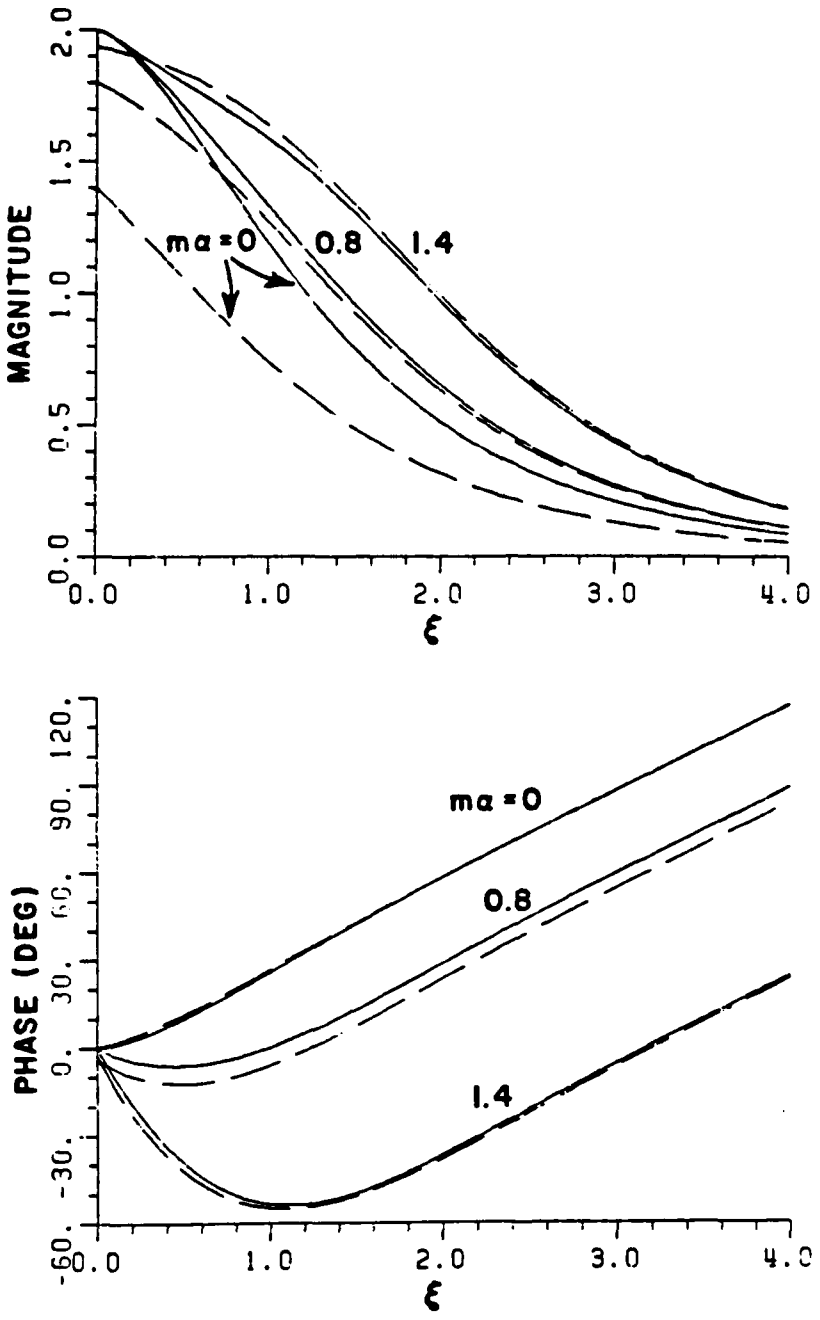

Figure B.1. Plots of the modified Fock function (solid curves) and the Fock function (dashed curves).

$$\frac{e^{-jm^3\alpha^3/3}}{\sqrt{\pi}} \int_{-\infty}^{\infty} \frac{e^{j(\xi-m\alpha)q}}{w_1'(q)}\, dq \ ,$$

which describes the current distribution on a complete parabolic convex surface. The modified Fock function can be applied to estimating the radar cross section of a cone-sphere. A paper [8] detailing this new modified Fock function has also been accepted for publication in IEEE AP.

(b) Diffraction By the Tip of a Perfectly-Conducting Cone

Recently, work has been initiated to analyze the problem of EM scattering by a semi-infinite circular cone via the type (i) hybrid GTD-MM approach. This is of importance in RCS applications where the diffraction by a cone tip can occur. The solution for the diffraction by a semi-infinite cone will also be useful in estimating the contributions to the scattering due to the cone tip-base wave interactions in the case of a finite circular cone. In this hybrid GTD-MM approach, it is being investigated if a known eigenfunction expansion for the currents induced near the cone tip when it is illuminated by an external plane wave is more efficient to use than the subsectional basis functions near the tip. Of course, far from the cone tip, the form of the UTD/GTD basis functions is being employed.

2. Problem of Diffraction by Edges Formed at Junctions Between Perfectly Conducting and Dielectric Boundaries

(a) Diffraction of a Surface Wave by a Step in a Conducting Surface Which Contains a Recessed Dielectric Slab

The study of surface wave diffraction by a truncated dielectric slab recessed in a perfectly conducting surface is of importance in designing flush-mounted dielectric covered antennas. The incident surface wave gives rise to waves diffracted and reflected by the junction at the termination of the dielectric. A strong reflected surface wave is undesirable in certain situations in that it may cause a problem in matching antenna impedances. One way to reduce the reflected surface wave is to use a different section of the dielectric near the junction. If the section of the dielectric near the junction is lossy, a substantial reduction of the reflected surface wave can be achieved as demonstrated in the present study. Because of the added complexity from the inclusion of different dielectric sections, this diffraction mechanism is treated using a type (iii) hybrid approach. Figure B.2 shows the reduction in the surface wave reflection coefficient by the inclusion of a small lossy dielectric section near the dielectric-conductor junction. In the figure, $|R|$ is the magnitude of the surface wave reflection coefficient, b is the thickness of the dielectric slab, ε_2 is the relative dielectric constant of the semi-infinite dielectric slab, and ε_1 is the relative dielectric constant of the lossy dielectric section of width $-x_1$. As shown in

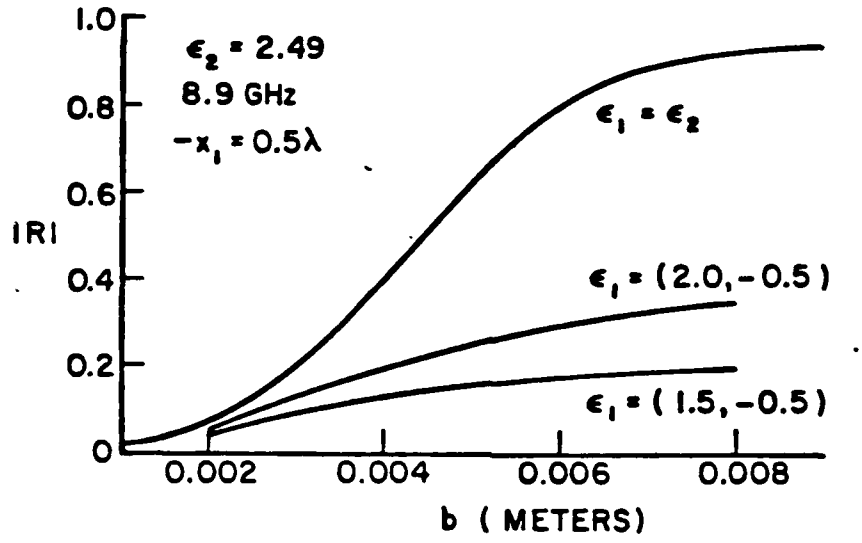

(a)

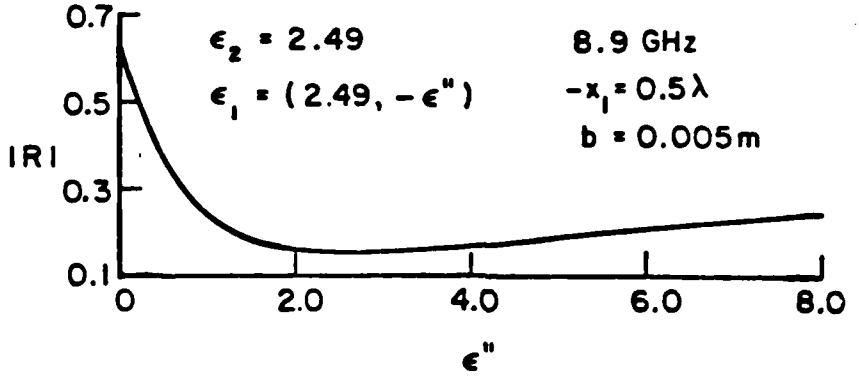

(b)

Figure B.2. Reduction in the surface wave reflection coefficient.

Figure B.2b, there is an optimal value of ε_1 where $|R|$ is minimal. A paper [9] detailing the hybrid approach solution of this problem has been accepted for publication in IEEE AP.

(b) Diffraction by Antenna and Inlet Cavities

It was mentioned earlier that the problem of EM scattering by cracks and notches in perfectly-conducting surfaces was studied under the JSEP contract (with some additional support from Rockwell and PMTC); in time however, most of the support for this type of work was picked up primarly by AFOSR, so that it is being continued only with a minimal support from JSEP. Specifically, the main topic of this AFOSR sponsored research deals with the EM scattering by dielectric loaded shallow antenna cavities and also notches in planar perfectly-conducting surfaces. This work is a natural extension of the work initiated on the scattering by cracks and notches under JSEP, Rockwell and PMTC. It may be remarked that a report describing the earlier work on crack scattering was written; namely:

> "EM Scattering by Slits and Grooves in Thick Perfectly-Conducting Planar Surfaces", R. Kautz, P.H. Pathak and L. Peters, Jr. The Ohio State Univ., Dept. of Electrical Engineering, Tech. Rpt. 714614-5, prepared under Contract No. N0429A-82-C-0396, for the Dept. of the Navy, Point Mugu, Calif. August 1984.

The above report was a direct outgrowth of the work submitted as an M.Sc. thesis on this research by R. Kautz. The newer geometries involving scattering by shallow open-ended cavities in

perfectly-conducting surfaces in which the cavities may be large or small (as in the case of a notch or a crack) is being analyzed via the type (iii) hybrid GTD-MM approach. It has been found that the GTD type basis functions involving surface waves work well for large apertures; whereas, an alternative set of basis functions simulating the proper edge conditions are more appropriate for small width apertures. These highly efficient solutions for both small and large width apertures provide an overlap in the numerical results to accommodate moderately sized apertures as well. Presently, an M.Sc. thesis describing this work is in progress and the papers based on that thesis will be prepared in the next few months.

Most shallow cavities are employed for housing antennas; on the other hand, an inlet cavity is deep. Work has been in progress to analyze the EM scattering by inlet type cavities as well on AFOSR, NASA/Langley and NWC sponsored research. Nevertheless, the technical approaches being utilized in analyzing these inlet cavities involve a combination of asymptotic high frequency and modal techniques which are used in conjunction with the multiple scattering method (MSM). Consequently, such approaches fall within the general framework of hybrid methods which combine the best features of two or more techniques. The MSM requires a knowledge of scattering matrices to characterize pertinent junctions corresponding to discontinuities (e.g., the inlet opening and the interior inlet termination). The elements of these scattering matrices are obtained via asymptotic high frequency methods; thse asymptotic techniques provide relatively simple and also

accurate expressions for the elements of the scattering matrices which describe the scattering from the open end, the coupling of the incident field into the modes of the inlet region and their subsequent radiation after single and multiple reflections from the termination within the inlet. As a result of such a combination of asymptotic and modal techniques used in conjunction with the MSM, inlets which are composed of piecewise linear sections can also be analyzed.

Another interesting outcome of this study has been the connection between the aspect of incidence on the inlet to the significant modes excited within the inlet by the incident wave. Such a relation is useful for efficiently computing the fields scattered by electrically large inlets which can support a large number of propagating modes. If the above connection is not employed the computations requiring the inclusion of a large number of inlet modes will become inefficient.

The aforementioned work on the EM scattering by inlets (with a dielectric termination inside) will be partially credited to JSEP because of its close association to the fundamental work in the area of hybrid techniques. The following papers are being prepared for publication in order to describe some of this research on inlet scattering; namely:

> "A Simple Modified GTD Equivalent Current Approach for Analyzing Modal Reflection Coefficients of Open Ended Waveguide Geometries", by P.H. Pathak and A. Altintas, paper to be submitted to IEEE Trans. Antennas and Propagation.
>
> "Ray Analysis of Reflection from Open-Ended Circular and Rectangular Waveguides", by C.W. Chuang, P.H. Pathak, and C.C. Huang, paper to be submitted to IEEE Trans. on Antennas and Propagation.

In addition, the following papers related to the inlet scatterng research were presented orally:

> "Ray Analysis of Reflection from a Class of Waveguide Discontinuities", by A. Altintas, P.H. Pathak and C.D. Chuang, IEEE/APS Symposium and National Radio Science Meeting at the University of British Columbia, Vancouver, Canada, June 1985.
>
> "An Efficient Approach for Analyzing the EM Coupling into Large Open-Ended Waveguide Cavities", by P.H. Pathak and A. Altintas, IEEE/APS Symposium and National Radio Science Meeting at the Universtiy of British Columbia, Vancouver, Canada, June 1985.

3. Analysis of Microstrip Antennas

Microstrip antennas are light-weight, relatively low-cost antennas which can be employed conformally on many practical structures including aircraft and missile shapes. It is therefore of interest to efficiently analyze the radiation from a single microstrip antenna element and also from an array of electrically small microstrip patch antennas which are placed conformally on an electrically large perfectly-conducting smooth convex surface. The latter problem can be handled efficiently if one combines low frequency techniques (for handling the electrically small microstrip patches) with the high frequency ray technique (for handling the electrically large convex surface). Presently, work has been initiated to analyze the asymptotic high frequency surface fields of an electric current source (such as that associated with a microstrip patch) on a "thin" grounded dielectric planar surface. This solution would provide the dominant contribution to the asymptotic high frequency

estimate of the Sommerfeld integral type surface Green's function which is useful for calculating the unknown current distribution only on the microstrip patch or on the array of microstrip patches. The remaining asymptotic contribution from the edges of the dielectric substrate will be accounted for separately using the results described in Work Units 1 (b) and 1 (c) dealing with the diffraction by a discontinuity in surface impedance and by the edge of thin dielectric half plane on a perfectly-conducting surface. The object here is to find a simple and accurate asymptotic approximation for the aforementioned surface Green's function which remains valid even for observation points reasonably close to the source so that the MM calculation can be made efficient using the hybrid GTD-MM approach of type (ii) discussed earlier. It is noted that a direct calculation of the Sommerfeld integral type represent of the microstrip surface Green's function makes the MM procedure extremely inefficient especially for an array of microstrip antennas. A simple approximation for the surface Green's function has been obtained in the past for a two-dimensional planar and convexly curved perfectly conducting surface with an extremely thin dielectric coating (which may thus be approximated by an impedance boundary condition). It is therefore felt that a similar approach could be employed in the three-dimensional situation as is presently being investigated. This approach would automatically account for the mutual coupling between various microstrip patch (or elements) in an array environment. The case of a moderatley thick dielectric substrate on a planar as well as a convexly curved perfectly conducting surface will be

dealt with in the future phases of this challenging study once the present approach is found to be sufficiently accurate and efficient on the thin dielectric planar substrate.

4. Reflector Antenna Synthesis

Large, offset array fed parabolic reflector antennas are being considered for use in multiple and contour beam type antenna applications. It would hence be of interest to investigate approaches for developing an efficient solution for the synthesis of such a multiple or contour beam type reflector antenna configuration, by combining high frequency techniques and appropriate numerical techniques. The object of this study is to essentially determine a feed distribution in the vicinity of the focal region which generates the desired multiple or contour beams. In addition, it is desirable that information on the size of reflector and feed region which would tend to optimize the design should be contained in this approach. Recently, work has been initiated to study such geometries from the reciprocal point of view in which the field within the focal region due to a plane wave incident on the reflector is investigated; here the direction of the incoming plane wave corresponds to that of any of the multiple or contour beam directions of interest via the reciprocity theorem for EM fields. The focal region fields are analyzed using a spectral procedure which has recently been found to be not only accurate but also very efficient as compared to the conventional approaches based on a direct

numerical evaluation of the physical optics approximation to the radiation integral for calculating these fields. Efficiency is of importance in synthesis problems. The solution to this reciprocal problem will be properly combined in the future phases of this study to deal with the general multiple and contour beam synthesis problems mentioned above. The preliminary results of this investigation have been recently reported in a M.Sc. thesis which is indicated below:

> "An Efficient Approach for Calculating the Focal Region Field of Parabolic Reflectors Illuminated by an Electromagnetic Plane Wave", by A. Nagamune, M.Sc. thesis, Department of Electrical Engineering, The Ohio State University, Columbus, Ohio, 1985.

The above thesis reports the analytical results for the focal region fields received by both, 2-D and 3-D parabolic reflectors. Numerical results are presented only for the 2-D case in the above thesis; however, more recently numerical results have also been obtained for the 3-D case. Of particular significance is the physical meaning that can be attached to the spectrum of the focal region fields in the 2-D case as described in the thesis. The spectrum has a simple ray interpretation as one might expect. Work is in progress to attempt a similar physical interpretation for the spectrum of the focal region fields in the 3-D reflector case. Also, additional work remains to be done to further improve the efficiency of the numerical evaluation of the focal fields in the 3-D reflector case by using a better procedure to subdivide the 3-D reflector with an arbitrary rim shape into only a few segments.

REFERENCES

[1] W.D. Burnside, C.L. Yu and R.J. Marhefka, "A Technique to Combine the Geometrical Theory of Diffraction and the Moment Method", IEEE Trans. AP-23, pp. 551-558, July 1975.

[2] G.A. Thiele and T.H. Newhouse, "A Hybrid Technique for Combining Moment Methods with the Geometrical Theory of Diffraction", IEEE Trans. AP-23, No. 1, January 1975.

[3] E.P. Ekelman, Jr. and G.A. Thiele, "A Hybrid Technique for Combining the Moment Method Treatment of Wire Antennas with the GTD for Curved Surfaces", IEEE Trans. Ap-S, pp. 831-839, November 1980.

[4] L.W. Henderson and G.A. Thiele, "A Hybrid MM-GTD Technique for the Treatment of Wire Antennas Near a Curved Surface", Radio Science, pp. 1125-1130, November-December 1980.

[5] C.W. Chuang and W.D. Burnside, "A Diffraction Coefficient for a Cylindrically Truncated Planar Surface", IEEE Trans. AP-S, Vol. 28, pp. 177-182, March 1980.

[6] W.D. Burnside and C.W. Chuang, "An Aperture-Matched Horn Design", IEEE Trans. AP-S, Vol. 30, pp. 790-796, July 1982.

[7] C.W. Chuang, "An Asymptotic Result for the Diffraction of Plane Waves Propagating Along a Cylinder Truncated Flat Surface", accepted for publication in April 1986 issue of IEEE AP, April 1986.

[8] C.W. Chuang, "An Asymptotic Solution for Currents in the Penumbra Region with Discontinuity in Curvature", accepted for publication in IEEE AP.

[9] C.W. Chuang, "Surface Wave Diffraction by a Truncated Inhomogeneous Dielectric Slab Recessed in a Conducting Surface", accepted for publication in April 1986 issue of IEEE AP.

C. INTEGRAL EQUATIONS

Researchers: E. Newman, Research Scientist
(Phone: 614/422-4999)

J. Richmond, Professor
(Phone: 614/422-7601)

J. Blanchard, Graduate Research Associate
Department of Mathematics
(Phone: 614/422-5049)

Integral Equation Studies of Material Coated Edges

1. Introduction

This section will review past and present research in the areas of integral equation and moment method techniques. The past work has been largly in the area of integral equation solutions for general shapes, with some work in penetrable surfaces and microstrip antennas. The present research is an integral equation formulation and method of moments solution to the problem of scattering by a dielectric/ferrite cylinder in the presence of a perfectly conducting cylinder. The cylinder shapes will be chosen so that they form a simple model for scattering by a material coated perfectly conducting edge.

In electromagnetics it is common to formulate radiation or scattering problems as boundary value problems. This often leads to a linear integral equation for the unknown of interest, usually a current

distribution. In most cases these integral equations have no known closed form solution. Thus, we resort to an approximate technique, known as the method of moment (MM) [1], to solve the integral equation. In the MM, we expand the unknown current in terms of a series N modes or basis functions. Next, N weighted averages or moments of the integral equation are enforced. The result is that the original integral equation is transformed into an NxN system of simultaneous linear algebraic equations. These equations can be solved (using standard matrix algebra) for the N coefficients in the expansion for the current, and thus provide an approximation to the current distribution. The number of terms retained in the expansion for the current is proportional to the electrical size of the body. As the electrical size of the body increases, N must increase, and so will the computer run time and storage requirements, which are usually proportional to N^2. For this reason, conventional MM solutions are referred to as low frequency solutions, and are restricted to bodies which are not too large in terms of a wavelength.

2. Review of Past Work

This section will review our past work under JSEP support. The main emphasis of our work has been in the development of MM solutions applicable to general perfectly conducting shapes, however, we have also done work in scattering from material surfaces, and microstrip antennas.

(a) General Modeling Techniques

Our approach to the modeling of general bodies has been to model them as an interconnection of thin-wires and polygonal plates. The polygonal plates are interconnected to form the (assumed) perfectly conducting surfaces of the body. For example, Figure C.1 shows 14 polygonal plates interconnected to model the Concord aircraft at a frequency where the Concord is about two wavelengths in length. One can envision how the polygonal plates could be interconnected to model other shapes, such as a satellite, a building, a ship, etc. Figures C.2 and C.3 show the magnitude and phase of the RCS of the Concord in the azimuth plane and compared with measurements. Thin-wires can be used to model wire antennas, such as dipoles, loops, etc. They can also be used to model a mast on a ship, a flagpole on a building, or other long thin shapes. Techniques for combining thin-wires with the polygonal plates, including the important problem of the wire to plate junction have been developed. The basic theory for the MM solution of the interconnection of wires and plates is described by several journal publications [2-10] as well as two Ph.D. dissertations and one Masters thesis [11-13]. In addition, the techniques have been implemented in terms of user-oriented codes [14,15] which have been distributed to over 50 members of industry, universities, and government.

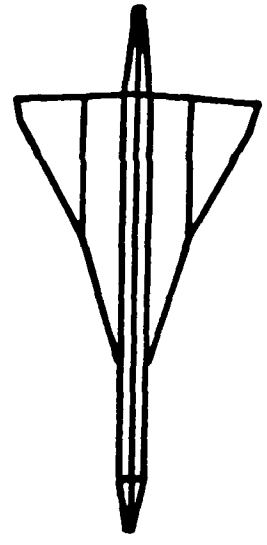

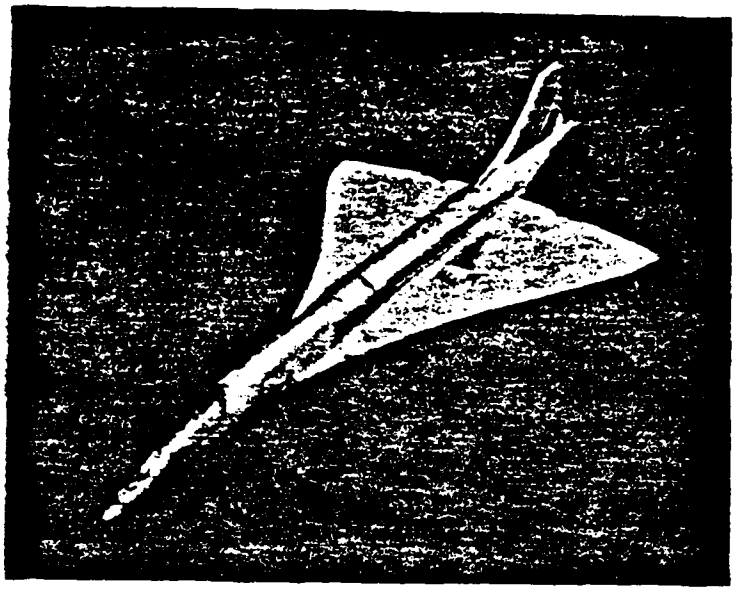

Z AXIS VIEW

SCALE = 0.62 λ

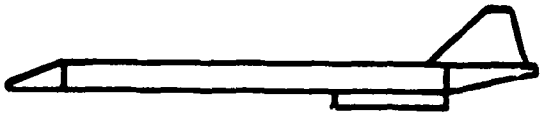

X AXIS VIEW

Y AXIS VIEW

Figure C.1. A 14 polygonal plate model of the Concord aircraft.

AD-A164 916 JOINT SERVICES ELECTRONICS PROGRAM(U) OHIO STATE UNIV 2/2
COLUMBUS ELECTROSCIENCE LAB DEC 85 ESL-710016-18
N00014-78-C-0049

UNCLASSIFIED F/G 9/5 NL

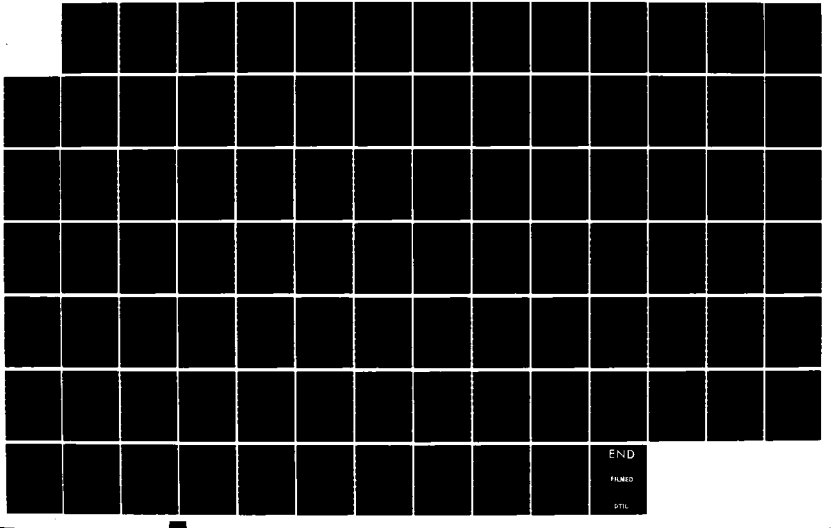

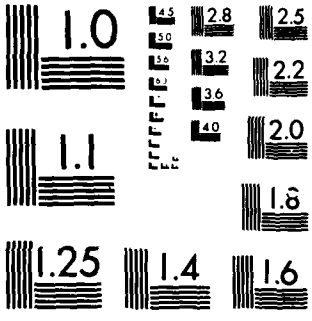

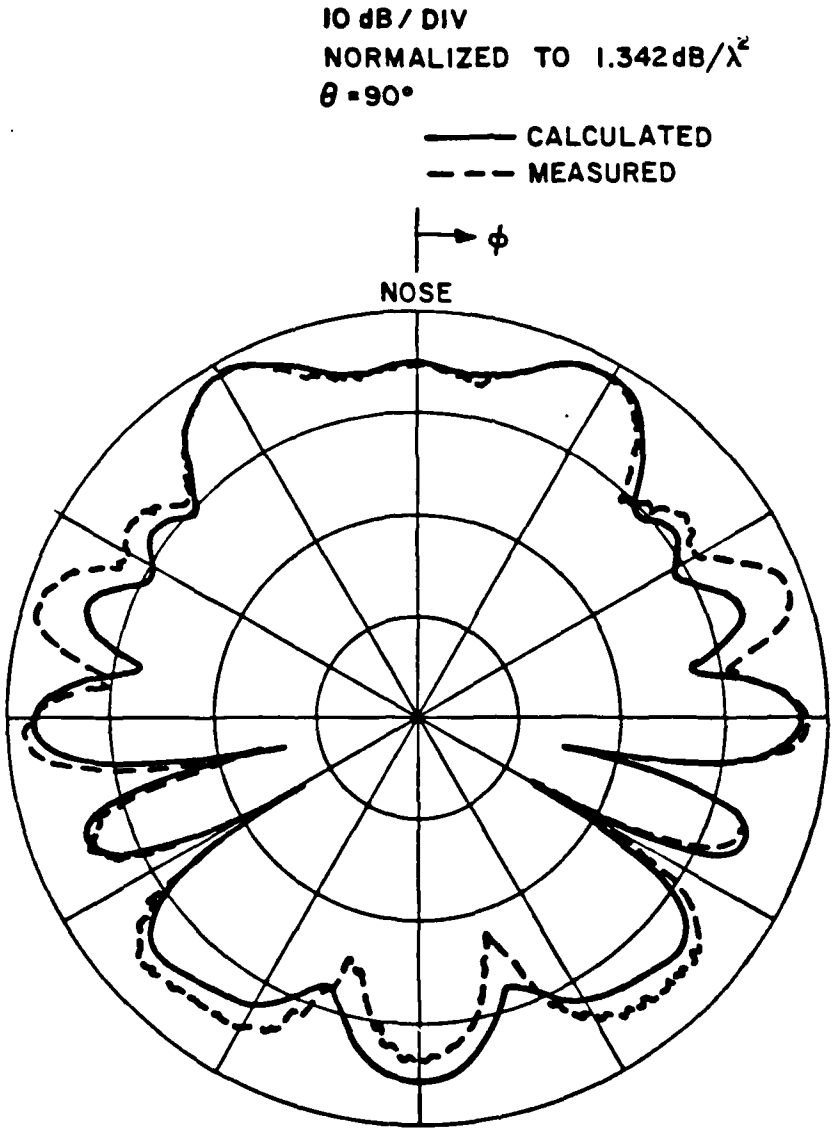

Figure C.2. $\hat{\phi}$ polarized RCS of the Concord in the azimuth plane.

(b) Scattering by a Material Plate

As described above, we have done a considerable amount of work on the problem of the modeling of perfectly conducting surfaces as an interconnection of perfectly conducting plates. However, this work is not applicable if the surface is composed of some material (i.e., dielectric/ferrite) medium. Thus, we would not be able to analyze composite materials or radar absorbing materials on an aircraft. One method of treating these material surfaces, and yet retaining much of the work and computer coding done for perfectly conducting plates, is to develop a solution for the material plate. Basically, we have developed an integral equation and MM solution for the scattering by a thin rectangular material plate. The basic theory is described in [16] or by the Ph.D. dissertation [17]. By a material plate we mean a thin three dimensional slab composed of some (possibly lossy) dielectric/ferrite material. Alternatively, it can mean a perfectly conducting plate coated on one or both sides by a thin dielectric/ferrite slab. We have formulated the material plate solution as a generalization of the perfectly conducting plate, so as to be able to take maximum advantage of past work on perfectly conducting plates. As an example, Figure C.4 shows the RCS of a square plate coated on one side by a dielectric/ ferrite absorbing layer. Note that the theory is in close agreement with measurements, and that it correctly predicts about a 20 dB drop in the RCS when the wave is incident from the abosrber side, as opposed to the perfectly conducting side.

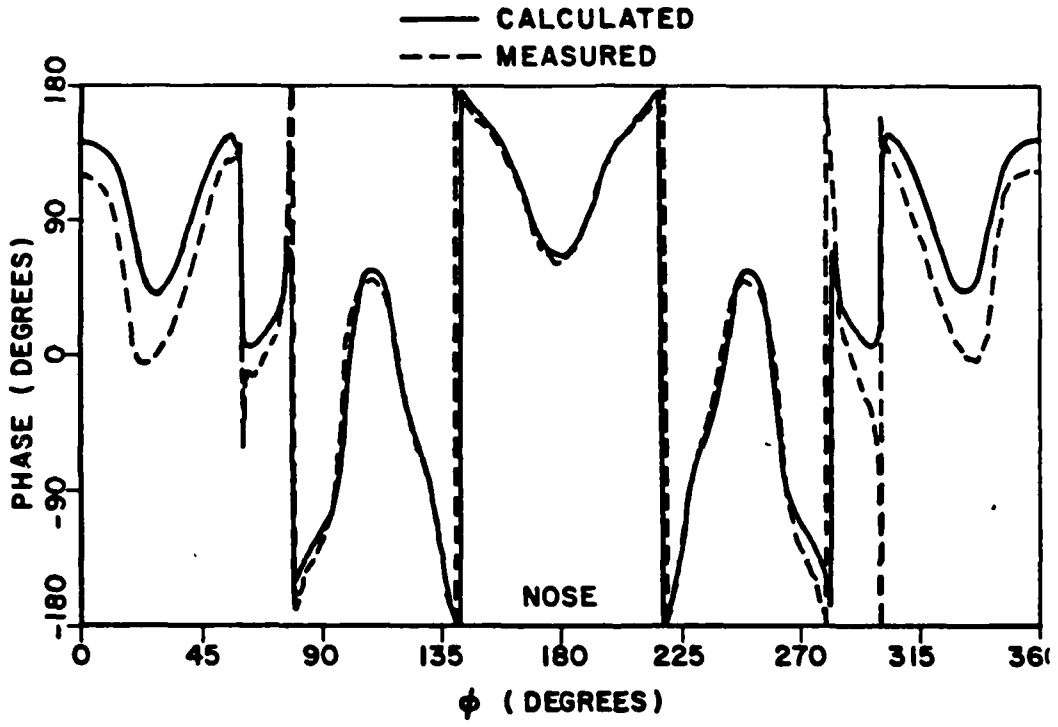

Figure C.3. $\hat{\phi}$ polarized RCS phase of the Concord in the azimuth plane.

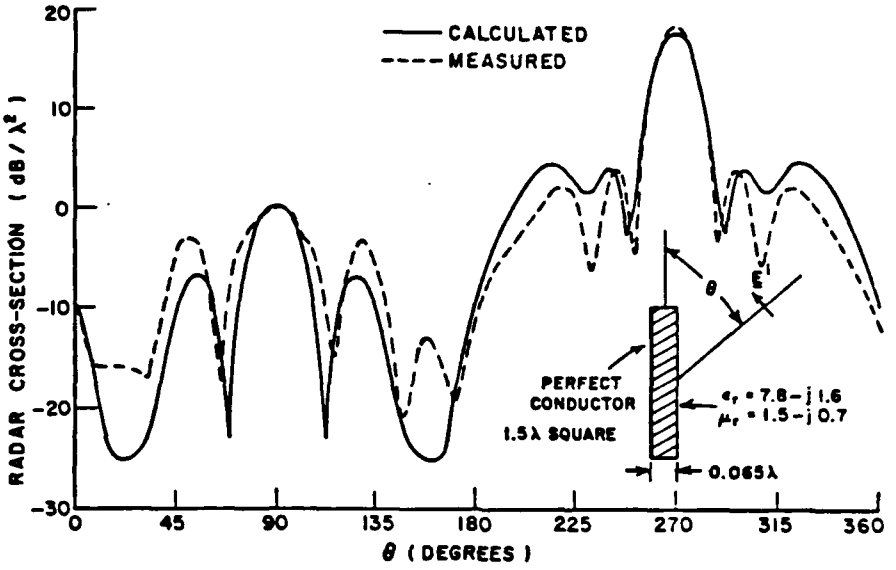

Figure C.4. TM radar cross-section of a 1.5 wavelength coated, perfectly conducting plate.

(c) Microstrip Antennas

A microstrip antenna consists of a metallic patch on a thin dielectric coated ground plane. Microstrip antennas and arrays have recieved considerable study and appplication in the last 20 years, since they are lightweight, flush-mountable, and can be easily fabricated using standard printed circuit etching techniques. The microstrip antenna can be analyzed using the basic techniques described above for the modeling of surfaces. Basically we begin with an exact integral equation for the currents on the microstrip patch. The integral equation contains the dielectric slab Green's function in the form of the Sommerfeld integrals. The integral equation is solved by the MM. This technique has been applied to the analysis of rectangular microstrip antennas and arrays [18,19]. An N port Thevenin theorem was used to account for the microstrip transmission line feed network. More recently, we have studied the problem of the self and mutual impedance between microstrip patches on a dielectric coated cylinder. This work included an exact eigenfunction solution, as well as asymptotic approximations for large cylinder radius. Figure C.5 shows the eigenfunction solution for the magnitude of the mutual impedance between microstrip patches on a dielectric coated cylinder versus their separation. Curves are shown for different cylinders radius. This work resulted in a Ph.D. dissertation [20], and two journal articles are in preparation [21,22].

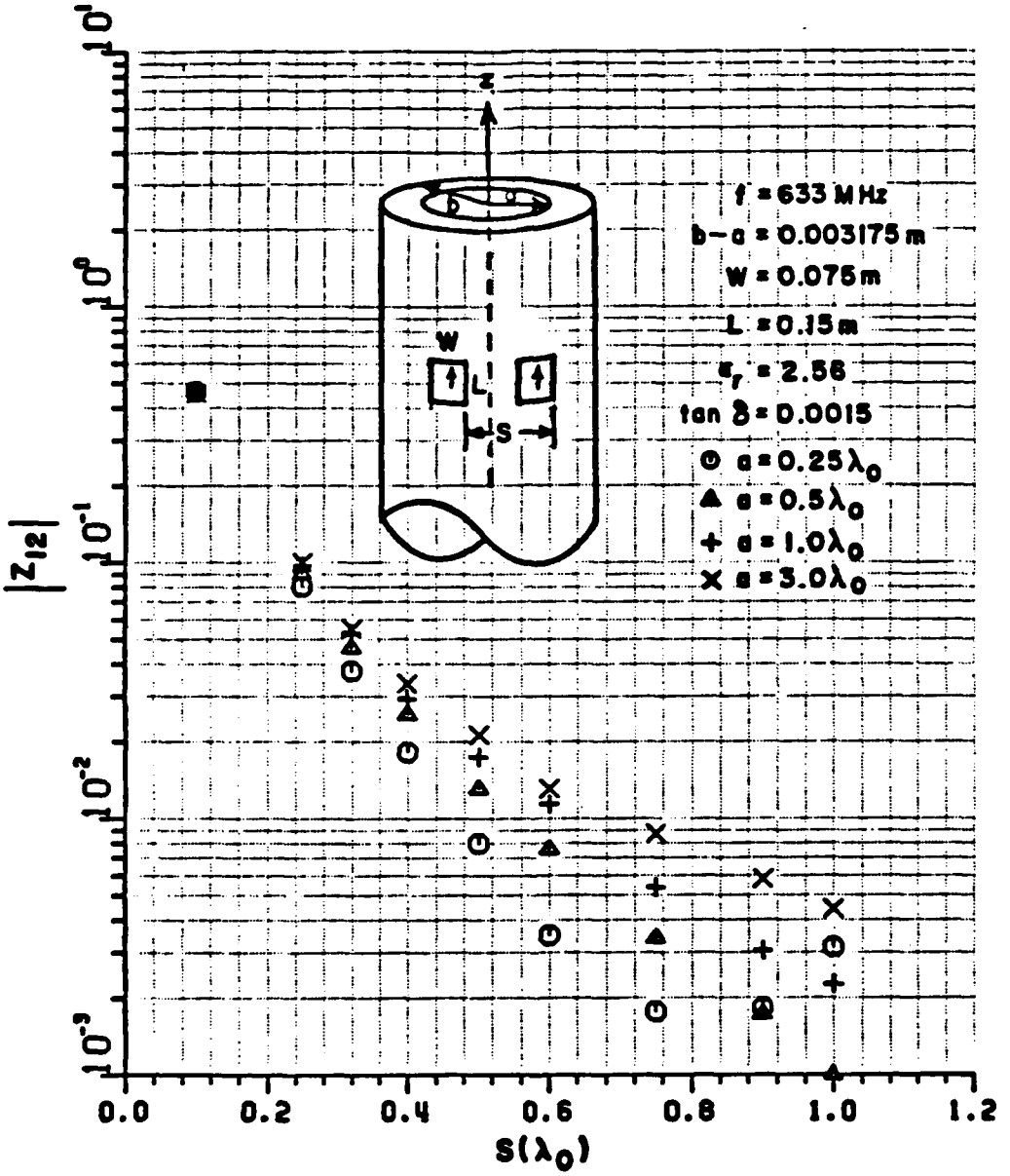

Figure C.5. H-plane coupling for identical microstrip patch modes on a dielectric coated cylinder.

3. Current Research

(a) Introduction

The current research is a departure from the work described above. We are studying various fundamental geometries associated with the plane wave scattering from material coated perfectly conducting edges. Reduction of the scattering from edges is one of the important problems in the design of low RCS bodies. For simplicity, all geometries considered are two dimensional, with the edge being the z axis.

Figure C.6a, b, c, and d show four geometries of interest. Each shows a material cylinder in the presence of a perfectly conducting cylinder. The perfectly conducting cylinder is chosen because it contains an edge, and it is intended that the material cylinder should coat or surround this edge. Thus, the four problems shown in Figure C.6 represent four ideal models applicable to the scattering from material coated perfectly conducting edges. The simplest model for an edge is the half-plane, shown in Figure C.6a. Figure C.6b shows a parabolic cylinder which is a model for a thick edge. Figure C.6c shows a right angle wedge which can model an edge in a thick ground plane. The elliptic cylinder of Figure C.6d can be used to represent a thick edge of finite width. The next section will outline the integral equation and MM solution for a class of problems, of which these geometries are special cases.

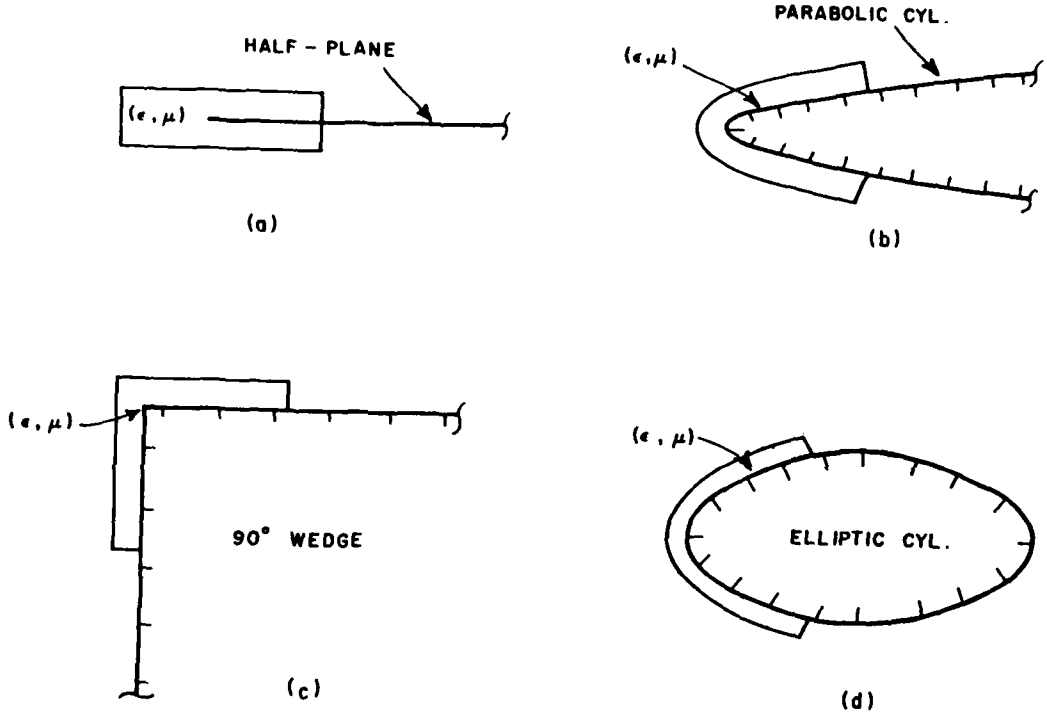

Figure C.6. Four examples of perfectly conducting cylinders with a dielectric/ferrite coating; (a) a half-plane, (b) a parabolic cylinder, (c) a right angle wedge, and (d) an elliptic cylinder.

(b) Theoretical Solution

The problem to be analyzed is shown in Figure C.7a. Here we have a plane wave illuminating a dielectric/ferrite cylinder in the vicinity of a perfectly conducting cylinder. Figures C.6a, b, c and d are special cases of Figure C.7a, where the perfectly conducting cylinder is a half-plane, a parabolic cylinder, a right angle wedge, or an elliptic cylinder, respectively. The method described below is most applicable when the shape of the perfectly conducting cylinder is such that its Green's function is known. This is the case for the shapes shown in Figure C.6 [23]. The ambient medium is homogeneous with permittivity and permeability (ε_0, μ_0), while the material cylinder may be inhomogeneous with parameters (ε, μ). The fields of the incident plane wave in the presence of the conducting cylinder are considered to be known and denoted $(\underline{E}_i, \underline{H}_i)$ while $(\underline{E}_T, \underline{H}_T)$ denotes the unknown total fields, i.e., the fields of the incident plane wave in the presence of the material and the conducting cylinders. All fields and currents are considered to be time harmonic, with the $e^{j\omega t}$ time dependence suppressed.

The first step in the solution is to replace the dielectric/ferrite cylinder by the ambient medium and the equivalent volume polarization currents $(\underline{J},\underline{M})$ confined to the region R and given by

$$\underline{J} = j\omega(\varepsilon-\varepsilon_0)\underline{E}_T \tag{1}$$

$$\underline{M} = j\omega(\mu-\mu_0)\underline{H}_T \tag{2}$$

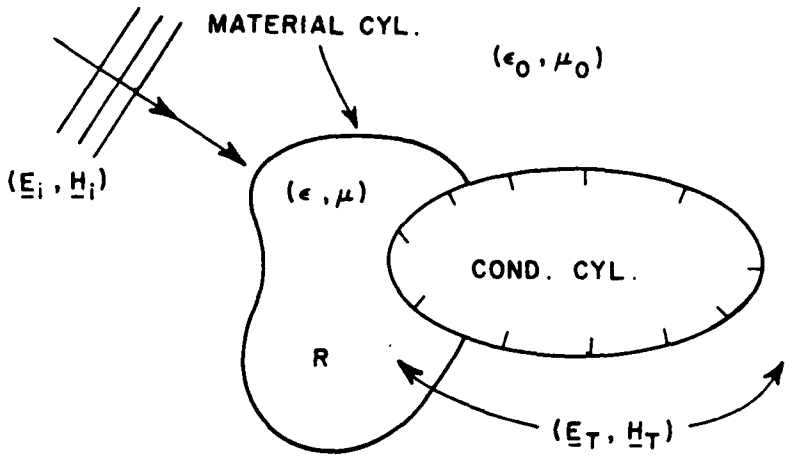

(a)

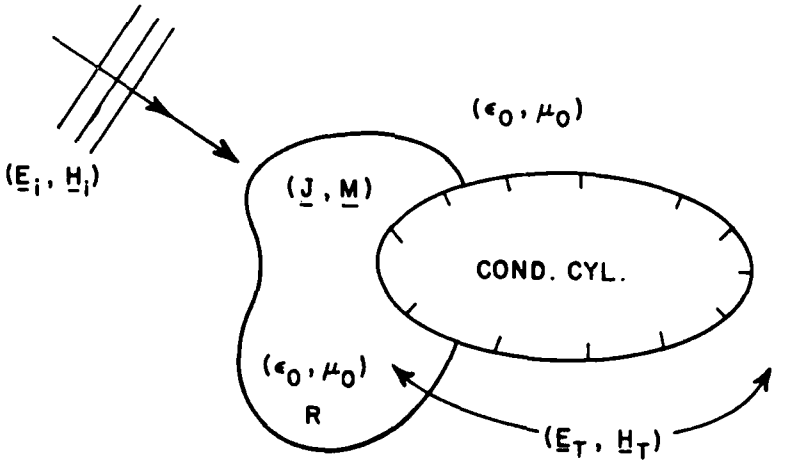

(b)

Figure C.7. (a) A material cylinder in the presence of a perfectly conducting cylinder illuminated by a plane wave. (b) The equivalent problem where the material is replaced by free-space and equivalent electric and magnetic volume polarization currents.

Note that $(\underline{J},\underline{M})$ are unknown since $(\underline{E}_T,\underline{H}_T)$ are unknown. $(\underline{J},\underline{M})$ radiate the scattered fields $(\underline{E}^S,\underline{H}^S)$ in the presence of the conducting cylinder. The total fields are the sum of the incident plus the scattered fields,

$$\underline{E}_T = \underline{E}_i + \underline{E}^S \tag{3}$$

$$\underline{H}_T = \underline{H}_i + \underline{H}^S \quad . \tag{4}$$

Substituting Equations (3,4) into (1,2) produces

$$\underline{E}_T = \underline{E}_i + \underline{E}^S = \underline{J}/j\omega(\varepsilon-\varepsilon_o) \qquad \text{in R,} \tag{5}$$

$$\underline{H}_T = \underline{H}_i + \underline{H}^S = \underline{M}/j\omega(\mu-\mu_o) \qquad \text{in R.} \tag{6}$$

Equations (5,6) represent two coupled integral equations which must be solved for $(\underline{J},\underline{M})$. These equations are exact, and it is only in their solution by the MM that approximations need be made. Any surface waves, creeping waves, or mutual coupling effects between the equivalent currents representing the dielectric/ferrite cylinder and the currents on the perfectly conducting cylinder are automatically included in Equations (5,6) (even though the electric surface current density on the conducting cylinder does not explicitly appear in (5,6)).

For simplicity, we will now consider the special case where the material cylinder is dielectric, but not ferrite. In this case $\mu = \mu_o$, $\underline{M} = 0$, and we need only solve Equation (5) for $\underline{J}$. The scattered electric field can be written as

$$\underline{E}^S = \int\int_R \underline{J} \cdot \underline{G}\, ds \tag{7}$$

where $\underline{\underline{G}}$ is the conducting cylinder dyadic Green's function. That is, $\underline{\underline{G}}$ is the electric field ($\hat{x}$,$\hat{y}$, or $\hat{z}$ polarization) of an electric line source ($\hat{x}$,$\hat{y}$, or $\hat{z}$ polarization) radiating in the presence of the conducting cylinder. If $\underline{\underline{G}}$ is not known in a closed analytic form, then it would have to be determined numerically, and the solution presented here would be less desirable. The Green's function (at least some of the nine components) for the shapes of Figure C.6 are well known [8].

The MM solution of Equation (5) would begin by expanding $\underline{J}$ as

$$\underline{J} = \sum_{n=1}^{N} I_n \underline{J}_n \tag{8}$$

where the $\underline{J}_n$ are a sequence of N known expansion functions or modes, and the I_n are a sequence of N unknown coefficients. If we now insert Equations (7,8) into (5), multiply both sides by the known weighting functions $\underline{W}_m$ m = 1,2, ... N, and integrate over the region R, then (5) is transformed into a system of simultaneous linear equations which can be written as

$$[Z]I = V. \tag{9}$$

Typical terms of the impedance matrix, [Z], and voltage vector, V, are given by

$$Z_{mn} = -\iint_R \left[\underline{E}_n^J \cdot \underline{w}_m + \frac{1}{j\omega} \frac{\underline{J}_n \cdot \underline{w}_m}{(\varepsilon - \varepsilon_o)} \right] ds \tag{10}$$

$$V = \iint_R \underline{E}_i \cdot \underline{w}_m \, ds \qquad Z_{mn} = \iint_R \underline{E}_n^J \cdot \underline{w}_m + \frac{\underline{J}_n \cdot \underline{w}_m}{j\omega (\varepsilon - \varepsilon_o)} \tag{11}$$

where $\underline{E}_n^J$ is the electric field of the n^{th} expansion mode radiating in the presence of the conducting cylinder and can be written as

$$\underline{E}_n^J = \iint_R \underline{J}_n \cdot \underline{\underline{G}} \, ds. \tag{12}$$

Note again that the evaluation of Equations (10-12) will be facilitated if the Green's function for the conducting cylinder is known. Equation (9) can now be solved for the current vector I, which contains the N coefficients I_n, n = 1,2, ... N. Once I is known, then using Equation (8), an approximation to $\underline{J}$ is known, and the scattered fields can be found in a straight-forward manner.

The MM solution should, in principle, appraoch the exact solution as the number of terms, N, in the expansion for $\underline{J}$ is increased. Generally, the number of terms required to achieve a given accuracy will be proportional to the cross-section area of the material cylinder.

Assuming that this effort is successful, we will have a number of idealized, but highly accurate, models for the scattering from material coated perfectly conducting edges. These models should be capable of providing basic information as to how a material coating can modify the scattering from perfectly conducting edges. A second use of the solutions will be to provide physical insight and numerical data to aide others who are developing high frequency asymptotic solutions to these problems.

(c) Most Recent Work

In the JSEP report dated June 1984 [24] and in [25] we reported that we had completed the solution for the material coated half-plane for the limited cases of dielectric only (i.e. no ferrite) and the TM polarization. In the past year this work has been extended to material cylinders which are both dielectric and ferrite, and for both the TM and TE polarization [26]. As an example of the results obtained, Figure C.8 shows a rectangular dielectric slab coating a half-plane. Figure C.8 also shows the TM edge on echo width for this geometry versus frequency. Note the good agreement between theory and experiment. These methods have been applied to the problem of reducing half-plane edge scattering by incorporating a properly designed dielectric coating [27].

Our present work deals with the scattering from the material coated parabolic cylinder shown in Figure C.6b. The parabolic cylinder is a model for a thick edge (as opposed to the half-plane which is a model for a thin edge). Comparison of the results for the material coated half-plane and the material coated parabolic cylinder should provide interesting and useful results concerning the effects of edge thickness.

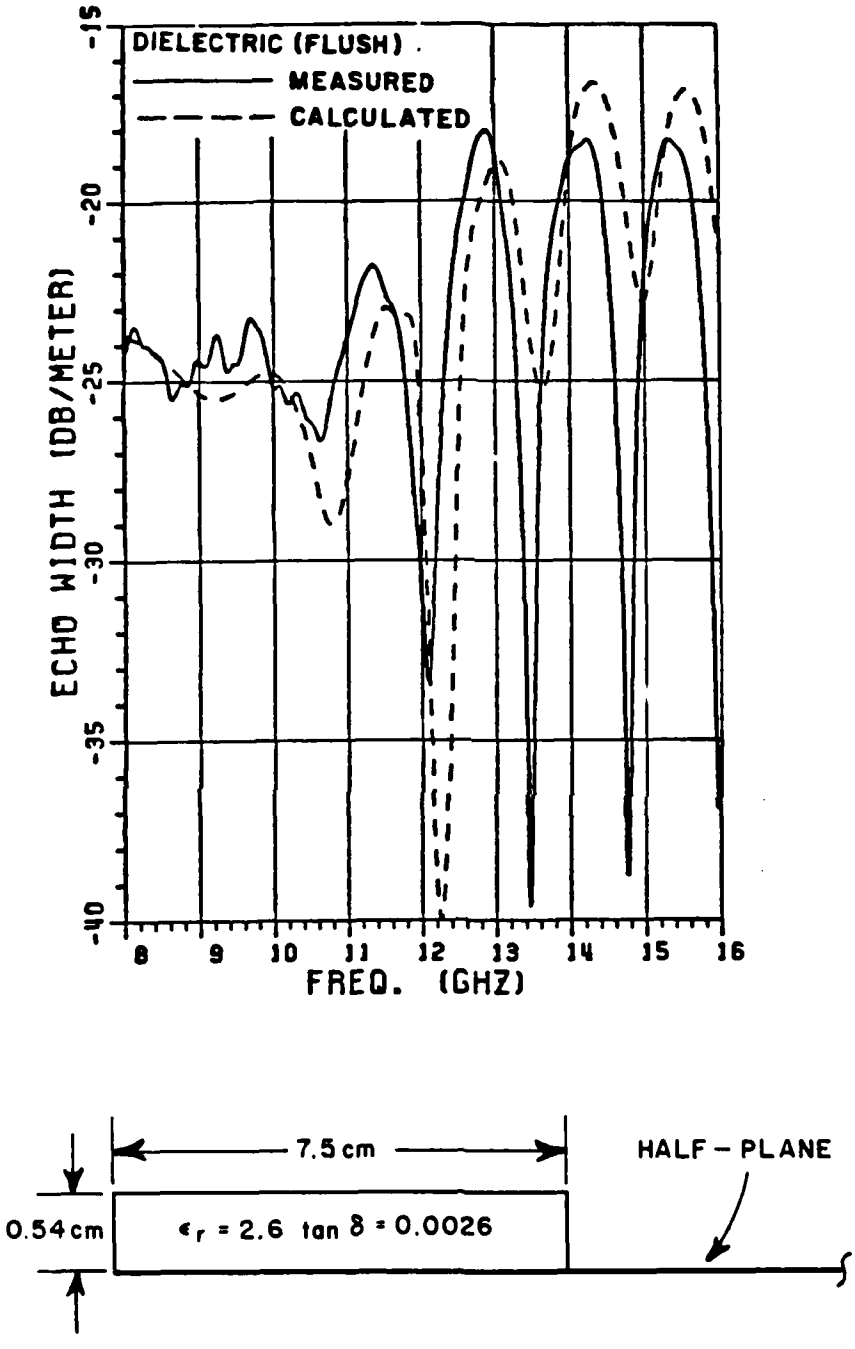

Figure C.8. The edge-on echo width of a dielectric coated half-plane.

Integral Equation Studies of Penetrable Objects

1. Introduction

The preceding sector of this work unit has discussed Dr. Newman's approaches to this important task. Earlier we had presented comparable studies of the same problem from an asymptotic viewpont. Professor Richmond is also pursuing several alternate approaches. This topic is most important because the increased use of penetrable materials on aerospace vehicles leads to requirements for more efficient analytic treatment of such configurations. We may list the following examples of penetrable geometries: the dielectric radome, ablation coatings, composite media, and ferrite absorbers.

In 1965 Richmond [28,29], published the first moment-method solutions for scattering by dielectric cylinders with arbitrary cross-sectional shape, and recently the technique was extended to ferrite cylinders by Rojas [30]. A dielectric cylinder is modeled with electric polarization currents, while a ferrite cylinder requires magnetic (as well as electric) polarization currents.

In 1973, Richmond [31] developed a user-oriented moment method for scattering by a perfectly conducting polygon cylinder. Later, Wang [32] extended the theory and computer program to include a thin dielectric coating on the polygon cylinder. While promising, Wang's results might be improved by including surface waves in the analysis. A user-oriented

program is still not available for a conducting polygon cylinder with a thin ferrite coating.

In the area of RCS control, Professor Leon Peters has suggested that a thin ferrite coating may offer unique properties that cannot be duplicated with a thin lossy dielectric coating. This idea has been reinforced by the numerical results of Hill [33] for the propagation constant of a surface wave on a thin lossy ferrite coating.

To take advantage of these unique properties, we require an analysis of scattering by a thin lossy ferrite slab, or a conducting strip with a thin ferrite coating. An analysis for the lossless case has been developed recently by Burnside and Burgener [34] with the GTD format. Their results agree closely with moment method calculations except for those situations where surface wave effects are dominant. The surface waves are not included in their analysis.

As discussed in an earlier section, Pathak and Rojas-Teran have applied the Wiener-Hopf Technique to the thin dielectric half-plane. They have obtained excellent results, with some difficulty in the vicinity of grazing incidence.

In the next sections we consider some examples of scattering by thin ferrite geometries and conducting surfaces with a thin ferrite coating. These examples are: a thin planar dielectric strip, a conducting circular cylinder partially coated with a thin ferrite layer, and a thin curved ferrite strip. In each of these sections we outline our accomplishments in the area.

2. Scattering by Thin Planar Dielectric Strip

Richmond [35] has developed an efficient moment-method solution (with only three equations and three unknowns) for plane-wave scattering by a thin lossy dielectric strip. Although this was accomplished in 1983, it is summarized here to facilitate a discussion of our more recent research.

Figure C.9 illustrates a thin planar dielectric strip with thickness t which is much smaller than the wavelength, and infinite length. The width w can range from zero to infinity. The electric field intensity in the dielectric strip is expressed in "physical basis functions" as the sum of three traveling waves:

$$E_z(x,y) = \sum_{1}^{3} C_n \exp(f_n x) \cosh(g_n y) \qquad (13)$$

The first term represents the "forced wave", or the field induced in an infinitely-wide dielectric slab. The last two terms represent surface waves traveling in opposite directions across the dielectric strip. The propagation constants f_n and g_n are known from an analysis of an infinitely-wide dielectric slab. Galerkin's method is employed to determine the constants C_n, and then the far-zone scattered field is calculated by considering the polarization currents radiating in free space.

Figure C.10 illustrates the backscattering pattern for a thin dielectric strip as calculated with the new method. Each point on the curve requires a CPU time of 0.3 seconds on a VAX 11/780 computer. The results obtained with the new method (physical basis) show excellent agreement with the old method (pulse basis) which involves a system of 200 simultaneous linear equations and a CPU time of 5 seconds in this example.

More recently, Kent [36] has extended this technique to the thin dielectric strip with TE polarization. His computer program requires approximately 3 hours on a large modern digital computer for each point on a scattering curve. Some additional work is needed here to make the program useful.

An analysis is still needed for a thin planar ferrite strip, which involves the magnetic polarization currents in addition to the electric polarization currents we used so successfully for the dielectric strip. We need to extend the technique to near-zone scattering problems in addition to the plane-wave scattering case which we analyzed. Finally, the physical basis approach should be applied to a perfectly conducting strip with a thin ferrite coating.

Going beyond the planar penetrable structures, we also require an insight into the scattering mechanisms for curved ferrite bodies and curved ferrite-coated conductors. These geometries are considered in the next two sections.

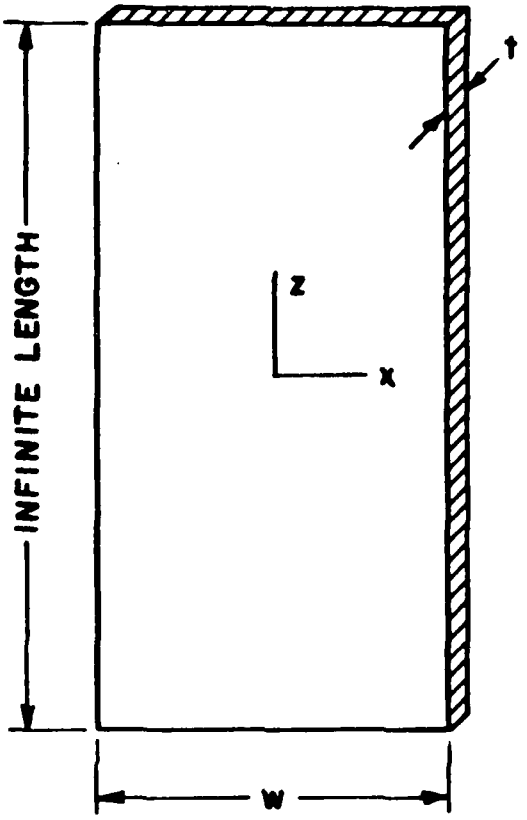

a) Side view

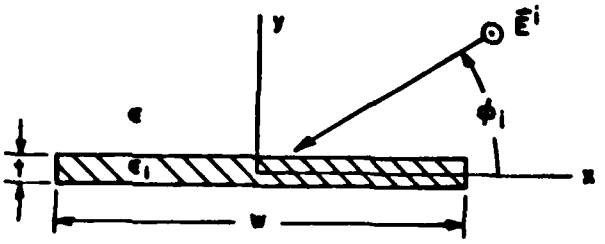

b) Cross-sectional view

Figure C.9. Thin planar dielectric strip.

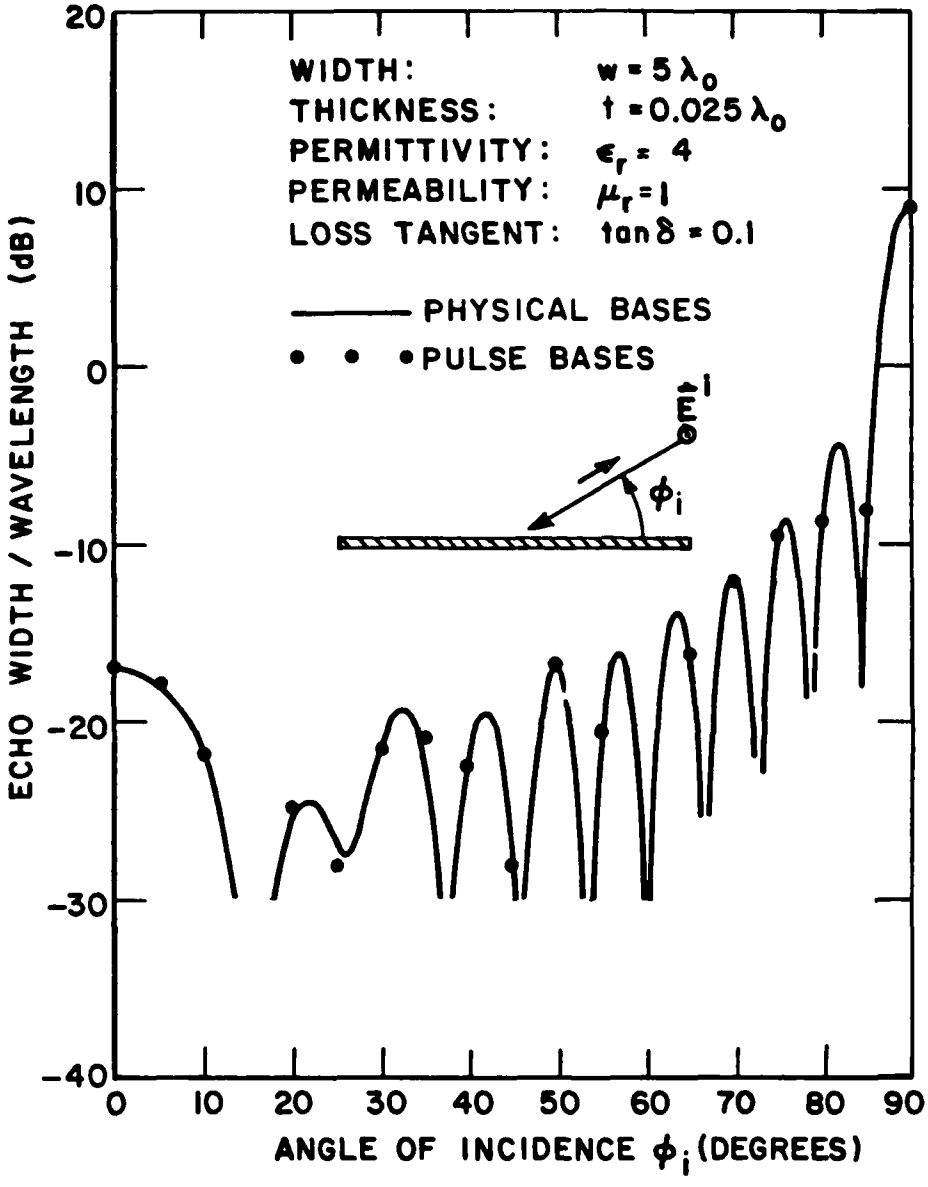

Figure C.10. Backscatter pattern for thin dielectric strip.

3. Conducting Circular Cylinder Partially Coated with Thin Ferrite Layer

In 1984, Richmond combined the moment method with the eigenfunction approach to analyze the scattering properties of an infinitely-long conducting circular cylinder which is partially coated with a thin ferrite layer. As illustrated in Figure C.11, the ferrite coating is flush mounted on the surface of the cylinder.

In the exterior free-space region, the field is expanded in cylindrical waves with integer order. In the interior ferrite region, the field is expressed in cylindrical waves with non-integer orders as determined by the angular extent of the region. The expansion coefficients in each region represent an infinite series of unknown constants.

A system of simultaneous linear equations is developed by enforcing the boundary conditions and applying Galerkin's method. For two reasons, the interior expansion coefficients are selected as the unknowns in the simultaneous linear equations. First, the series expansion converges more rapidly in the interior region than in the exterior region. Second, each of the exterior coefficients can be expressed in terms of the interior coefficients. Thus, we may regard the interior coefficients as a set of independent unknowns, and the exterior coefficients form a set of dependent unknowns.

Figures C.12 and C.13 illustrate typical results for the bistatic scattering patterns of a perfectly conducting circular cylinder partially coated with a thin ferrite layer. Results are shown for lossy coatings as well as lossless coatings.

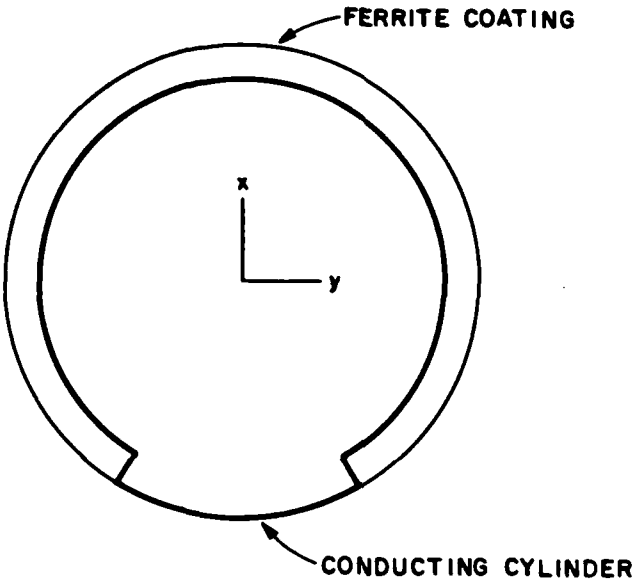

Figure C.11. Cross-sectional view of perfectly conducting circular cylinder partially coated with thin ferrite layer.

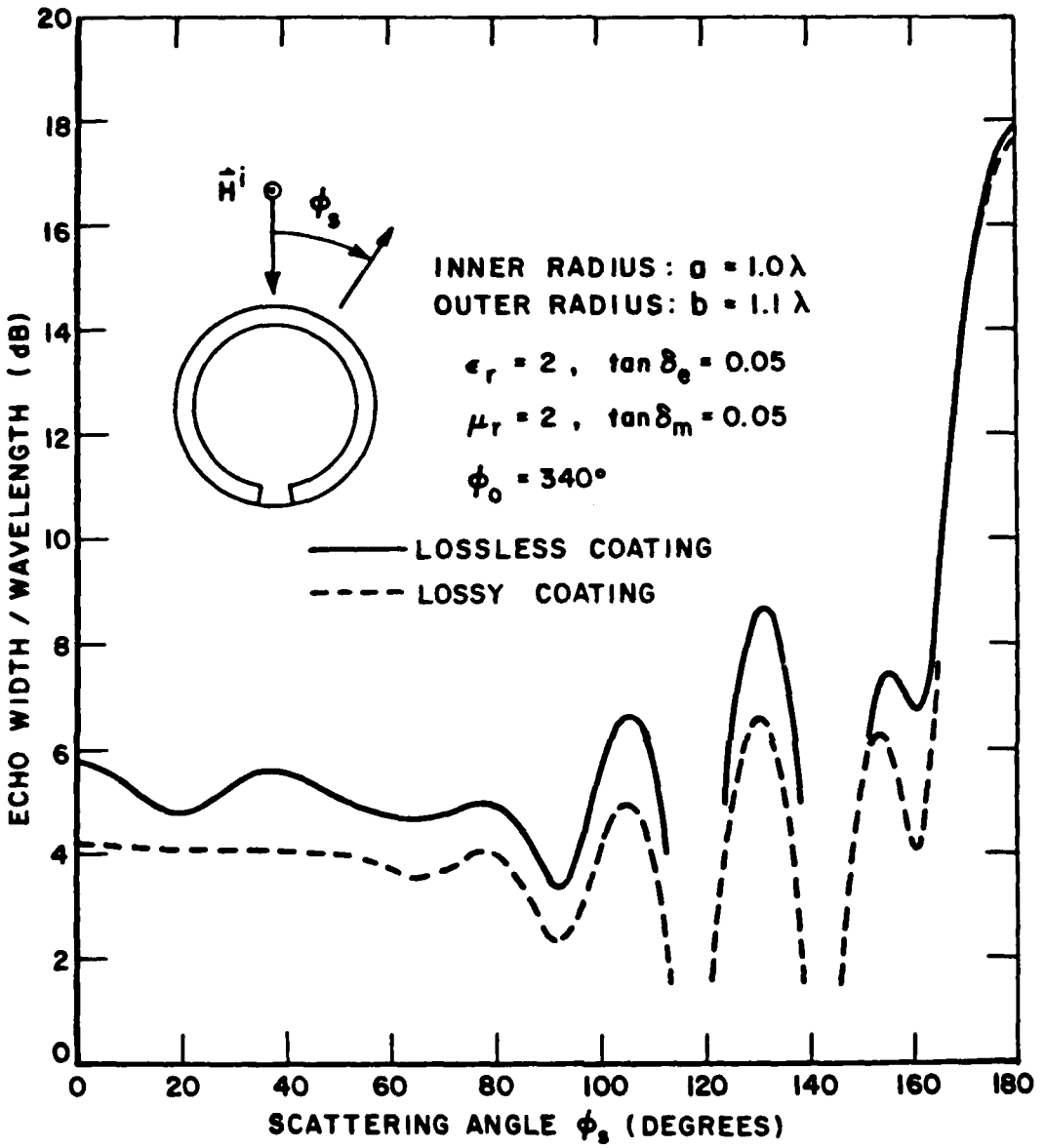

Figure C.12. Bistatic scattering pattern of perfectly conducting circular cylinder with thin ferrite coating for TE polarization.

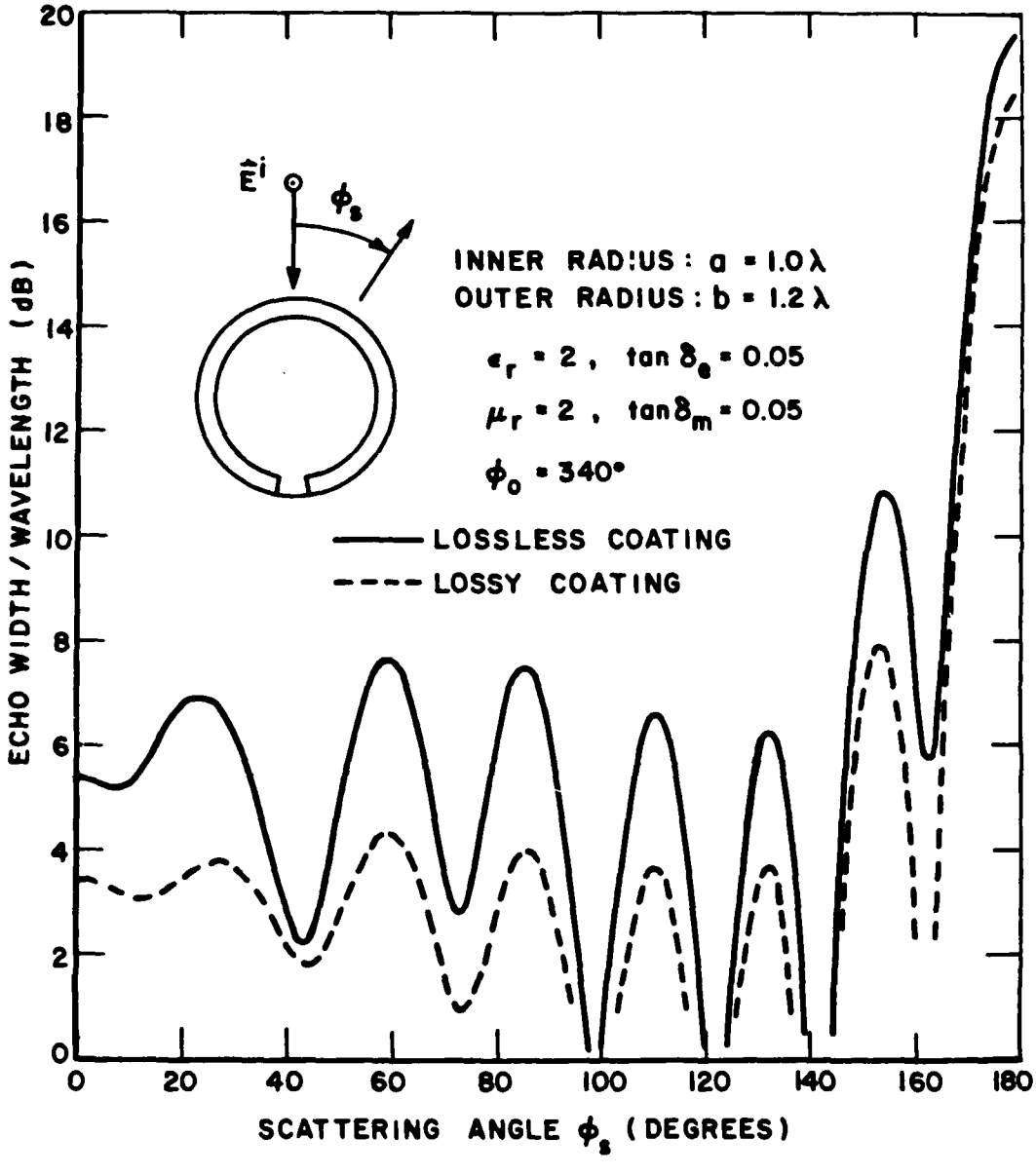

Figure C.13. Bistatic scattering pattern of perfectly conducting circular cylinder with thin ferrite coating for TM polarization.

To increase greatly the computational efficiency, and to understand the scattering mechanisms i volved in this geometry, we need to introduce the physical basis technique into the theory and the computer program.

4. Diffraction by Thin Curved Ferrite Strip

Figure C.14 illustrates a thin curved ferrite strip with infinite length, inner radius "a", and thickness t. In several ways, this geometry is more challenging than the planar ferrite strip considered earlier. We analyzed the thin curved ferrite strip by two methods in the current reporting period (October 1984 through September 1985). The first method is the "exact" eigenfunction approach, and the second is an extension of Andreasen's thin-shell theory.

Andreasen [37] presented a simple approximate boundary condition for thin dielectric shells, and he included numerical calculations for scattering by a thin dielectric spherical shell. In a subsequent paper [38], he presented numerical results for a dipole radiating through a thin dielectric spherical shell. The accuracy of his method was uncertain, as he did not compare it with the exact solution. Therefore, we calculated the bistatic scattering pattern of a thin cylindrical dielectric shell with Andreasen's method and with the exact eigenfunction approach. The results are illustrated in Figure C.15 where one may note the excellent agreement between the two methods.

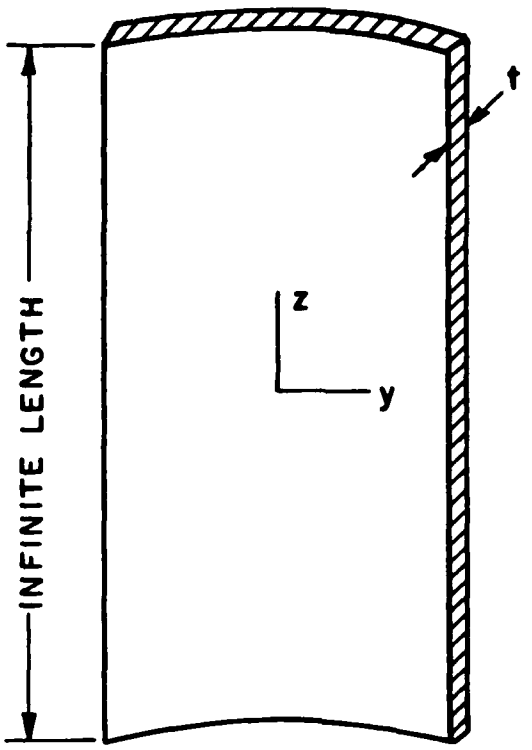

a) Side view

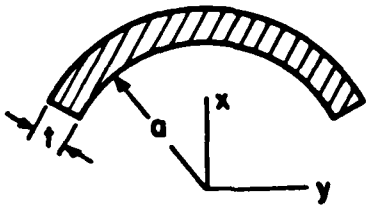

b) Cross-sectional view

Figure C.14. Thin curved ferrite strip.

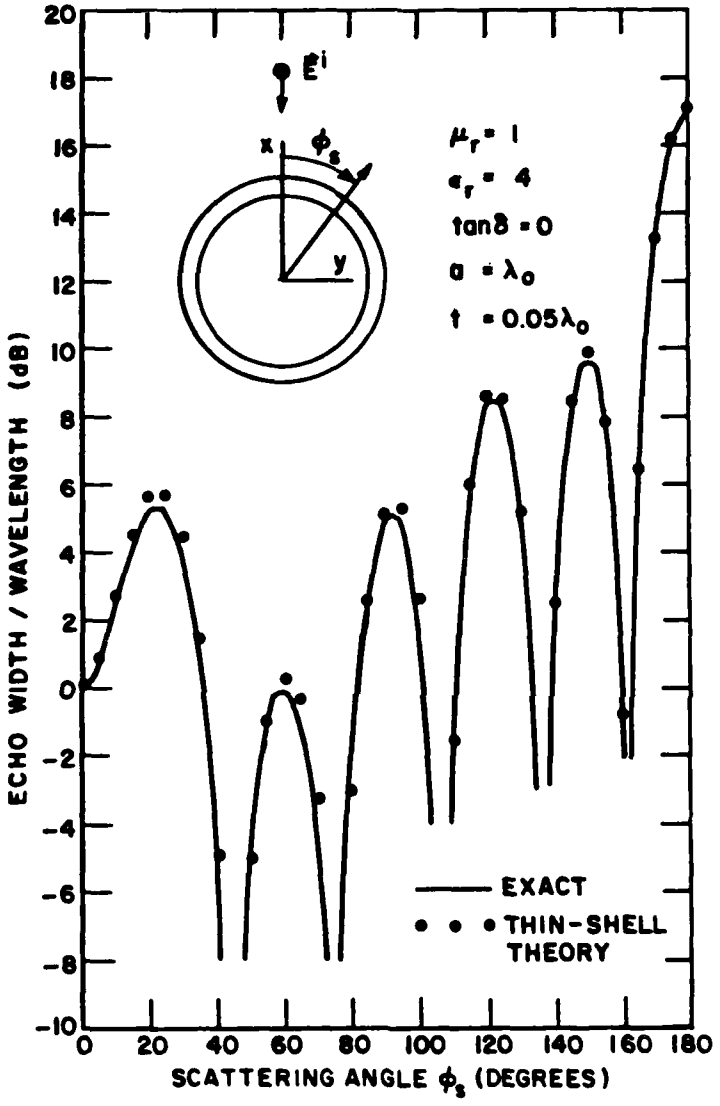

Figure C.15. Bistatic scattering pattern of thin cylindrical dielectric shell.

Andreasen presented no results for ferrite shells. Therefore, we calculated the bistatic scattering pattern of a thin cylindrical ferrite shell with Andreasen's method and with the exact eigenfunction approach. The results are presented in Figure C.16.

Having tested Andreasen's method as outlined above, we were ready to combine it with the moment method for the thin curved ferrite strip. As indicated in Figure C.17, space is divided into four regions. In the interior free-space region I, the field is expanded in integer-order cylindrical modes with Bessel functions $J_n(k\rho)$ and expansion coefficients A_n. In the exterior free-space region III, the scattered field is expanded in integer-order cylindrical waves with Hankel functions $H_n(k\rho)$ and expansion coefficients D_n. In the ferrite region II, the field is expanded in Fourier series with coefficients B_i for E_z and C_i for H_ϕ. In this region the field is considered to be a function only of the angular coordinate ϕ, and independent of the radial coordinate ρ.

Now we have four infinite sets of unknown constants: A_n, B_i, C_i and D_n. In this thin-film technique, it is not necessary to expand the field in region IV because the thin ferrite strip is replaced with an almost-equivalent strip having infinitesimal thickness and radius ρ_0 as indicated in Figure C.17. Thus, region IV also shrinks to an infinitesimal thickness. By enforcing the usual boundary conditions at radius ρ_0, and applying Galerkin's method, we develop a set of simultaneous linear equations in which the only unknowns are B_i and C_i. These equations are solved by matrix inversion, and then the remaining

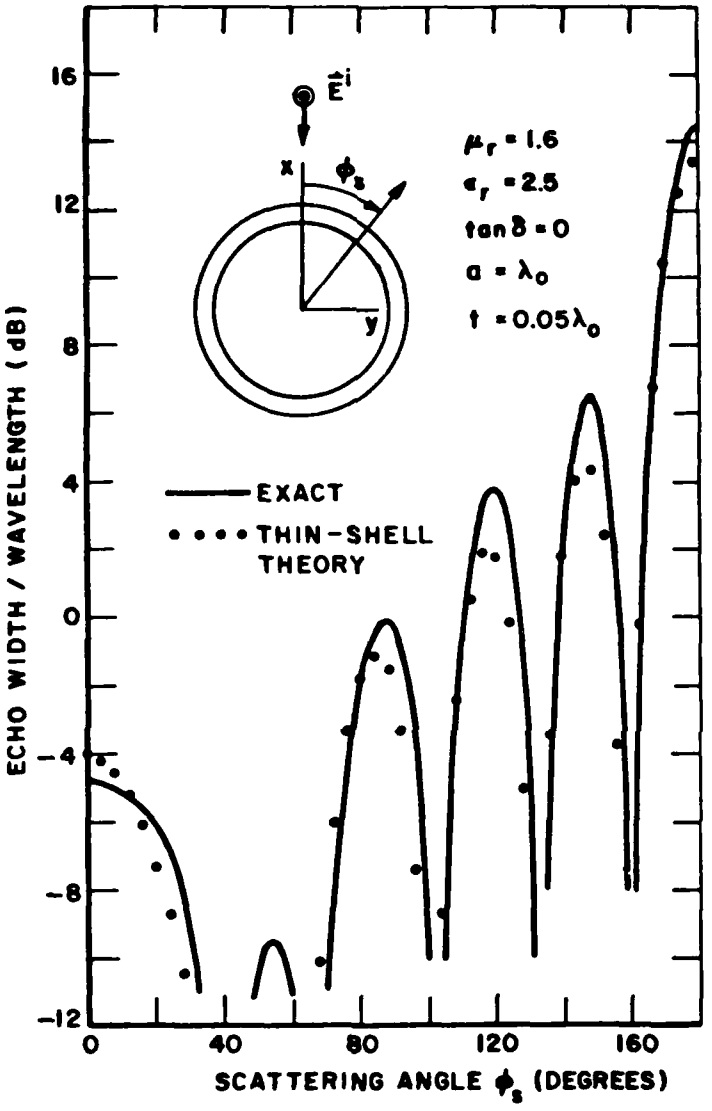

Figure C.16. Bistatic scattering pattern of thin cylindrical ferrite shell.

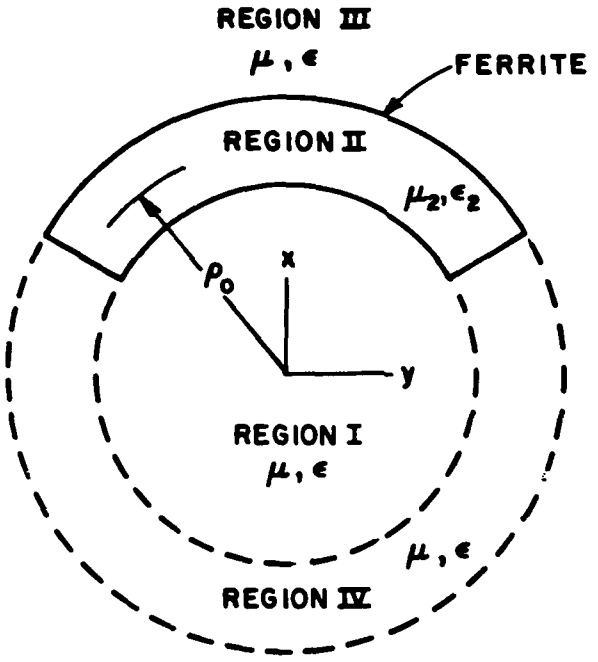

Figure C.17. Cross-sectional view of curved ferrite strip.

coefficients A_n and D_n are determined from the B_i and C_i. Finally, we calculate the far-zone scattered field and the radar cross section.

Figure C.18 illustrates the backscatter versus subtended angle for a thin curved dielectric strip, as calculated with the thin-shell theory outlined above. As the subtended angle varies from 0° to 360°, the radius ρ_o is also varied in such a way that the arc length L remains constant at five wavelengths. Figure C.18 also shows the results obtained with the original pulse-basis point-matching technique which we developed in 1965. It may be noted that the thin-shell theory shows excellent agreement with the pulse-basis technique. There are two limiting cases in which the data in Figure C.18 can be checked with independent results. When the subtended angle approaches zero, the curved dielectric strip becomes a planar dielectric strip and the data agree closely with our original results for that geometry. When the subtended angle approaches 360°, the curved dielectric strip becomes a cylindrical shell and the data agree closely with the exact eigenfunction approach.

Figure C.19 illustrates the backscatter versus subtended angle for a thin curved ferrite strip, as calculated with the thin-shell theory. It may be noted that the thin-shell theory shows excellent agreement with the eigenfunction data which are shown for comparison. Next let us outline the eigenfunction technique.

We developed the eigenfunction technique because our pulse-basis program in its present form cannot handle ferrite media. Referring to Figure C.17, the field in region I is again expanded in integer-order

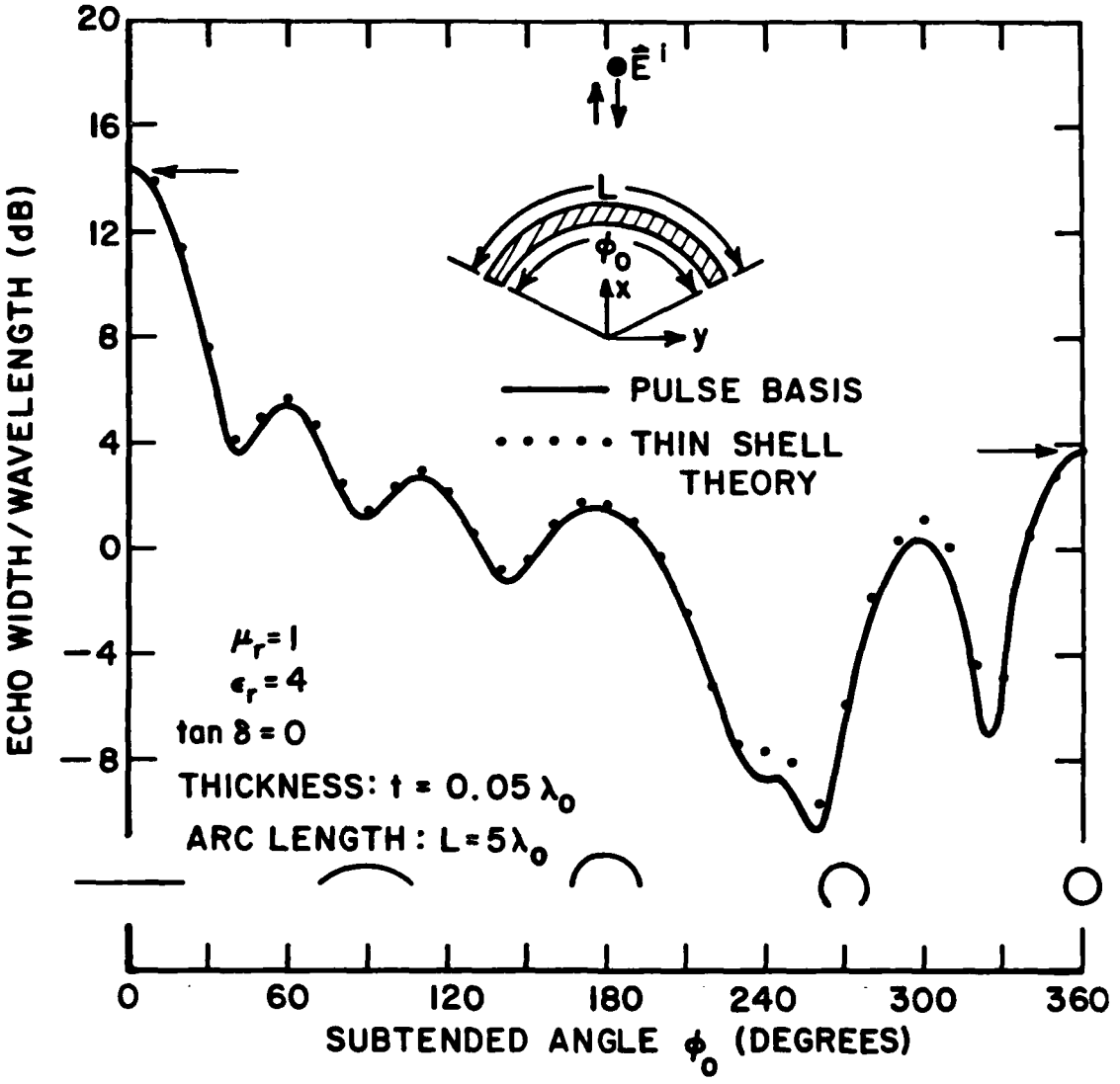

Figure C.18. Backscatter versus subtended angle for thin curved dielectric strip.

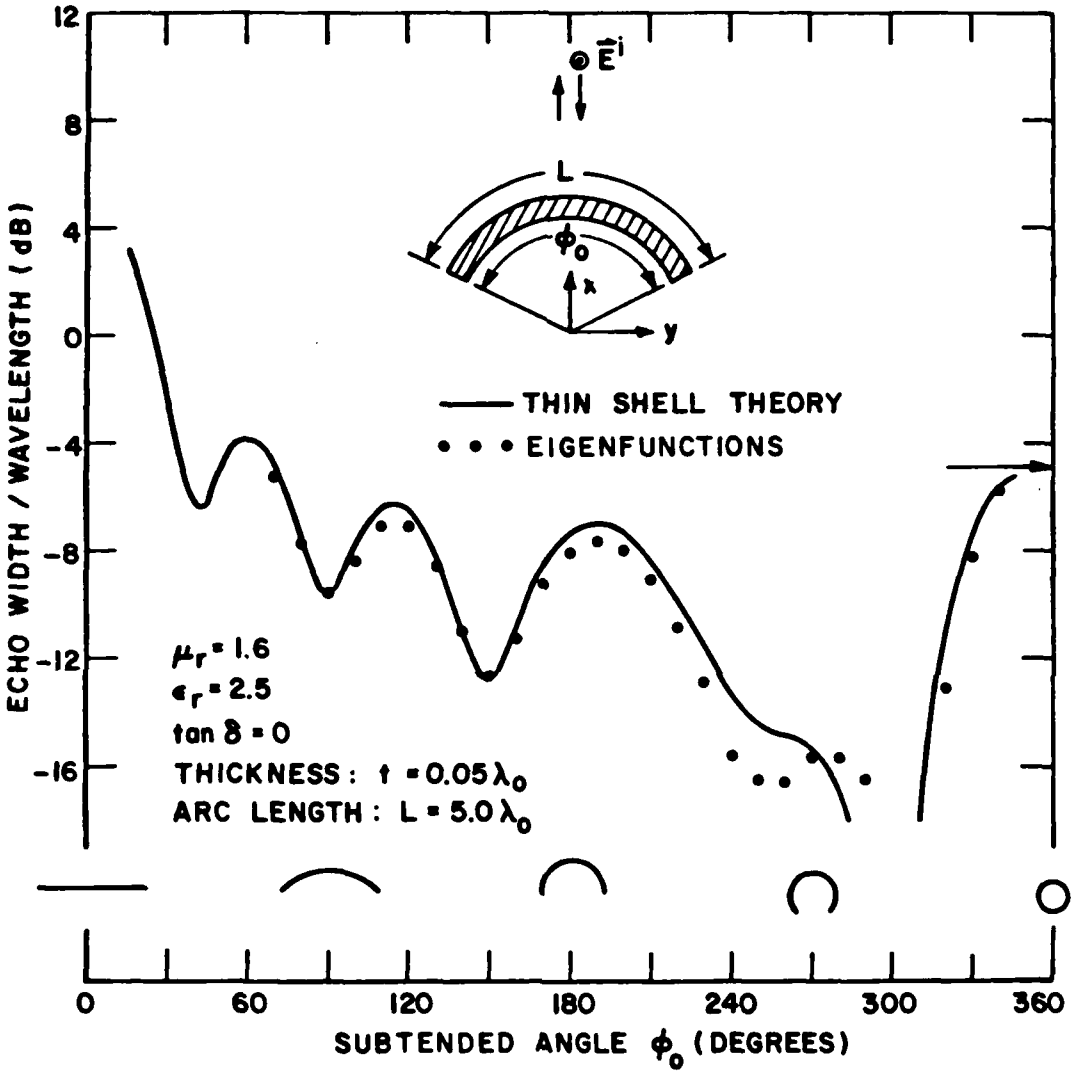

Figure C.19. Backscatter versus subtended angle for thin curved ferrite strip.

cylindrical modes with Bessel functions $J_n(k\rho)$ and coefficients A_n. The scattered field in region III is expanded in integer-order cylindrical waves with Hankel functions $H_n(k\rho)$ and coefficients D_n. Starting at this point, the eigenfunction technique differs from the thin-shell theory because we do not replace the ferrite shell with an "almost equivalent" shell having infinitesimal thickness. The field in the ferrite region II is expanded in non-integer cylindrical modes with Bessel functions $J_\nu(k_2\rho)$ and Neumann functions $N_\nu(k_2\rho)$ with coefficients B_ν and C_ν, respectively.

Similarly, the field in the free-space region IV is expanded in non-integer cylindrical modes with Bessel functions $J_u(k\rho)$ and Neumann functions $N_u(k\rho)$ with coefficients E_u and F_u respectively. Now we have defined six infinite sets of unknown constants: A_n, B_ν, C_ν, D_n, E_u and F_u. By enforcing the boundary conditions at the inner radius "a" and the outer radius "b", and applying Galerkin's method, we develop a system of simultaneous linear equations in which the only unknowns are the expansion coefficients A_n in region I. The constants A_n are determined by matrix inversion, and then the remaining constants are calculated from the A_n. Finally, we calculate the far-zone scattered field and the radar cross section. This procedure is actually a combination of the eigenfunction technique and the moment method.

It would be useful to introduce the physical basis functions into our analysis for the thin curved ferrite strips, as this would increase the computational efficiency and permit greater insight into the scattering mechanisms. It would also be useful to work out the analysis

for the TE polarization in a manner similar to the above work which concerns the TM polarization.

5. Accomplishments

During this annual reporting period, we performed a theoretical and numerical analysis of diffraction by thin curved ferrite strips. This work is summarized in Section 3 above, and it may be outlined as follows:

First we investigated the accuracy of Andreasen's thin-shell theory by comparing it with the exact eigenfunction solution for thin cylindrical ferrite shells. Then we combined Andreasen's theory, the eigenfunction approach and the moment method to develop a thin-shell theory for curved ferrite strips.

To verify the accuracy of our thin-shell program, we had to compare the results with independent formulations. For thin curved dielectric strips, our new calculations showed excellent agreement with the old pulse-basis point-matching method. For thin curved ferrite strips, our calculations showed excellent agreement with a new eigenfunction method which avoids the thin-shell approximations. Our thin-shell program was found to be considerably more efficient than the point-matching program or the eigenfunction program for the thin curved strips.

6. Future Research

In a project supported in part by Rockwell International, we will investigate the scattering properties of a conducting sphere with a thin ferrite coating. We will develop the exact eigenfunction solution, the physical-optics approximation, and the geometrical-optics form. Numerical results will be calculated to permit comparisons among these three techniques. This initial study could lead eventually to investigations of other ferrite-coated bodies with three-dimensional geometries.

We will attempt to extend the techniques in Section 3 to diffraction problems involving a curved conducting strip with a thin ferrite coating. The geometry will be the same as in Figures C.14 and C.17 with the addition of a conducting strip on the inner radius of the ferrite strip. The angular extent of the conductor will coincide with that of the ferrite. This is a very challenging task in several ways, but it appears to be within the realm of feasibility.

As summarized in Section 1, we have developed an efficient solution for scattering by a thin planar dielectric strip. In its present form, this solution is restricted to dielectric strips (as opposed to ferrite strips), and plane-wave incidence. By introducing the plane-wave spectral expansion, we will attempt to eliminate these restrictions while retaining the advantages of the physical basis functions.

REFERENCES

[1] R.F. Harrington, Field Computation by Moment Method, New York, MacMillan, 1968.

[2] E.H. Newman and D.M. Pozar, "Electromagnetic Modeling of Composite Wire and Surface Geometries", IEEE Trans. on Antennas and Propagation, Vol. AP-26, No. 6, November 1978, pp. 784-789.

[3] E.H. Newman and D.M. Pozar, "Considerations for Efficient Wire/Surface Modeling", IEEE Trans. on Antennas and Propagation, Vol. AP-28, No. 1, January 1980, 121-125.

[4] E.H. Newman and M.R. Schrote, "On the Current Distribution for Open Surfaces", IEEE Trans. on Antennas and Propagation, Vol. AP-31, May 1983, pp. 515-518.

[5] D.M. Pozar and E.H. Newman, "Near Fields of a Vector Electric Line Source Near the Edge of a Wedge", Radio Science, Vol. 14, No. 3, May/June 1979, pp. 397-403.

[6] E.H. Newman and D.M. Pozar, "Analysis of a Monopole Mounted Near or at the Edge of a Half-Plane", IEEE Trans. on Antennas and Propagation, Vol. AP-29, May 1981, pp. 488-496.

[7] E.H. Newman and D.M. Pozar, "Analysis of a Monopole Mounted Near an Edge or a Vertex", IEEE Trans. on Antennas and Propagation, Vol. AP-30, May 1982, pp. 401-408.

[8] E.H. Newman and P. Tulyathan, "Moment Method Solution for Polygonal Plates", IEEE Trans. on Antennas and Propagation, Vol. AP-30, July 1982, pp. 588-593.

[9] E.H. Newman, P. Alexandropoulos and E.K. Walton, "Polygonal Plate Modeling of Realistic Structures", IEEE Transactions on Antennas and Propagation, Vol. AP-32, July 1984, pp. 742-747.

[10] J.H. Richmond, D.M. Pozar, and E.H. Newman, "Rigorous Near-Zone Field Expressions for Rectangular Sinusoidal Surface Monopole," IEEE Trans. Antennas and Propagation, Vol. AP-26, May 1978, pp. 509-510.

[11] P. Tulyathan, "Moment Method Solutions for Radiation and Scattering from Arbitrarily Shaped Surfaces", Ph.D. Dissertation, Ohio State University, Dept. of Electrical Engineering, Columbus, Ohio, March 1981.

[12] M.R. Schrote, "An Open Surface Integral Formulation for Electromagnetic Scattering by a Material Plate", Ph.D. Dissertation, The Ohio State University, Dept. of Electrical Engineering, Columbus, Ohio, August 1983.

[13] P. Alexandropoulous, "Electromagnetic Modeling of Arbitrary Surfaces by Polygonal Plates and/or Wires", M.Sc. Thesis, The Ohio State University, Dept. of Electrical Engineering, Columbus, Ohio, August 1983.

[14] E.H. Newman, "A User's Manual For: Electromagnetic Surface Patch Code (ESP)", Report 713402-1, July, 1981, The Ohio State University ElectroScience Laboratory, Dept. of Electrical Engineering; prepared under Contract DAAG29-81-K-0020 for the Department of the Army, U.S. Army Research Office, Research Triangle Park, North Carolina.

[15] P. Alexandropoulos nd E.H. Newman "A User's Manual for Electromagnetic Surface Patch (ESP) Code: Version II, Polygonal Plates and Wires", Technical Report 712692-3, September 1983, The Ohio State University ElectroScience Laboratory, Department of Electrical Engineering; prepared under Contract N00014-78-C-0049 for the Department of the Navy, Office of Naval Research, Arlington, Virginia 22217.

[16] E.H. Newman and M.R. Schrote, "An Open Surface Integral Formulation for the Radiation and Scattering from a Material Plate", IEEE Transactions on Antennas and Propagation, Vol. AP-32, July 1984, pp. 672-678,

[17] M.R. Schrote, "An Open Surface Integral Formulation for Electromagnetic Scattering by a Material Plate", Ph.D. Dissertation, The Ohio State University, Department of Electrical Engineering, 1983.

[18] E.H. Newman, J.H. Richmond and B.W. Kwan, "Mutual Impedance Computation between Microstrip Antennas", IEEE Trans. Microwave Theory and Tech., Vol. MTT-31, November 1983, pp. 941-945.

[19] E.H. Newman and J.E. Tehan, "Analysis of a Microstrip Array and its Feed Network", IEEE Trans. Antennas and Propagation, Vol. AP-33, April 1985, pp. 397-403.

[20] B.W. Kwan, "Mutual Coupling Analysis for Conformal Microstrip Antennas", Ph.D. Dissertation, The Ohio State University, Department of Electrical Engineering, December 1984.

[21] B.W. Kwan, E.H. Newman, and R.G. Kouyoumjian, "Mutual Coupling Between Microstrip Modes on a Dielectric Coated Cylinder", IEEE Trans. on Antennas and Propagation, in preparation.

[22] B.W. Kwan, R.G. Kouyoumjian, and E.H. Newman, "An Asymptotic Evaluation of the Mutual Impedance Between 2-D Strips on a Dielectric Coated Circular Cylinder", IEEE Trans. on Antennas and Propagation, in preparation.

[23] J.J. Bowman, T.B.A. Senior, and P.L.E. Uslenghi, Electromagnetic and Accoustic Scattering by Simple Shapes, North-Holland, Amsterdam, Ch. 8, 1969.

[24] Joint Services Electronics Program, Seventh Annual Report, prepared under Contract N00014-78=C-0049 between The Ohio State University Research Foundation and the Office of Naval Research, Report 710816-17, June 1984.

[25] E.H. Newman, "TM Scattering by a Dielectric Cylinder in the Presence of a Half-Plane", IEEE Trans. on Antennas and Propagation, Vol. AP-33, pp. 773-782, July 1985.

[26] E.H. Newman, "TM and TE Scattering by a Dielectric/Ferrite Cylinder in the Presence of a Half-Plane", IEEE Trans. on Antennas and Propgation, submitted for publication.

[27] E.H. Newman, "TM Scattering by a Dielectric Cylinder in the Presence of a Half-Plane", prepared under Contract No. L4XN-11073-907 between The Ohio State University Research Foundation and Rockwell International Corporation, ElectroScience Lab Report No. 715994-4, October 1984.

[28] J.H. Richmond, "Scattering by a Dielectric Cylinder or Arbitrary Cross Section Shape", IEEE Trans. on Antennas and Propagation, Vol. AP-13, May 1965, pp. 334-341.

[29] J.H. Richmond, "TE-Wave Scattering by a Dielectric Cylinder of Arbitrary Cross-Section Shape", IEEE Transactions on Antennas and Propagation, Vol. AP-14, July 1966, pp. 460-464.

[30] R.G. Rojas-Teran, "A Uniform GTD Analysis of the EM Diffraction by a Thin Dielectric/Ferrite Half-Plane and Related Configurations", Ph.D. Dissertation, The Ohio State University, March 1985.

[31] J.H. Richmond, "An Integral-Equation Solution for TE Radiation and Scattering from Conducting Cylinders", Report 2902-7, October 1972, The Ohio State University ElectroScience Laboratory, Department of Electrical Engineering; prepared under Grant No. NGL 36-008-138 for National Aeronautics and Space Administration, Langley Research Center, Hampton, Virginia.

[32] N. Wang, "Reaction Formulation for Radiation and Scattering from Plates, Corner Reflectors and Dielectric-Coated Cylinders", Ph.D. Dissertation, The Ohio State University, Spring 1974.

[33] R.A. Hill, "Propagation Characteristics of Parallel Polarized Surface Waves on a Grounded Lossy Dielectric Slab", Masters Thesis, Spring 1983, The Ohio State University, Columbus, Ohio.

[34] W.D. Burnside and K.W. Burgener, "High Frequency Scattering by a Thin Lossless Dielectric Slab", IEEE Transactions on Antennas and Propagation, Vol. AP-31, January 1983, pp. 104-110.

[35] J.H. Richmond, "Scattering by Thin Dielectric Strips", IEEE Transactions, Vol. AP-33, January 1985, pp. 64-68.

[36] W.J. Kent, "Plane Wave Scattering by Thin Linear Dielectric-Coated Wires and Dielectric Strips: A Moment Method Approach with Physical Basis Functions", Ph.D. Dissertation, The Ohio State University, Spring 1985.

[37] M.G. Andreasen, "Back-scattering Cross Section of a Thin Dielectric Spherical Shell", IEEE Transactions, Vol. AP-5, July 1957, pp. 267-270.

[38] M.G. Andreasen, "Radiation from a Radial Dipole through a Thin Dielectric Spherical Shell", IEEE Transactions, Vol. AP-5, October 1957, pp. 337-342.

D. TIME DOMAIN STUDIES

Researchers: David L. Moffatt, Professor
(Phone: 614/422-5749)

John T. Scheick, Professor (Mathematics)
(Phone: 614/422-4012)

Nan Wang, Senior Research Associate
(Phone: 614/422-0020)

1. Introduction

It is perhaps simplest to report the progress of our research by reviewing the contents of papers which have been published, accepted for publication, submitted for publication or are in the process of being prepared for submission for publication. The background of our studies and our long range goals have been reviewed in previous annual reports on this contract and will not be repeated here. The time domain portion of our research was initially based primarily on the problem of radar target identification under the direction of Professor Moffatt with a small effort on the K-pulse concept conducted by Professor Kennaugh, now deceased. All of the target identification research is now supported on other research programs and effort now is concentrated on the K-pulse problem which it is felt to have significant potential in antenna development, radar cross section control and in target identification.

2. "Time-domain electromagnetic scattering by open ended circular waveguide and related structure" (Published in WAVE MOTION 6 (1984) 363-387) North-Holland)

The axial electromagnetic backscattering by four objects characterized in part by either a circular aperture or a circular conducting surface were studied. Impulse response waveforms for finite and open circular waveguides, a circular loop and a circular disk were synthesized using either exact and/or approximate frequency domain scattering data. Complex natural resonances of the four objects were obtained to illustrate similar and dissimilar features. It was also demonstrated that approximate scattering solutions for a loaded open circular waveguide could be obtained by properly combining low frequency and high frequency estimates.

It is felt that this paper made several important contributions. First it was shown that the loop, disk and open circular waveguide provide acceptable averages for the scattering by finite loaded circular waveguide with potential applications to the understanding and control of the scattering by the intake and exhaust cavities of jet aircraft. The impulse response waveforms for these targets provide clear and simple interpretations of the various scattering mechanisms. In particular this paper provides a clear understanding of the waveguide modes coupled into the guide and then reflected and reradiated. The usefulness of time domain response waveforms was further illustrated by their use in the proper treatment of rational function approximations which were used to link the low frequency and high frequency data. It would be possible for example to apply simple methods to existing

measured data on a good model (electromagnetically) of a representative jet engine configuration.

3. "Natural resonance estimation", (Published in IEEE Trans. Instrumentation, Measurements, Vol. IM-34, No. 4, pp. 547-550, December, 1985)

In this paper the complex natural resonances of two good models of modern aircraft are extracted from measured electromagnetic scattering data. Models for the extraction process are extremely important because for complicated (geometrically) objects in the resonance region analytical methods fail. That is, an integral equation formulation and numerical search requires excessive computer time for other than electrically small objects. Asymptotic methods are only now beginning to be applied to targets such as aircraft for backscatter and their use for natural resonance extraction, while feasilble, has not yet been initiated.

The primary contribution of this paper is the illustration of a new scattering model which approximately accounts for the data. This is best understood in the time domain. When an aperiodic excitation is incident on an object, the first response as the wavefront moves across the object is a forced response. After the wavefront moves beyond the object the response is a natural response. For geometrically simple targets the separation is distinct and for resonance extraction in the time domain one could simply wait until the response corresponds to a natural response. For complicated objects, the picture is no longer

simple. Substructures on the object resonate long before the wavefront moves off the body. Thus the time domain response is generally a complicated combination of forced and natural response. This same process dictates the presence of an entire function in the frequency domain data. Our model, a frequency domain model, adds a constant and a term linear with frequency to the residue series. These additional terms are found at the same time as the residues. It is demonstrated that complex natural resonances with stable (with orientation) oscillatory parts can be extracted from measured scattering data on realistic aircraft. It is also demonstrated that in the use of a residue series to predict the target's scattering spectrum, poles with oscillatory parts outside the frequency span of interest must be included.

4. "K-pulse for a thin circular loop" (To be published in IEEE Trans. Antennas Propagation, December 1985)

This paper uses a pole elimination concept to obtain a time-limited input waveform, the K-pulse, for a thin conducting circular loop. The resultant response waveforms are also found to be time-limited. Therefore, by employing a K-pulse input waveform the resonance ringing associated with the cirular loop can be eliminated.

The approach used to obtain the spectrum of the K-pulse was initially suggested for a lumped parameter system. The loop however is a distributed parameter system yet the approach worked very well. It was found, however, that when the method is applied to a low Q system

such as a sphere or cylinder that the spectrum did not converge. The loop is a high Q system. To illustrate the difference, the impulse response for the loop endures for at least 8 transit times for the loop circumference whereas the impulse response for the sphere or circular cylinder endures for less than 2 transit times for the sphere circumference.

In this paper the response waveforms for K-pulse excitation were shown for broadside, 45 degrees and edge-on incidence and for two orthogonal polarizations where appropriate. The results show very clearly both the K-pulse and the response to the K-pulse are time-limited waveforms.

5. "The K-pulse and response waveforms for non-uniform transmission lines", (To be published in IEEE Trans. Antennas Propagation, January 1986)

In this paper the K-pulse concept is applied to a class of distributed-parameter systems which can be modelled by finite lengths of non-uniform transmission lines. The K-pulse for such systems is an input waveform of finite duration which yields response waveforms of finite duration at all points of the system. Numerical techniques using a finite element method are developed to derive accurate estimates of the K-pulse and response waveforms for both uniform and non-uniform transmission lines. A comparison is also made with exact results to demonstrate the accuracy and utility of the method.

The finite element analysis is developed for lines with distributed shunt conductance and also for lines with non-uniform characteristic

impedance. The effects of various terminations of the line is developed. Specific results are shown for a lossless grounded dielectric slab, a shorted uniform lossy slab and a shorted tapered line. The K-pulse and response waveform for a line with continuously varying permittivity are also given.

The next logical step in this analysis is to address the inverse problem, i.e., given the K-pulse and response waveforms, what are the electrical parameters of the line? It has been demonstrated that this can be done for lines where the impedance termination is the same at both ends of the line. Research is continuing on development of the inverse problem for the general case. The key role of the K-pulse in factoring the system before attempting synthesis is clearly established in this approach which differs from other one-dimensional inversion techniques.

6. "A method for K-pulse generation directly in the time domain", (In preparation for submission to IEEE Trans. Antennas Propagation)

Low Q scatterers such as the conducting sphere and the conducting circular cylinder have for some time defied various methods for K-pulse generation. Product expansions which work so well to generate the K-pulse spectrum for high Q structures were not effective for low Q targets. For this reason, a method for expanding the K-pulse directly in the time domain using a series of Lengendre polynomials was developed. The coefficients of this expansion come from the moments of

the K-pulse which are found indirectly from a spectral product expansion.

A direct expansion in the time domain has been shown to work well for the case of a conducting sphere. The K-pulse and the K-pulse spectrum have been obtained for this target. It has also been demonstrated that the approach works well for a simulated K-pulse.

A paper describing the time domain K-pulse expansion is in preparation. At this time, the number of terms to retain in the time domain expansion is determined by examining the spectrum of the K-pulse. It is intended to supplement this approach by showing that convergence can also be demonstrated in the time domain.

7. "K-pulse generation using the impulse response waveform of a target", (Submitted to IEEE Trans. Antennas Propagation)

All of the previous methods developed for generating the K-pulse waveform of an object required knowledge of the complex natural resonances of the object. In this paper, a method for generating the K-pulse is developed which requires only an estimate of the impulse response waveform of the target. The response to the K-pulse waveform comes from convolution of the K-pulse with the impulse response waveform of the traget. We are ideally suited to obtain target impulse response waveform estimates using the state-of-the-art compact scattering range at the ElectroScience Laboratory. The K-pulse is modelled as a weighted string of delta functions and the energy in the response

waveform in the time interval beyond the estimated response waveform duration is minimized. An exisitng minimization program is used because the matrices involved usually represent an ill-conditioned problem. This approach has been shown to yield excellent results for both real targets (wires, loop, etc.) and simulated K-pulse results.

It is felt that the material in this paper represents a very significant contribution because we are now no longer dependent on complex natural resonance extraction for K-pulse estimation. The next step, as a follow-on to this paper, is to isolate the response from particular substructures using our broadband scattering range and time domain gating. The K-pulse estimation procedure developed in this paper would then be used to obtain K-pulse waveforms for the substructures. This paper also develops a procedure whereby once the K-pulse has been estimated, the dominant complex natural resonances of the target can be extracted from the K-pulse.

8. Summary

Three methods for generating the K-pulse input waveform of a target have been developed. Generation of the K-pulse directly in the time domain using an expansion of Legendre polynomials is considered to be a major step since it permits K-pulse development for low Q targets. Also, the ability to obtain K-pulse waveform estimates from multiple frequency real ($j\omega$) scattering data is considered to be another major step. K-pulse development without a prior knowledge of the complex

natural resonances of the scatterer is a significant achievement which will permit extended use of the state-of-the-art compact scattering range at the ElectroScience (ESL) Laboratory. We have been aided recently in our studies by the Ohio State University Mathematics Department* and can now state confidently that our assumed mathematical properties of the K-pulse spectrum are correct.

The K-Pulse concept can be used with an asymptotic theory such as the geometrical theory of diffraction (GTD) to obtain complex natural resonances of simple shapes. It does not appear, however, that GTD can be used to obtain a first estimate of the K-pulse.

In our opinion, all of the major tools for applying the K-pulse concept to practical problems in target identification, antenna development and cross section control are now in hand. We are ready then to utilize the scattering data on realistic targets available from our compact range facility.

*Professor J.T. Scheick

PUBLICATIONS

"Time-domain electromagnetic scattering by open ended circular waveguide and related structure", D.L. Moffatt, C-Y Lai and T.C. Lee, WAVE MOTION 6, (1984) pp. 363-387.

D.L. Moffatt and T.C. Lee, "Time-Dependent Radar Target Signature, Synthesis and Detection of Electromagnetic Authenticity Features", Inverse Methods in Electromagnetic Imaging-Part 1, pp. 441-460, D. Reidel Publishing Co., Netherlands, 1985.

E.M. Kennaugh, D.L. Moffatt, "Transient Current Denisty Waveforms on a Perfectly Conducting Sphere", Inverse Methods in Electromagnetic Imaging-Part 1, pp. 1-31, D. Reidel Publishing Co., Netherlands, 1985.

ACCEPTED FOR PUBLICATION

"Natural resonance estimation", D.L. Moffatt and C-Y Lai, to be published in IEEE Trans. Antennas Measurements, December 1985.

"K-pulse for a thin circular loop", H.T. Kim, N. Wang and D.L. Moffatt, To be published in IEEE Trans. Antennas and Propagation, December 1985.

"The K-pulse and response waveforms for non-uniform transmission lines", E.M. Kennough, D.L. Moffatt, and N. Wang, To be published in IEEE Trans. Antennas Propagation, January 1986.

9. Results

The purpose of this section is to show selected results taken from the papers described above.

"TIME-DOMIAN ELECTROMAGNETIC SCATTERING BY OPEN ENDED CIRCULAR WAVEGUIDE AND RELATED STRUCTURE".

The targets considered are shown in Figure D.1*, and the axial normalized radar cross sections from the structures are shown in Figure D.2. Figure D.3 shows the exact axial impulse response waveform of an open circular waveguide as obtained by inverse fast Fourier transform (IFFT) of the exact Wiener-Hopf solution. Also shown is the impulse response waveform given by an asymptotic high frequency approximation. As shown in Figure D.3, every other term in the asymptotic result (an infinite series) is non-causal. This is an anticipated result when caustic corrections are required. A modified impulse response for the open circular waveguide is shown in Figure D.4, where the non-causal portion has been corrected. Figure D.5 compares the normalized axial radar cross section for the open circular waveguide as predicted by the exact solution, the asymptotic estimate and the corrected asymptotic estimate. It is clear that the corrected version does as well as the uncorrected version in the frequency region where the estimates are reasonable.

*(Note: For the convenience of the reader Figures D.1 through D.30 and Table 1 have been grouped together at the end of the "Results" section.

The axial impulse response waveforms of a finite circular waveguide with an open or shorted rear termination are shown in Figure D.6. Predictably, the leading part of the waveforms corresponding to diffraction across the front rim are identical for both waveforms. It is also clear that the shorted termination contributes a stronger return. Not all of the second portion of the returns can be attributed to waveguide modes as there is also diffraction at the base of the guide, diffraction across the base of the guide and, in the case of the open termination, diffraction-guided wave combinations. The axial impulse response waveforms of a circular disc and a thin circular loop with the same radii are shown in Figure D.7. A doublet contribution of weight unity has been removed from the disc waveform. It is clear that the loop is a "high Q' target and the disc a "low Q" target.

Figure D.8 shows a comparison of the exact axial backscatter for a circular disc and that obtained from a rational function approximation. From approximations of this type, estimates of the complex natural resonances (CNR's) can be obtained. Estimates of the CNR's of the targets in this study are given in Figure D.9.

Various configurations for the loading of an open circular waveguide are shown in Figure D.10. It is possible to obtain an estimate of the axial backscatter spectrum of the targets shown in Figure D.10 by using a rational function to span the spectral range between the first cutoff frequency $D/\lambda=0.586$ and the frequency where asymptotic solutions are valid, $D/\lambda\approx2.6$. Figure D.11 shows the magnitude, a, and phase, b, estimates. The amplitude spectrum obtained

with this model for the case of a non-shorting disc (Figure D.10) is shown in Figure D.12, and the impulse response waveform for the model is given in Figure D.13. As noted earlier, it appears that similar rational function models could be used to combine integral equation computations and asymptotic estimates.

"NATURAL RESONANCE ESTIMATION"

Table D.1 shows the imaginary part of the complex natural resonances (CNR's) extracted from scattering data on an aircraft target. The aircraft was a good electroplated model and the measurements were made on the ESL compact range using vertical polarization and a model frequency span from 1.0 to 5.0 GHz. The incident angle given is measured from nose-on and the rotation was with the wings in a horizontal plane. With the present theoretical model which includes a first order estimate of the entire function, the extracted poles show excellent stability. However, at certain aspects the poles are simply too weakly excited to permit extraction.

Figure D.14 illustrates that CNR's on either side of a particular frequency span which is being tested must be included if the rational function model is to give a reasonable fit to a measured amplitude spectrum. In Figure D.14a, only those CNR's with imaginary parts within the spectral span being tested (2.1 to 3.2 GHz) are used for the calculated spectrum. In Figures D.14b and D.14c additional CNR's with imaginary parts outside the testing region are added to the model and the improvement is dramatic.

"K-PULSE FOR A THIN CIRCULAR LOOP"

The thin wire loop is centered at the origin of a rectangular frame and lies in the xy plane. The incidence angle is the standard polar angle measured from the z axis. Figure D.15 shows the impulse response waveform of the loop for incidence angles (theta) of 0, 45 and 90 degrees for phi polarization. Figure D.16 gives the impulse response waveform of the loop for an incidence angle of 45 degrees and theta polarization. All of the impulse response waveforms shown endure for eight or more transit times for the loop circumference.

The K-pulse for the loop is shown in Figure D.17 and the response of the loop to the K-pulse for the same incidence angles and polarizations as in Figure D.15 and D.16 are shown in Figures D.18 and D.19. In all cases, the long time ringing of the loop has been eliminated. All of this is accomplished using a single incident waveform.

THE K-PULSE AND RESPONSE WAVEFORMS FOR NON-UNIFORM TRANSMISSION LINES

Figure D.20 shows the K-pulse and response waveform for a lossless grounded dielectric slab with a relative dielectric constant of 4.0. The K-pulse and reflected waveform for a shorted uniform lossy slab are given in Figure D.21 and compared to the exact solution. Figure D.22 gives the same waveforms for the case of a shorted tapered line and Figure D.23 shows the results for a line with a continuously varying relative dielectric constant. With the finite element approach, any arbitrary finite line can now be treated.

A METHOD OF K-PULSE GENERATION DIRECTLY IN THE TIME DOMAIN

The K-pulse waveform for a perfectly conducting sphere is shown in Figure D.24, the amplitude spectrum of the K-pulse in Figure D.25 and the response of the sphere to K-pulse excitation in Figure D.26. What makes the results in Figures D.24, D.25 and D.26 remarkable is that the K-pulse for a low Q scatterer has not previously been obtained.

K-PULSE ESTIMATION FROM THE IMPULSE RESPONSE OF A TARGET

A sampled version of the K-pulse waveform for a grounded dielectric slab, reproducing the top of Figure D.20 but now obtained directly from the impulse response, is given in Figure D.27. Figure D.28 illustrates that with this approach the response of the grounded slab to the K-pulse is essentially the same as the bottom of Figure D.20. This approach is also independent of the initial guess, as two other initial guesses (Figure D.29a and b) also converged to the same result. In Figure D.30, the exact (a simulated waveform) and approximated K-pulse obtained from real frequency samples are shown. The documented proof of this method for K-pulse estimation, which does not require a priori knowledge of the CNR's of the scatterer, completes the K-pulse generation problem.

> We are now in a position to obtain the K-pulse waveform of any arbitrary scatterer or substructure of a scatterer regardless of high Q or low Q or knowledge of the CNR's.

TABLE D.1

IMAGINARY PART OF POLES OF AIRCRAFT AT VARIOUS ANGLES

	0°	15°	30°	60°	90°	120°	150°	180°	Ave
(1)	1.051	1.047	1.034	-----	-----	1.070	-----	1.098	1.060
(2)	1.345	1.311	1.348	1.321	1.354	1.381	1.373	1.365	1.350
(3)	1.611	1.747	1.635	1.536	1.575	1.663	1.620	1.627	1.627
(4)	1.995	2.039	1.920	1.944	2.028	2.055	1.994	2.017	1.999
(5)	2.293	2.160	2.332	2.253	2.257	2.375	2.344	2.402	2.302
(6)	2.663	2.635	2.503	2.647	2.615	2.578	2.666	2.549	2.607
(7)	2.995	3.005	2.841	3.073	3.021	2.958	2.893	2.972	2.970
(8)	3.320	3.345	3.321	3.384	3.320	3.238	3.231	-----	3.308
(9)	3.732	3.691	3.738	-----	-----	3.639	-----	3.507	3.661
(10)	4.036	4.182	-----	3.955	4.151	3.995	-----	-----	4.064
(11)	4.663	-----	4.394	4.739	4.482	4.510	4.551	4.549	4.555

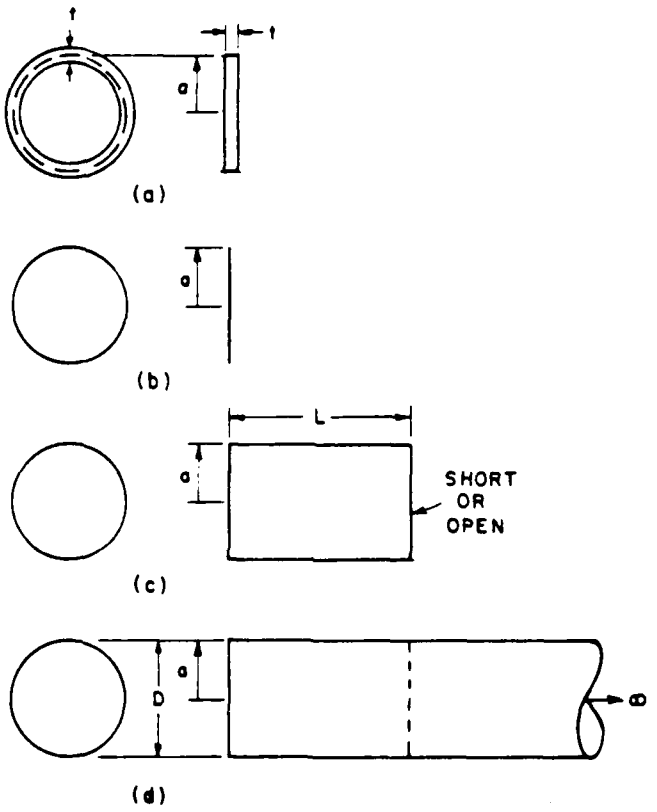

Figure D.1. Scattering geometries, 1) circular loop, b) circular disc, c) truncated circular waveguide, d) open circular waveguide.

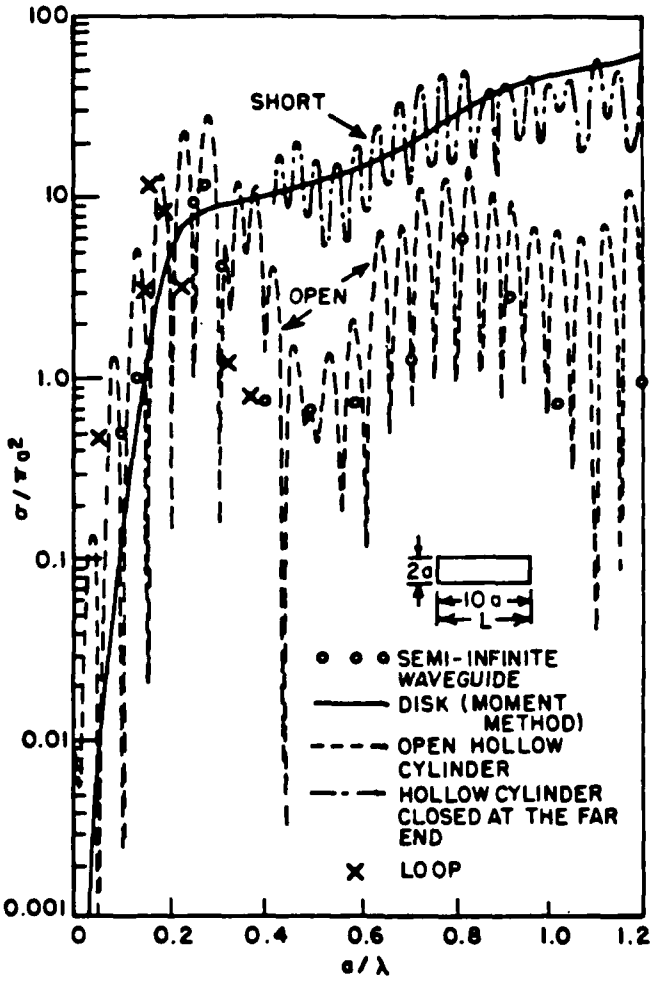

Figure D.2. Normalized axial radar cross section of finite hollow cylinders (open and shorted at far end), a circular disc and a semi-infinite circular waveguide.

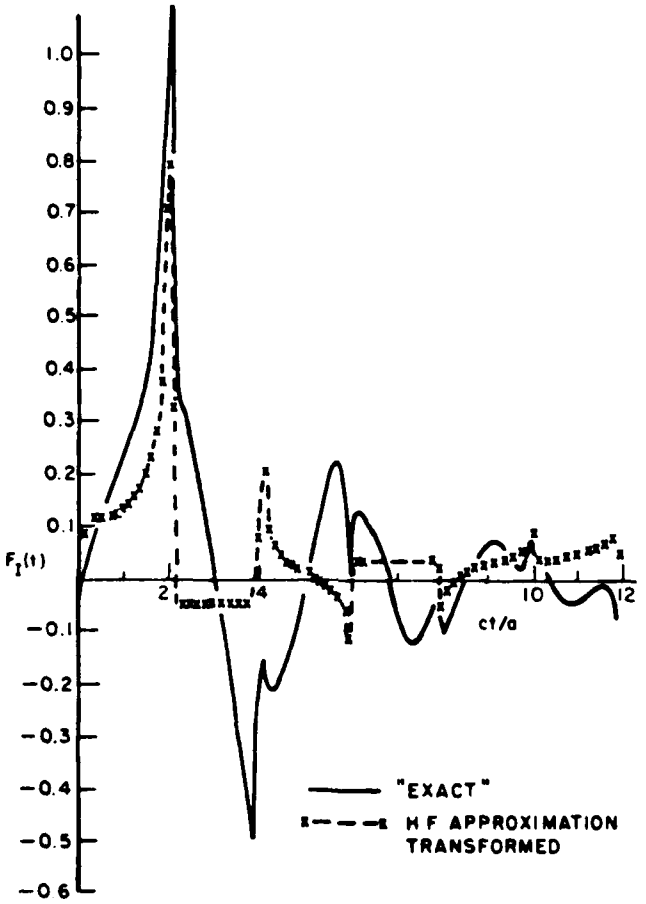

Figure D.3. Inverse Laplace transform of on-axis backscatter, comparing exact numerical results with asymptotic approximation.

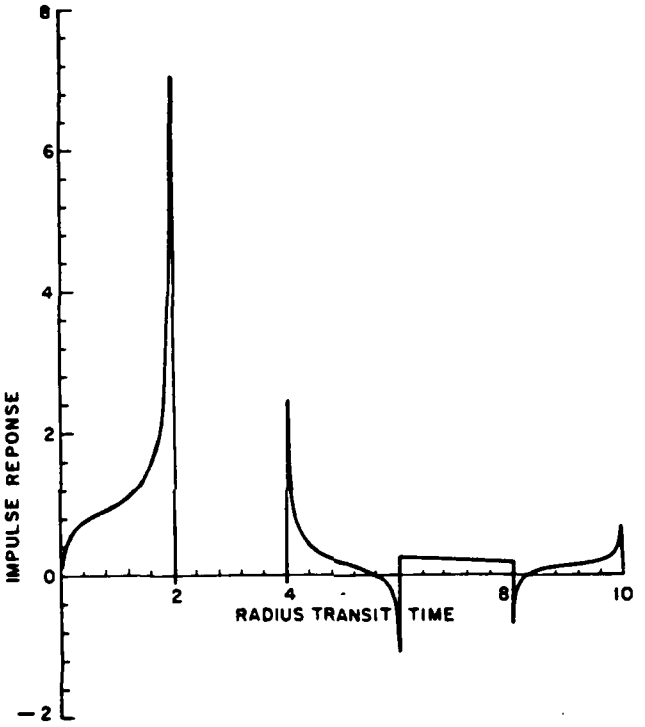

Figure D.4. Modified impulse response of on-axis backscatter with asymptotic approximation $\alpha t_0 = 8$.

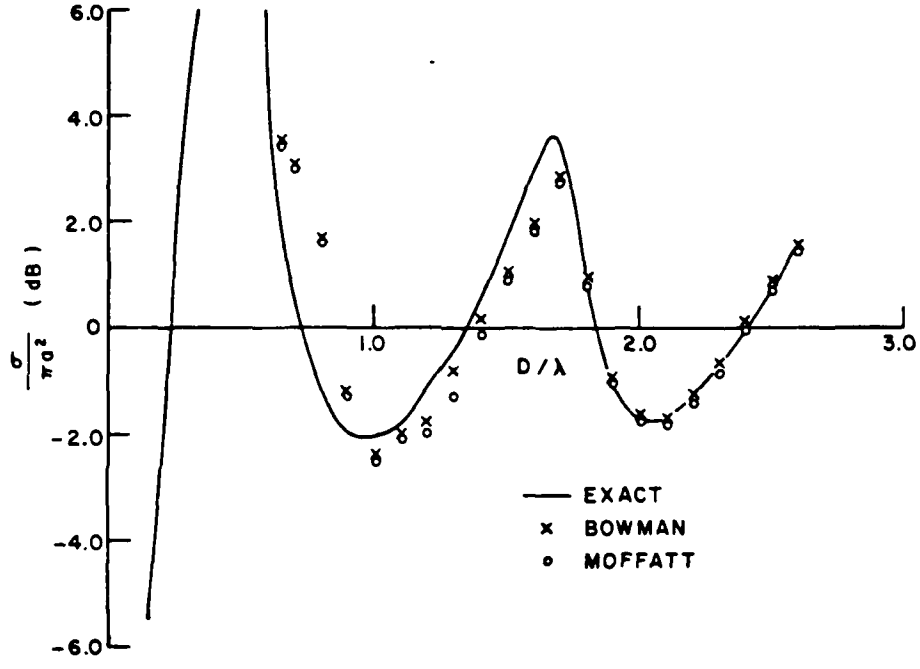

Figure D.5. Normalized axial radar cross section of an open circular waveguide. Asymptotic estimates compared to the exact result.

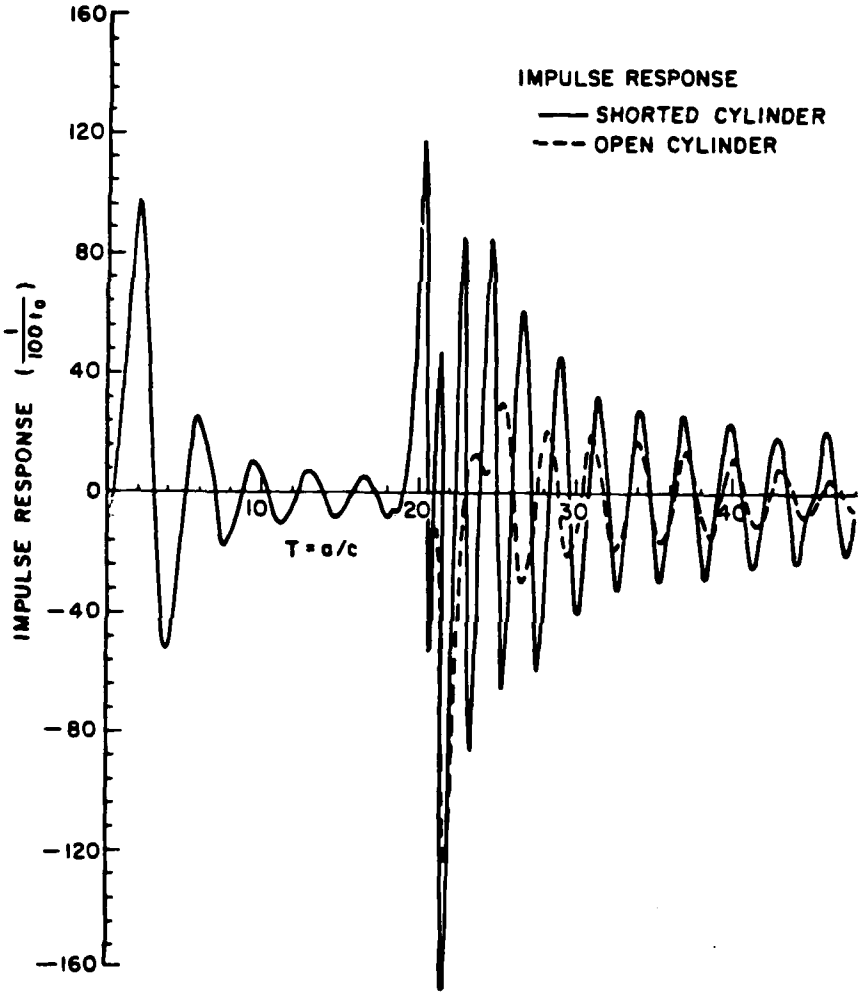

Figure D.6. On axis backscatter impulse response of finite circular waveguide shorted (solid) or open (dashed) at the rear.

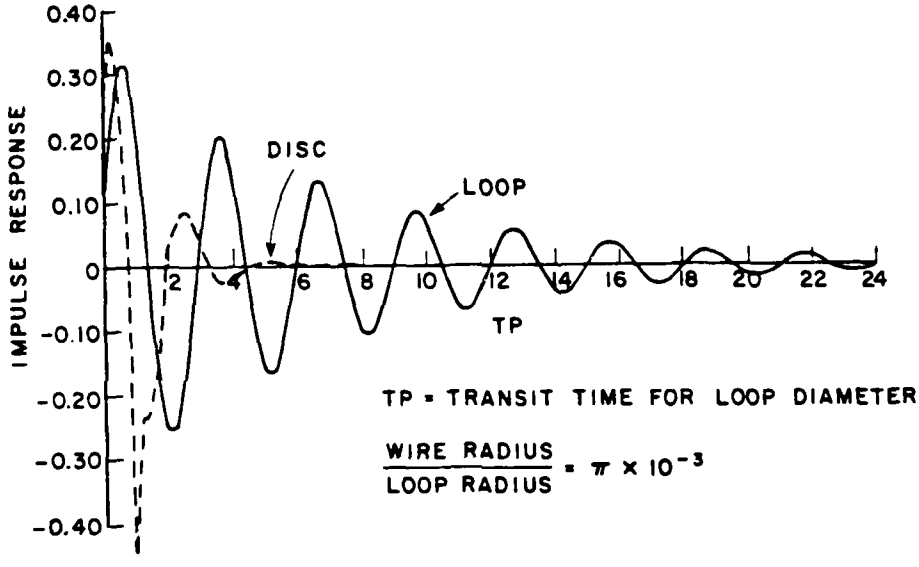

Figure D.7. Axial impulse response waveforms of a circular loop and a circular disc. The nominal radius of the loop and the radius of the disc are equal.

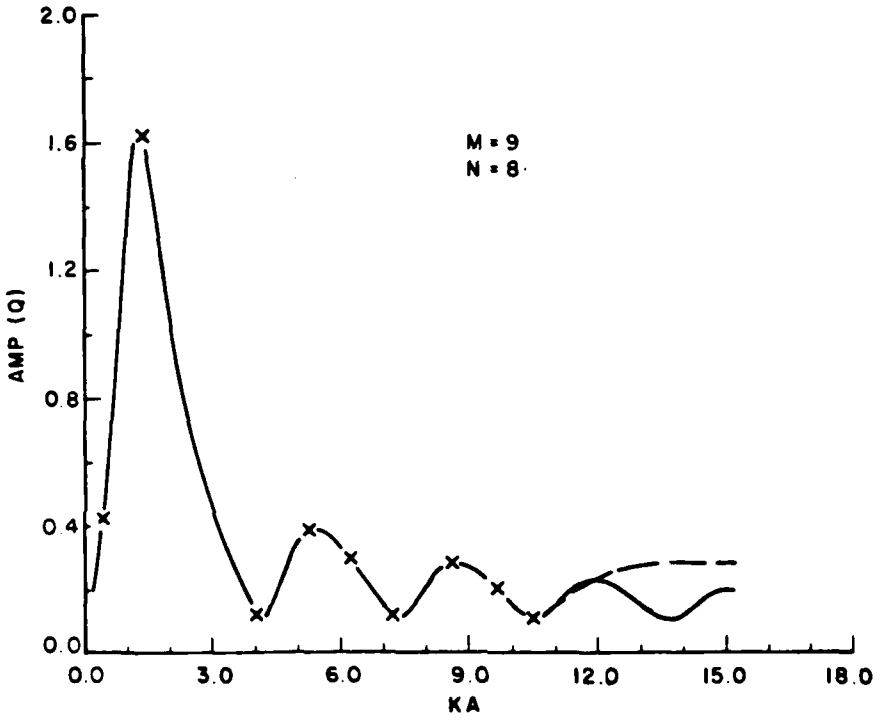

Figure D.8. A comparison of the exact backscatter and rational function approximation for the axial incidence case. Dashed curve is the rational function and the crosses are the input data points used to achieve the fit.

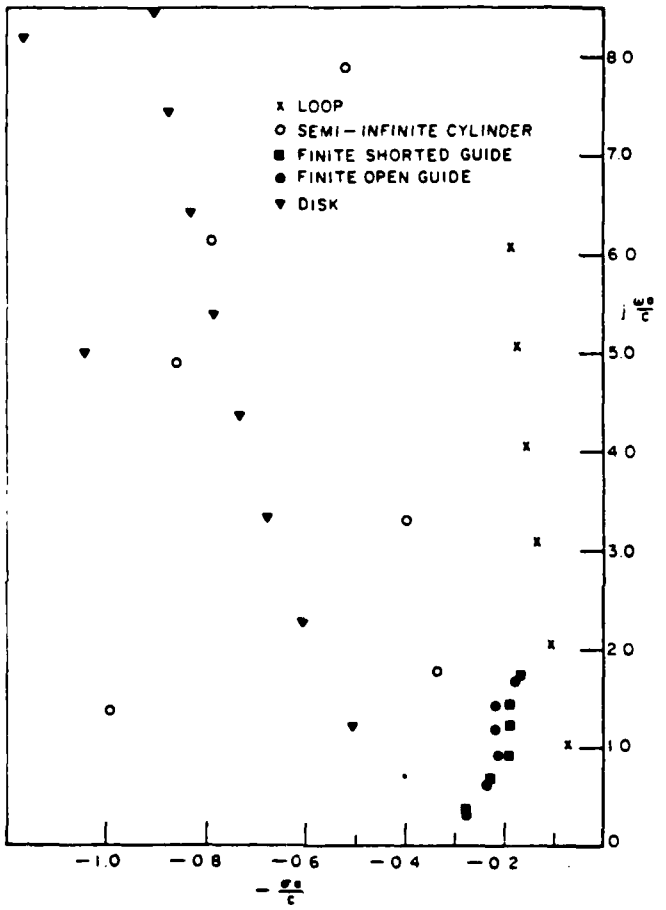

Figure D.9. Complex natural resonances extracted for the various target geometries. The resonances are in the wavenumber radius plane.

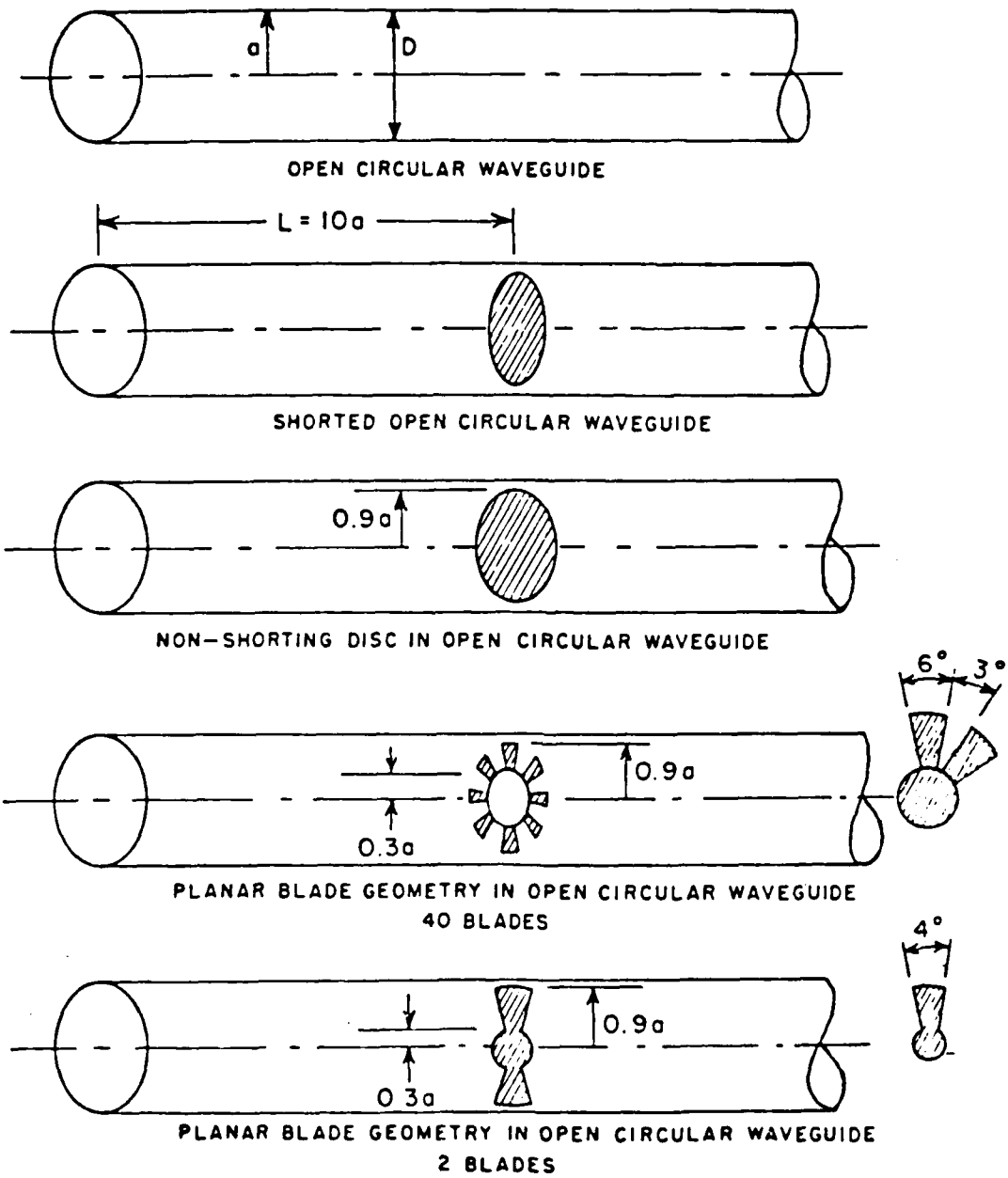

Figure D.10. Configurations of various loadings inside a semi-infinite circular cylinder.

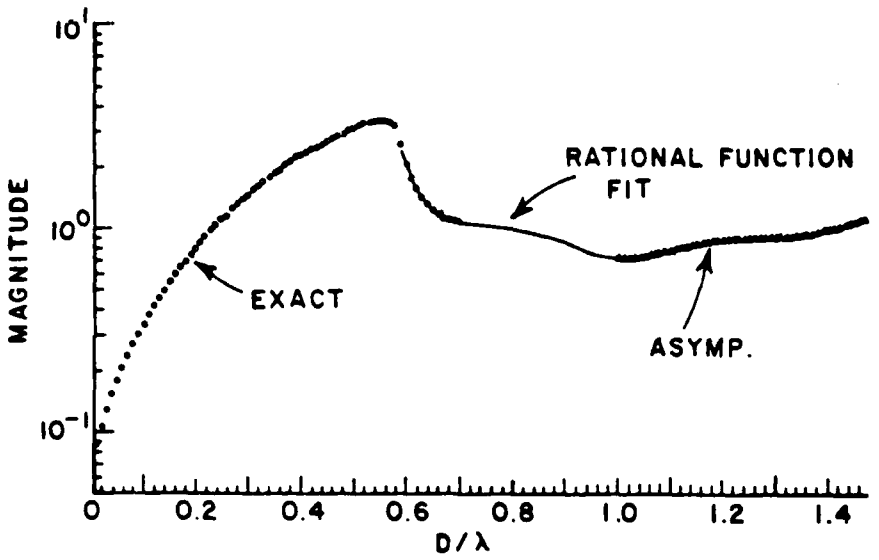

(a) Magnitude

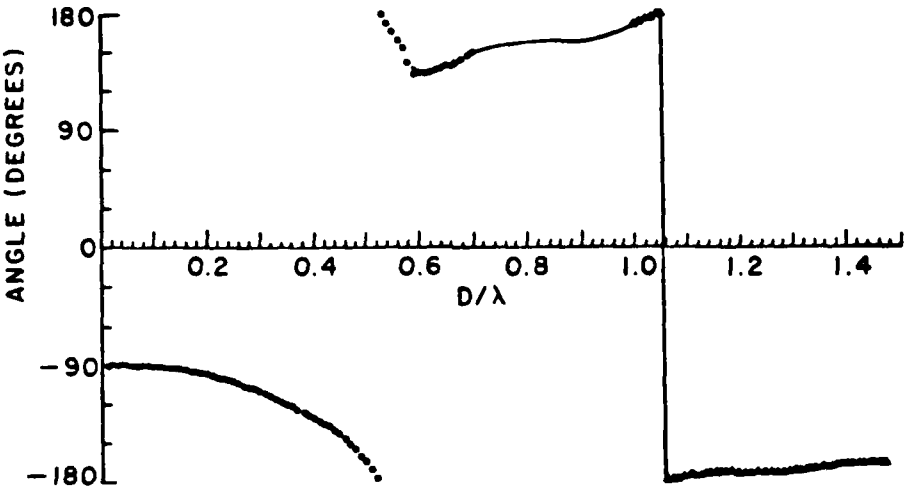

(b) Phase

Figure D.11. Frequency spectrum (phase) of semi-infinite hollow cylinder.

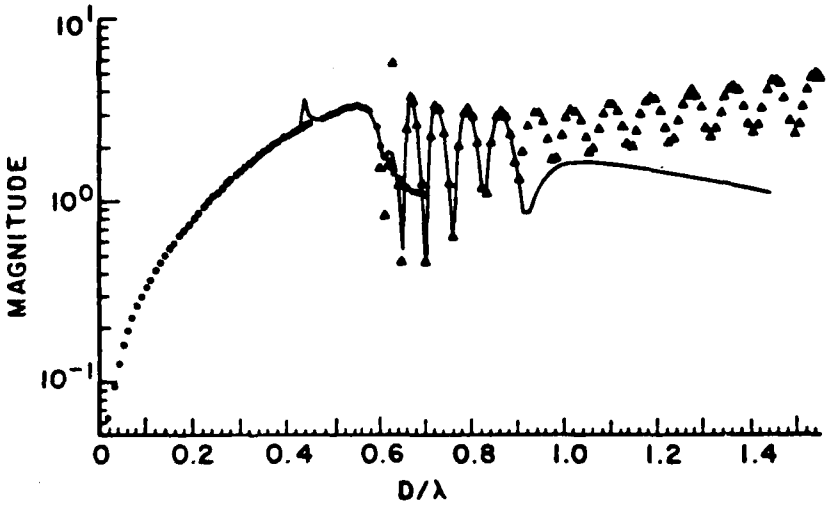

Figure D.12. Frequency spectrum (magnitude) for cylinder loaded with non-shorting disc showing behavior of rational function fit (solid line) and inside and outside the unknown region.

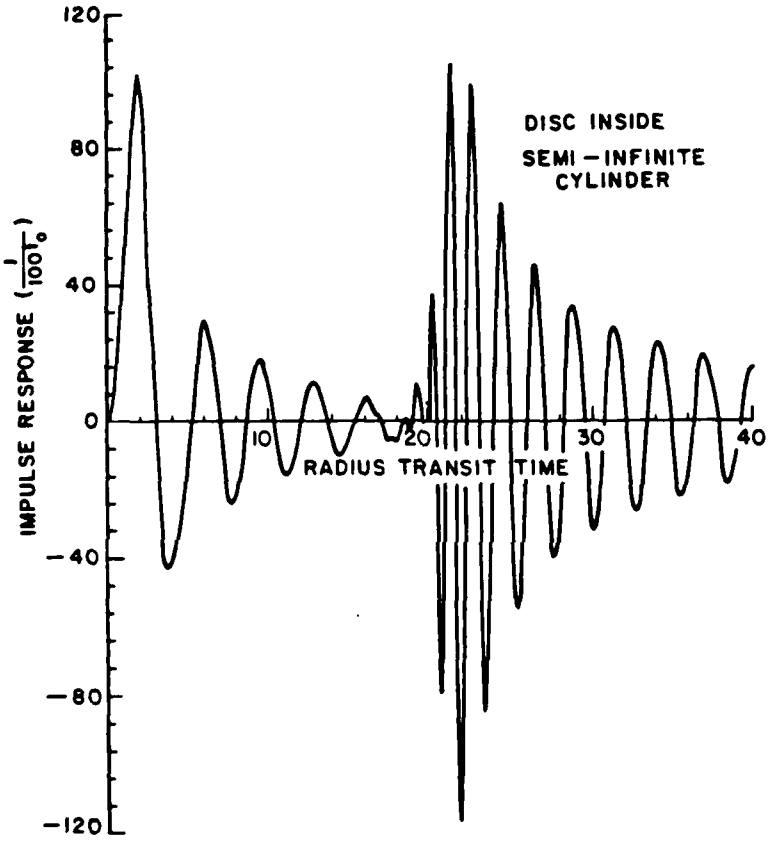

Figure D.13. Impulse response for semi-infinite cylinder loaded with non-shorting disc.

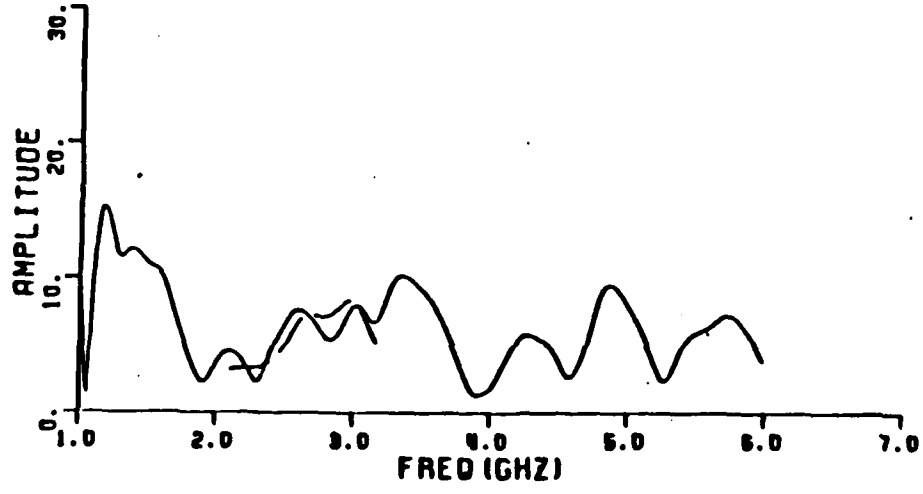

(a) Poles No. 5-7 used.

Figure D.14. Aircraft B, 15°.

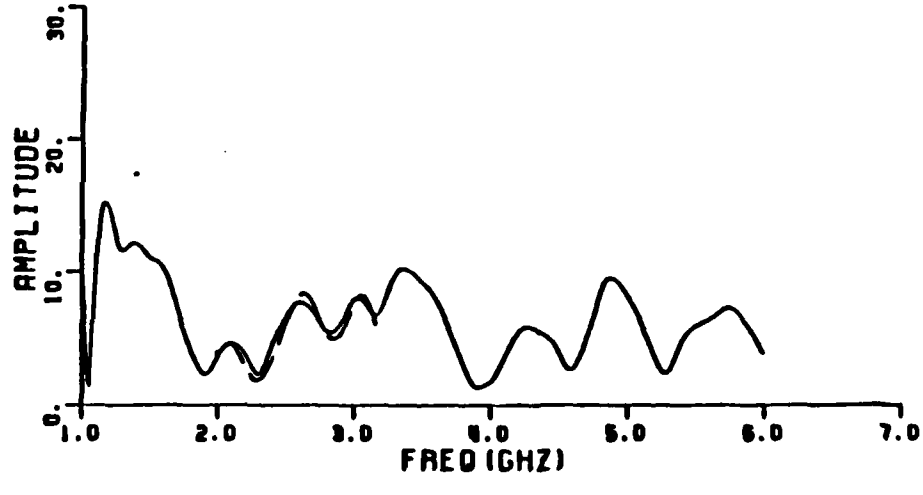

(b) Poles 3-9 used.

Figure D.14. (continued)

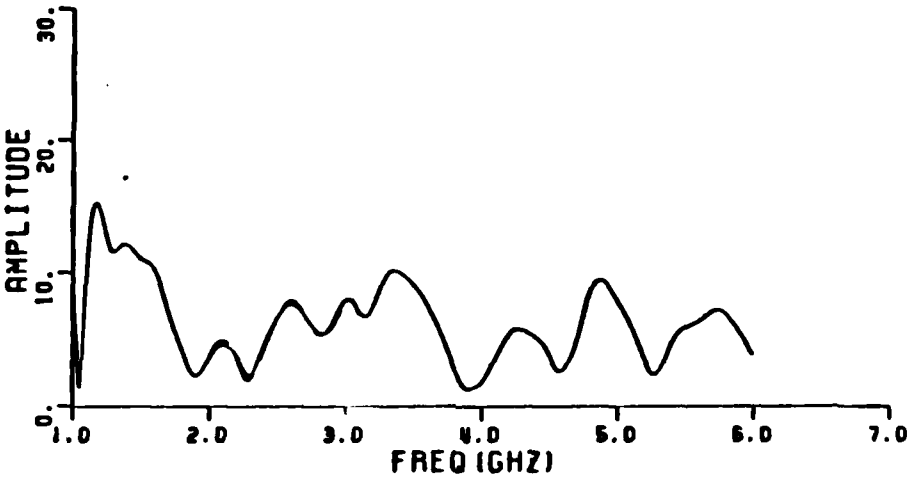

(c) Poles No. 1-10 used.

Figure D.14. (continued)

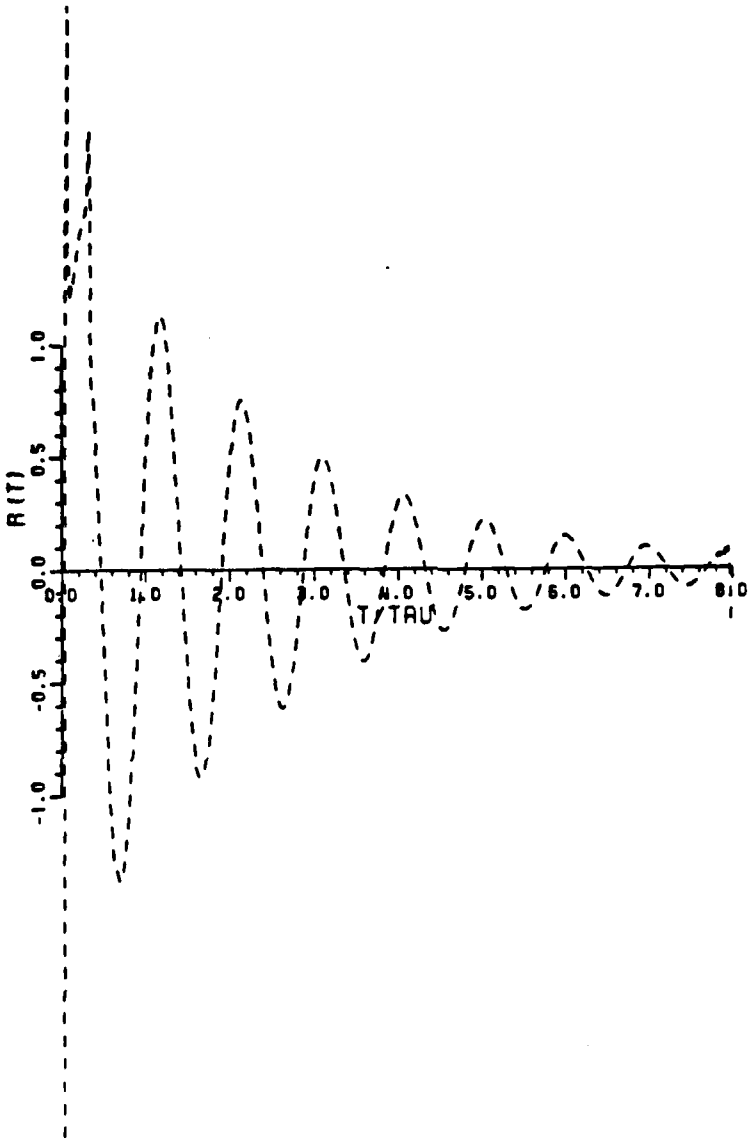

(a) $\theta_i = 0°$

Figure D.15. Impulse response waveforms for backscattering by a thin circular loop ($\hat{\phi}$-polarized incidence).

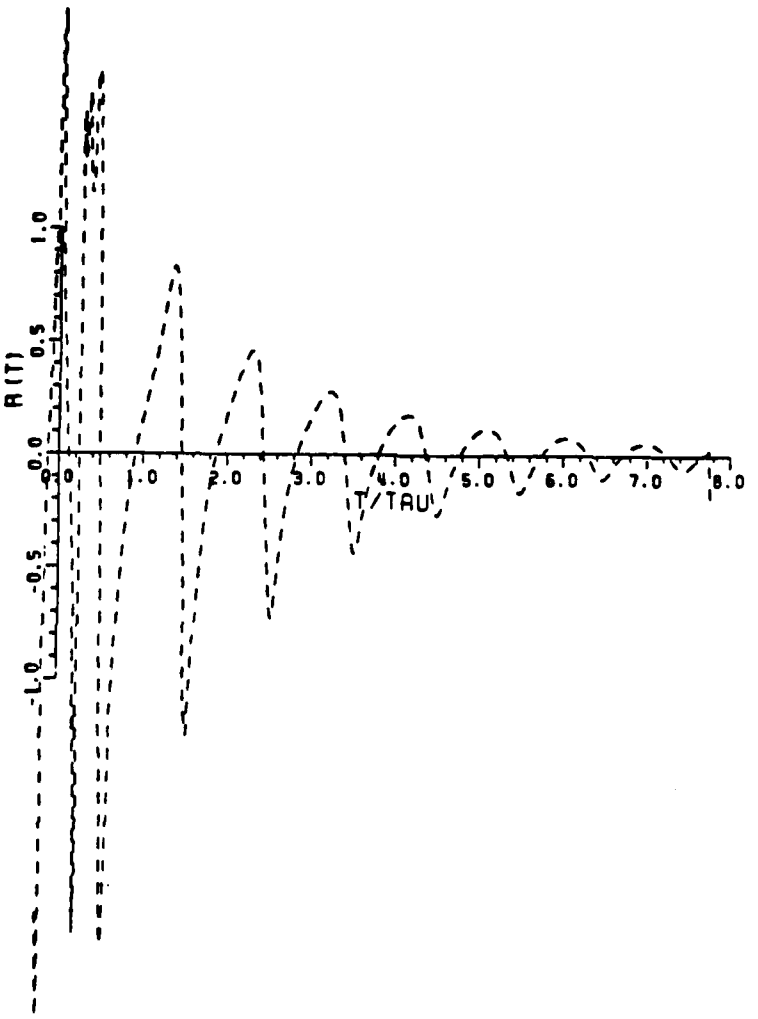

(b) $\theta_i = 45°$

Figure D.15. (continued)

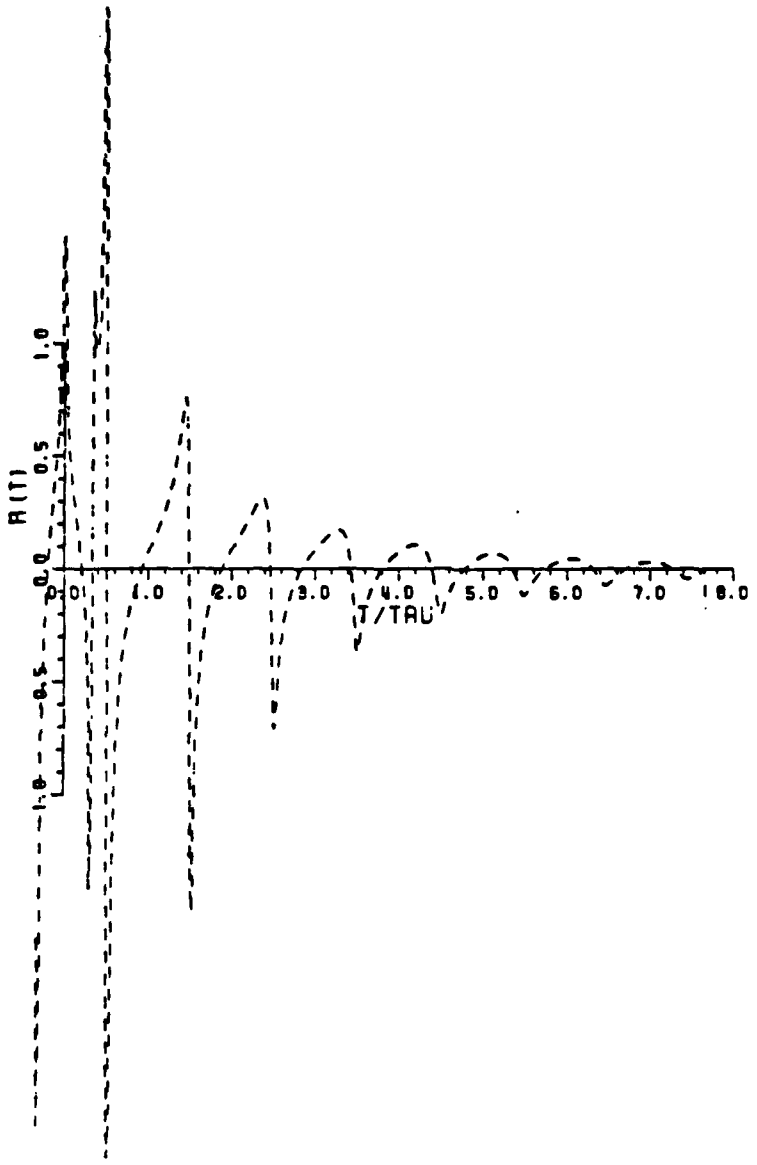

(c) $\theta_i = 90°$

Figure D.15. (continued)

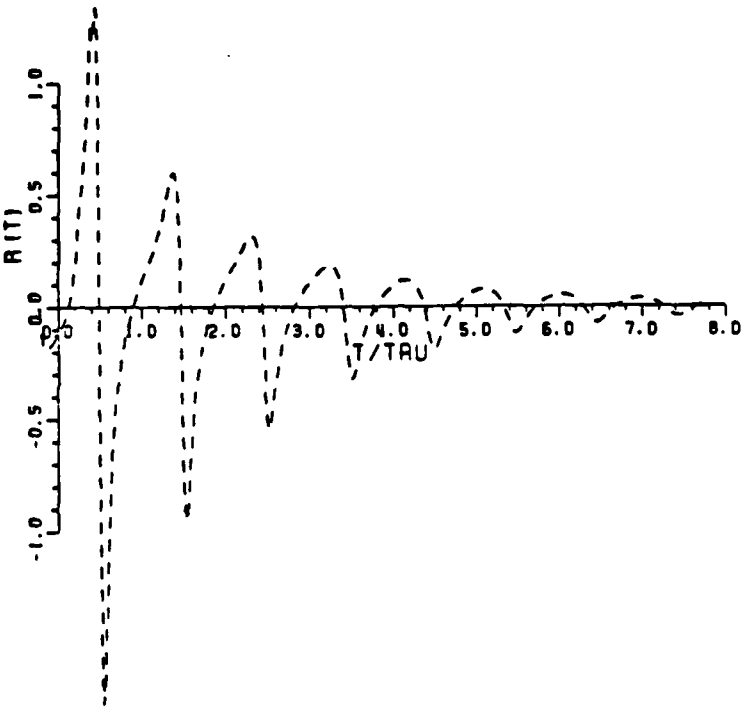

Figure D.16. Impulse response waveform for backscattering by a thin circular loop ($\hat{\theta}$ polarized incidence); $\theta_i = 45°$.

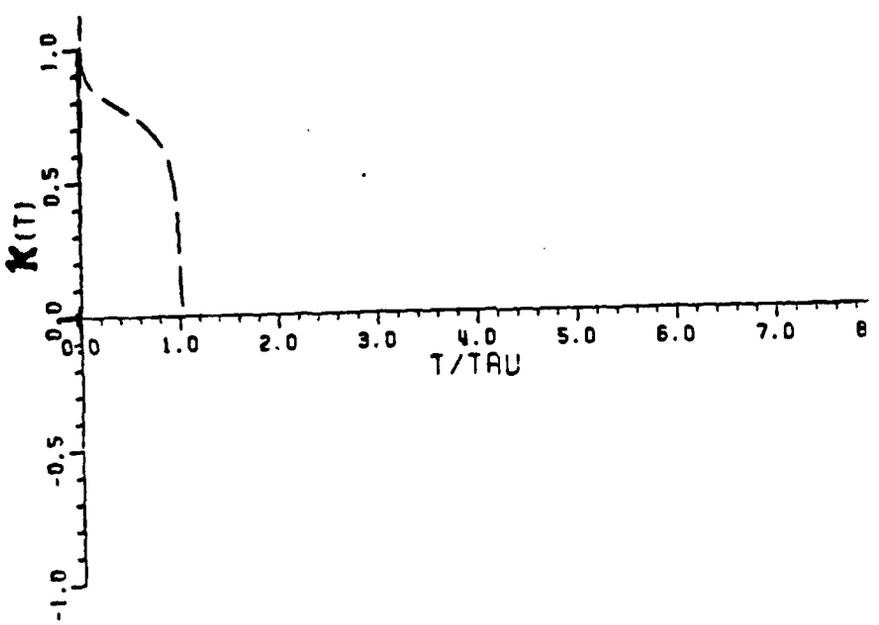

Figure D.17. Approximate K-pulse for a thin conducting circular loop.

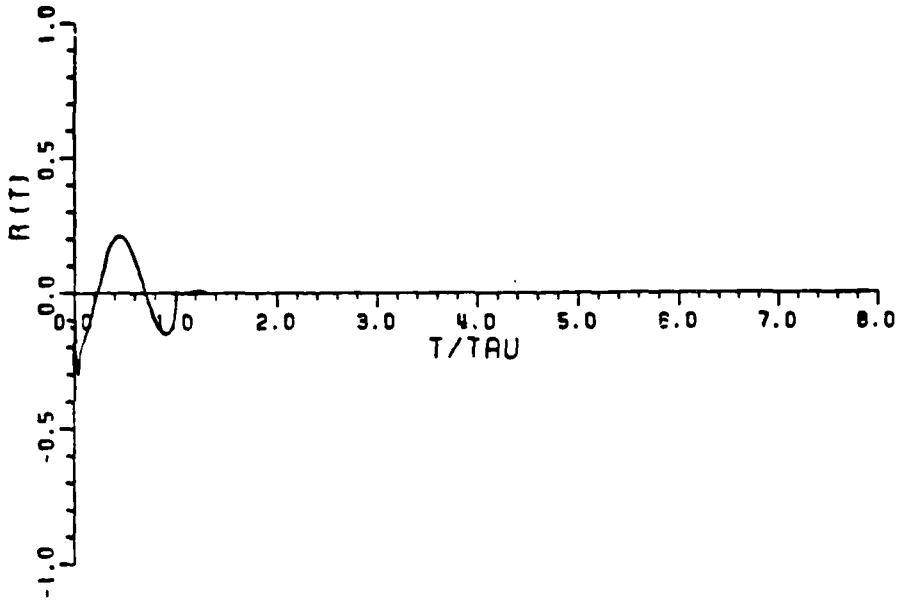

(a) $\theta_i = 0°$

Figure D.18. K-pulse response waveforms for $\hat{\phi}$-polarized incident plane wave.

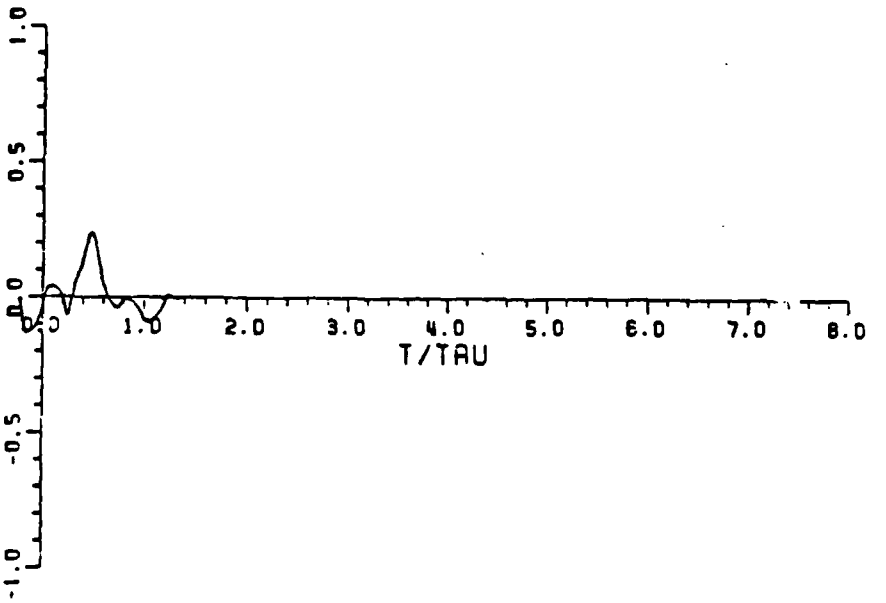

(b) $\theta_i = 45°$

Figure D.18. (continued)

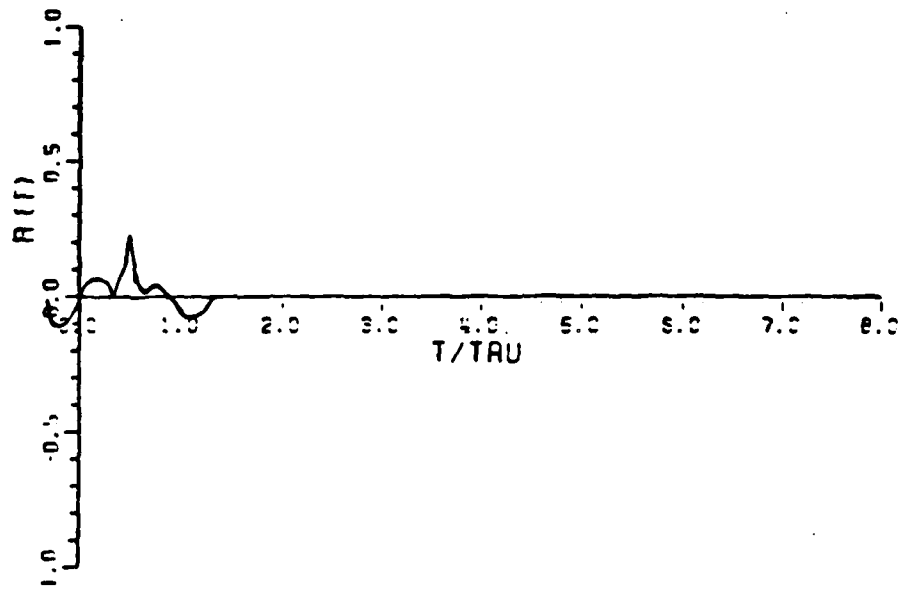

(c) $\theta_j = 90°$

Figure D.18. (continued)

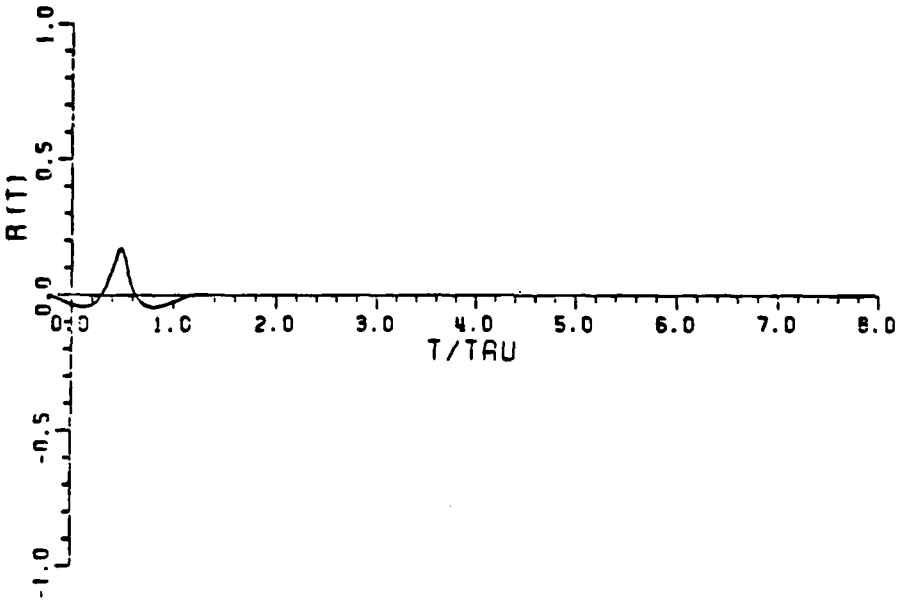

Figure D.19. K-pulse response waveforms for $\hat{\theta}$ polarized incident plane wave; $\theta_i = 45°$.

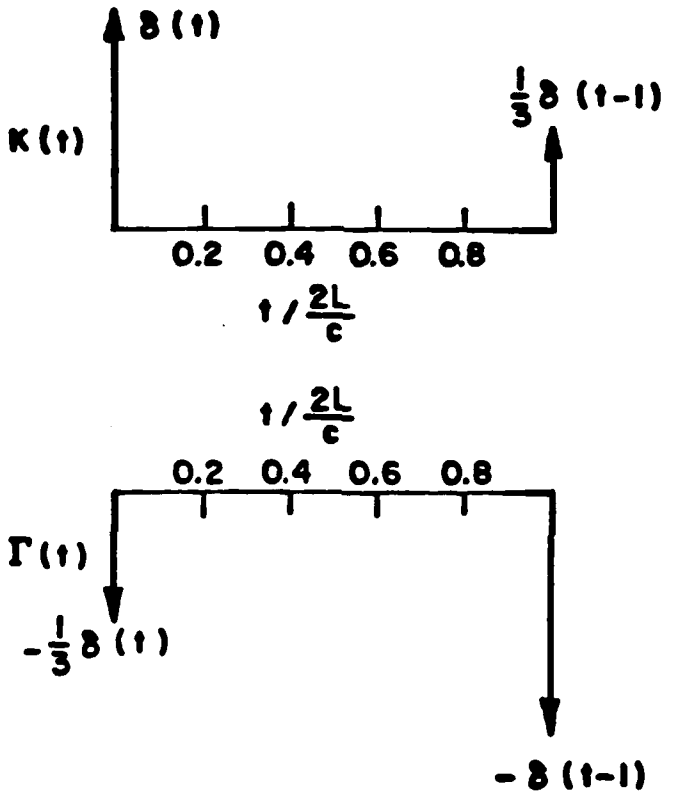

Figure D.20. K-pulse and reflected waveform for a lossless grounded slab.

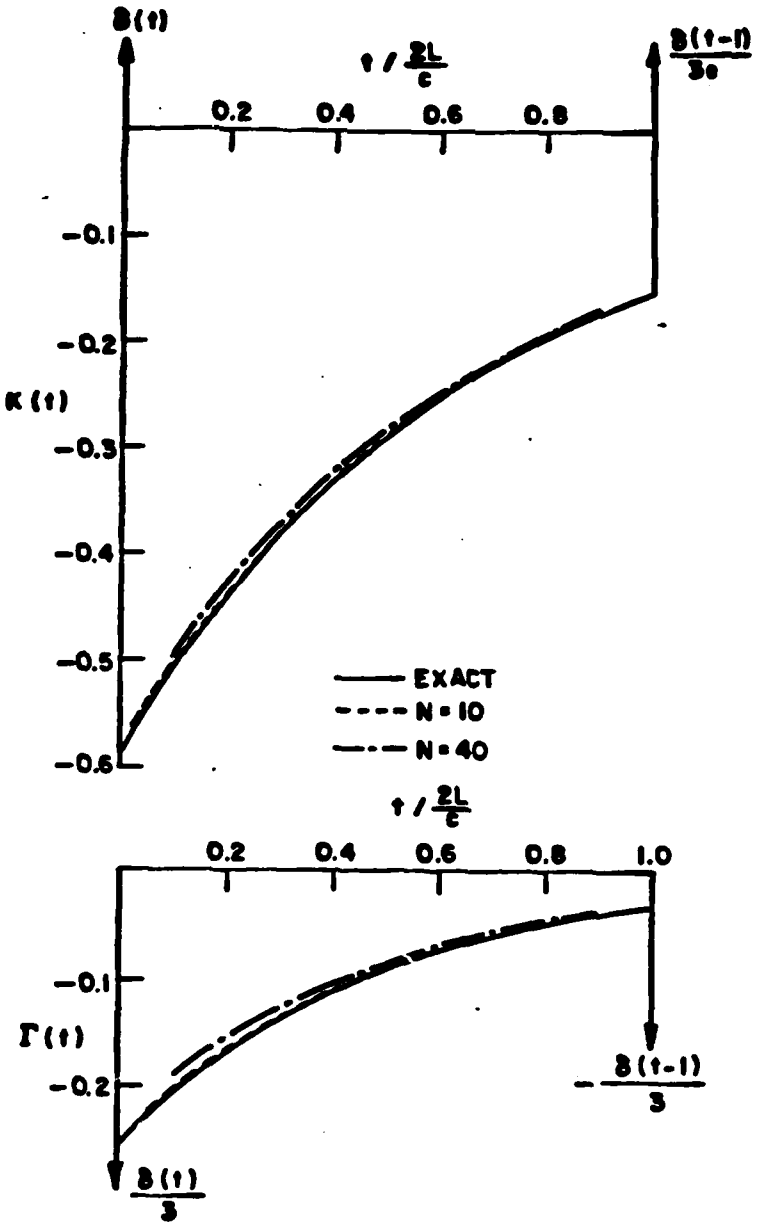

Figure D.21. K-pulse and reflected waveforms for a shorted uniform lossy slab.

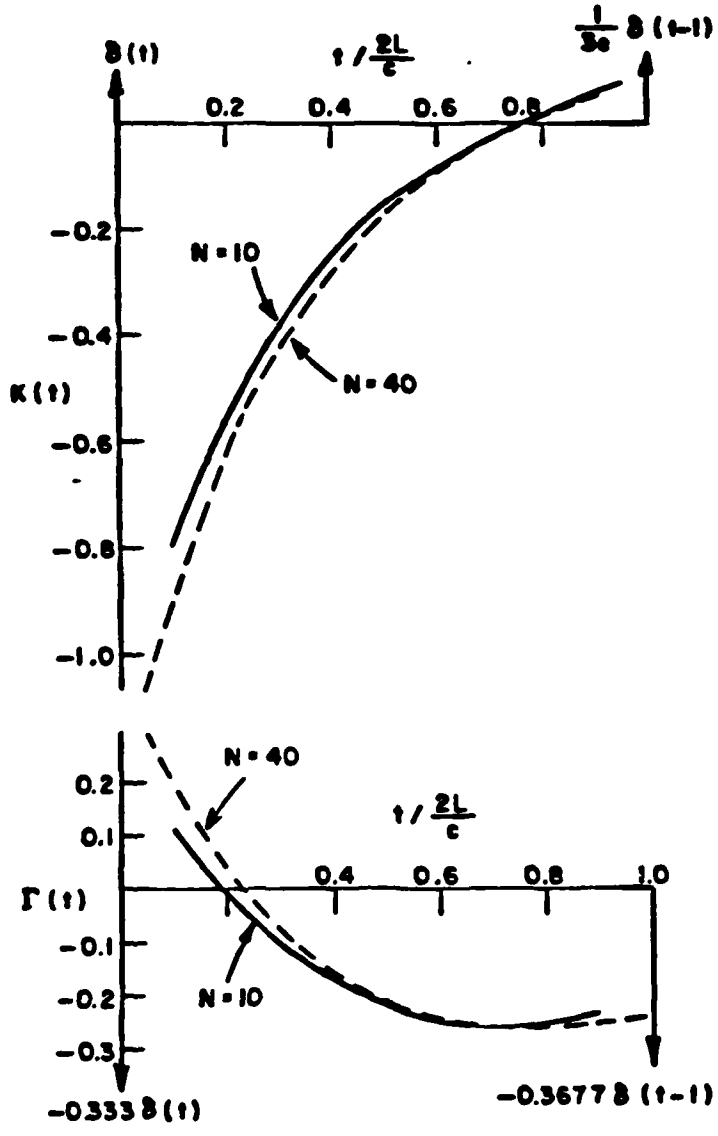

Figure D.22. K-pulse and reflected waveforms for shorted tapered line (Z_s=2.0, Z_d=0.0, k=1)

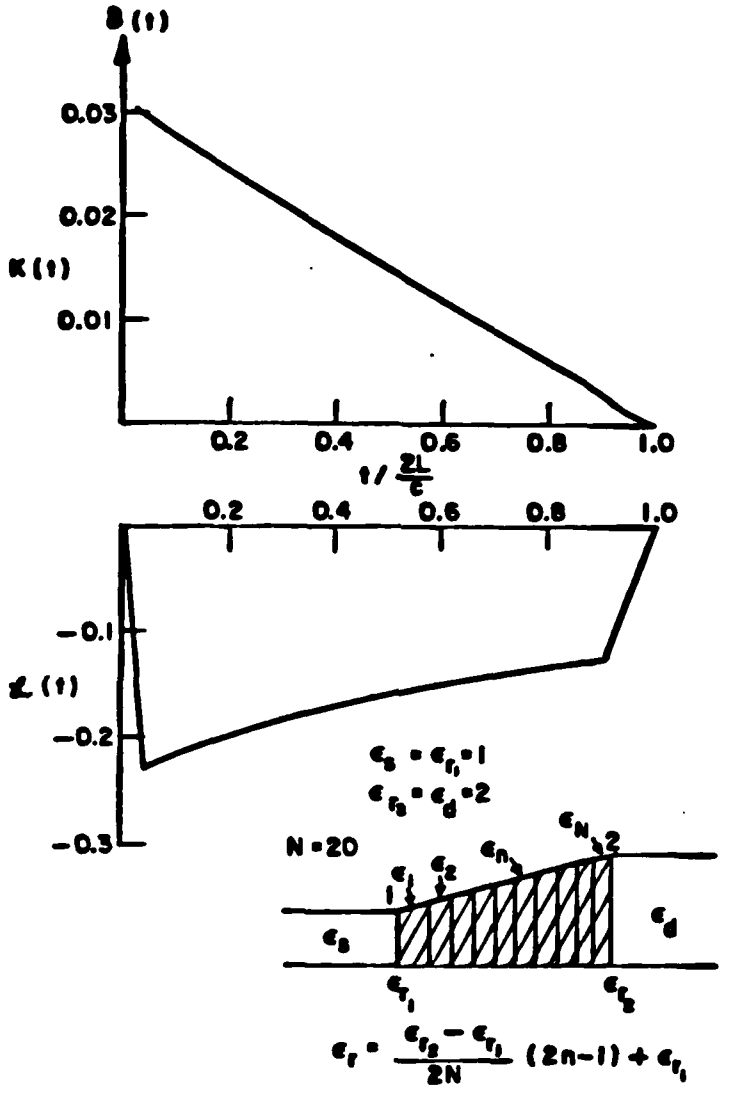

Figure D.23. K-pulse for line with continuously varying ϵ_r.

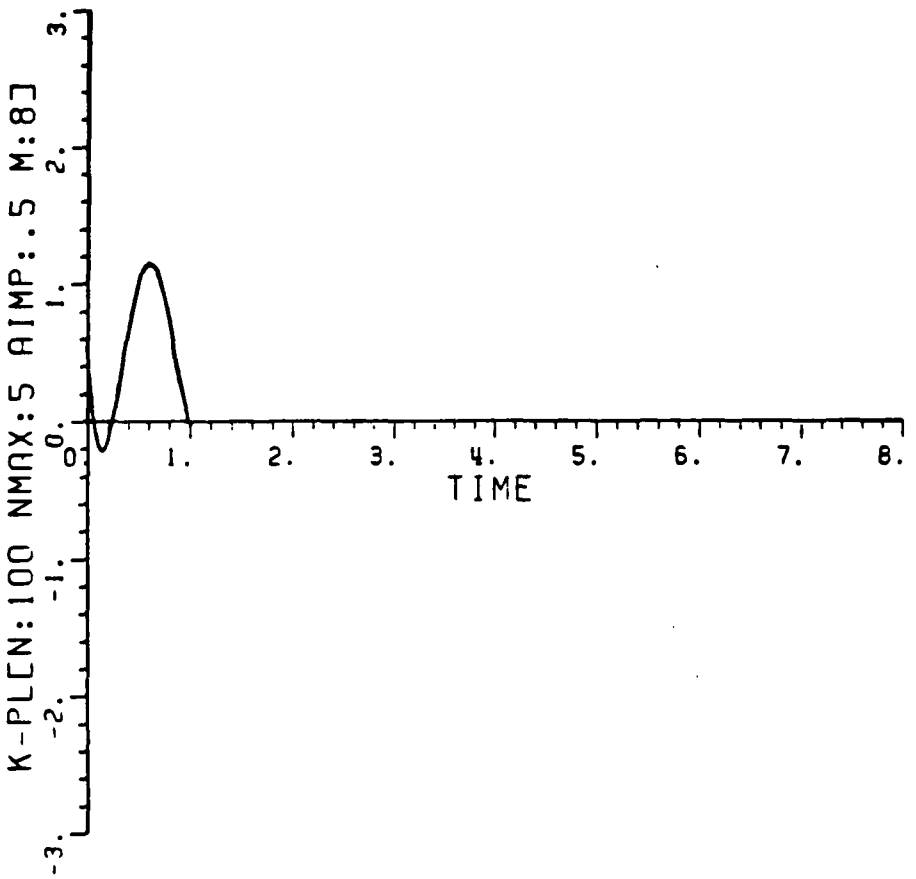

Figure D.24. Approximate K-pulse for the conducting sphere impulse of weight 1/2 at origin not shown.

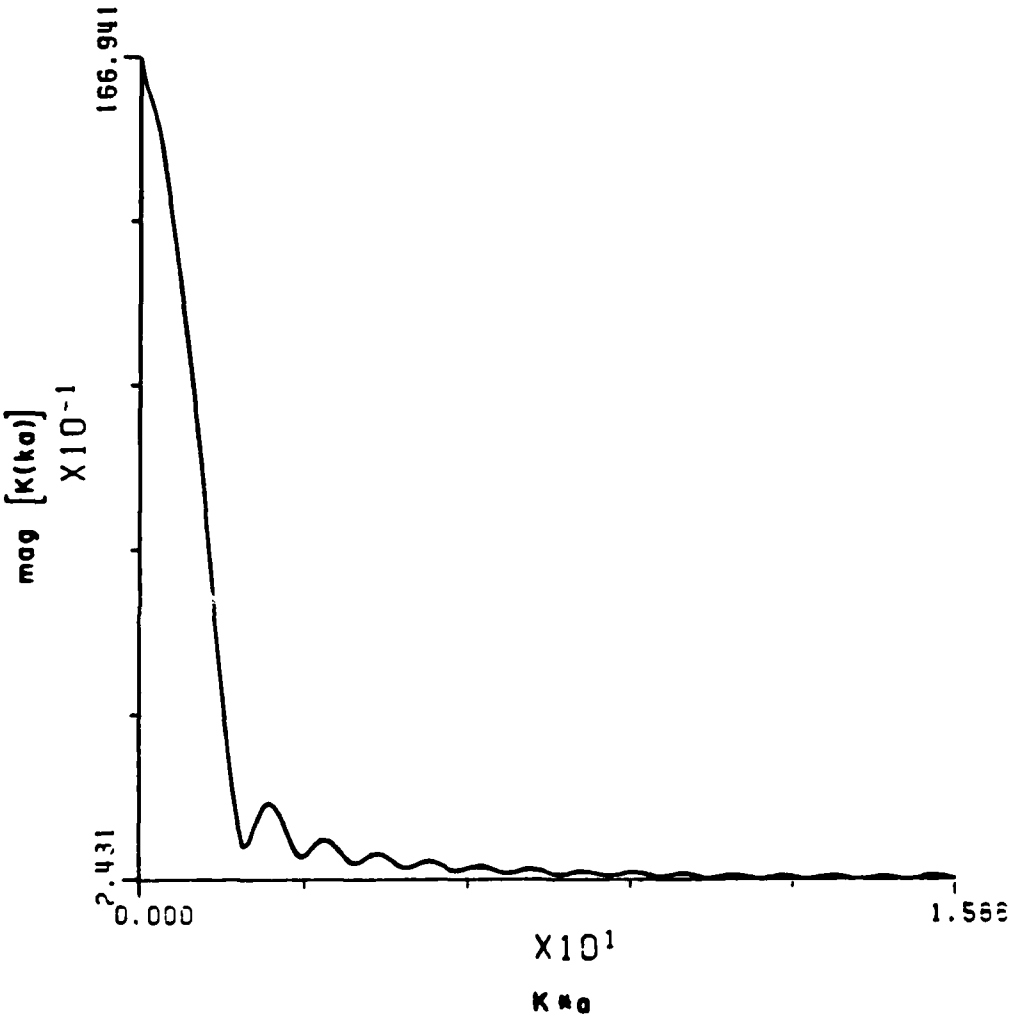

Figure D.25. Approximate K-pulse spectrum for the conducting sphere.

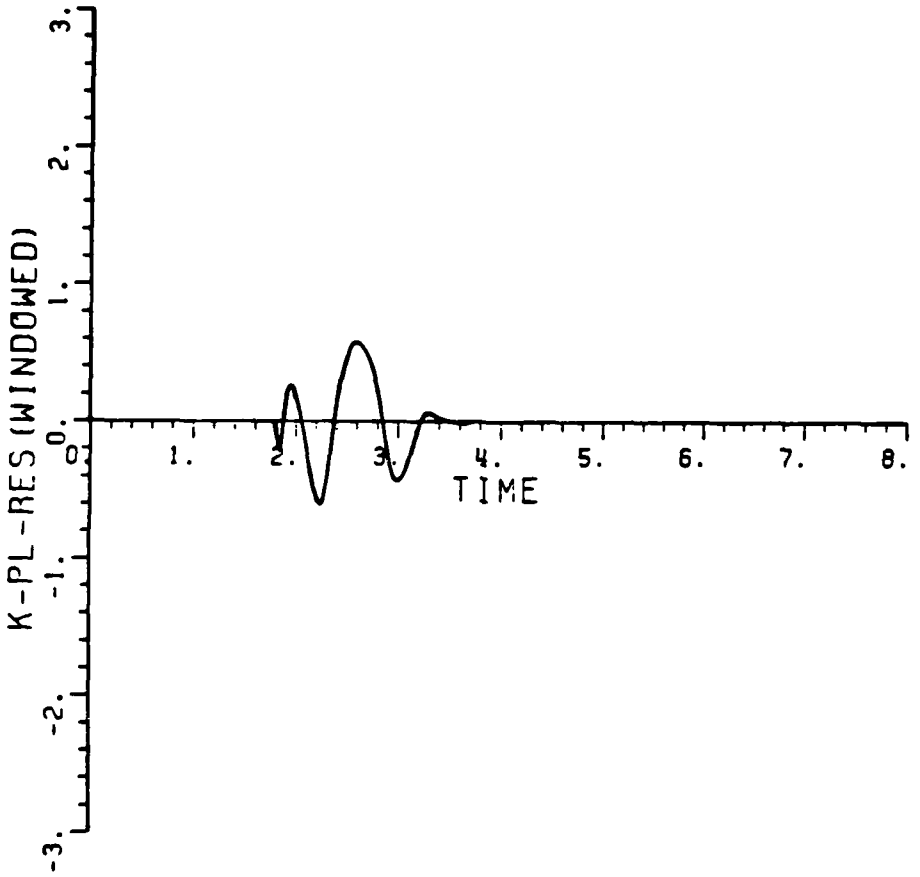

Figure D.26. Conducting sphere response to K-pulse excitation.

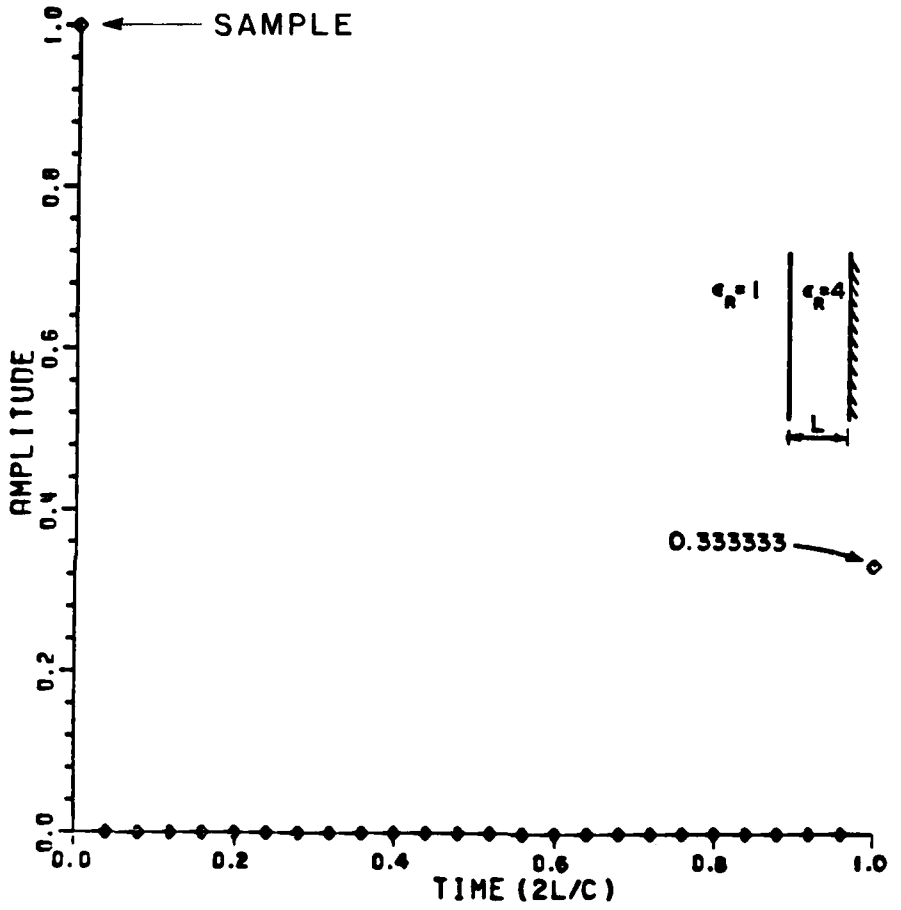

Figure D.27. K-pulse for a plane wave normal incident onto a grounded dielectric slab. (each dot represents an impulse) (Resembles a sampled version of Figure 20).

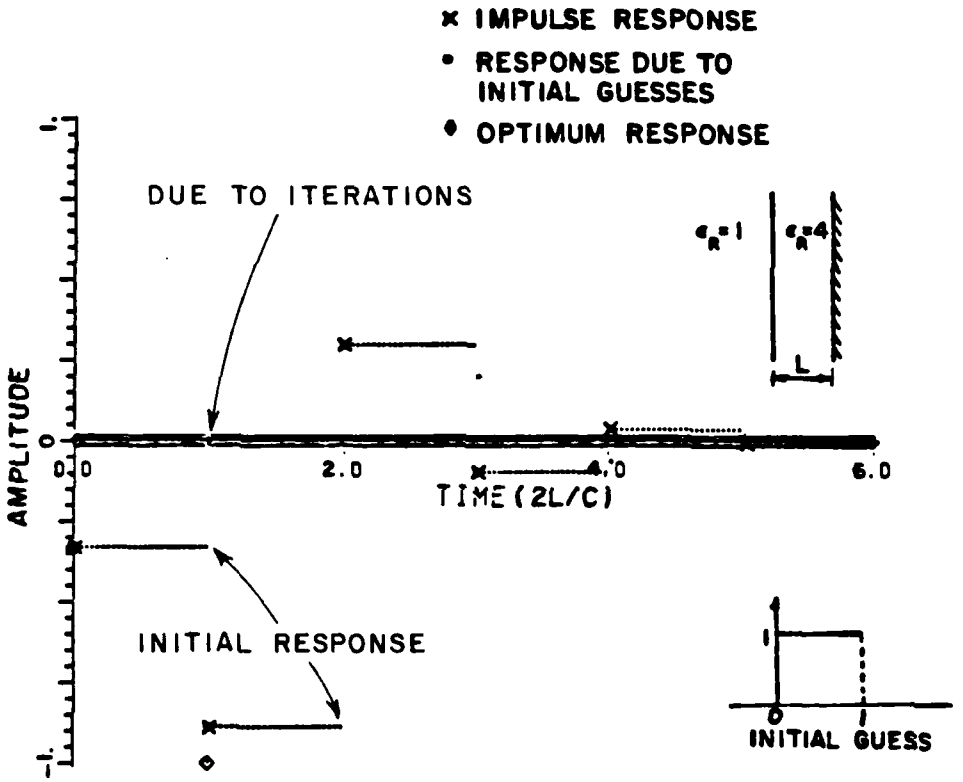

Figure D.28. Target responses for three different inputs. (each dot represents an impulse)

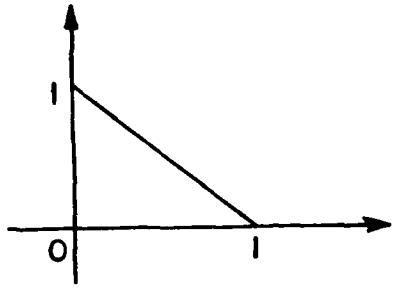

(a)

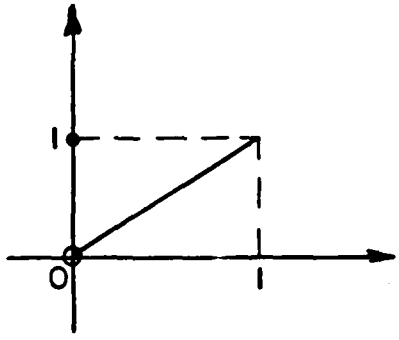

(b)

Figure D.29. Other initial K-pulse guesses which converge to the same results as Figure 28.

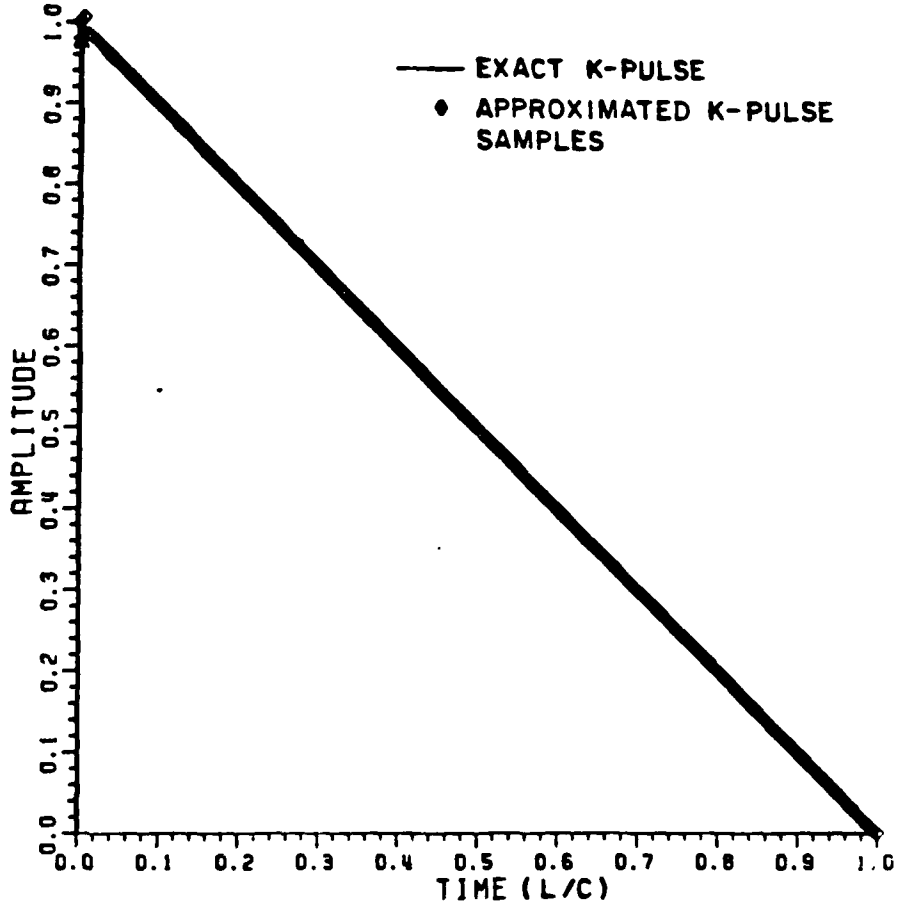

Figure D.30. Exact and approximated K-pulse.

END

FILMED

4-86

DTIC